

DTIC FILE COPY

2

# NAVAL POSTGRADUATE SCHOOL Monterey, California

AD-A224 139



DTIC  
ELECTE  
JUL 23 1990  
S B D

## THESIS

EFFECTS OF FLOWFIELD TURBULENCE  
ON ASYMMETRIC VORTICES  
OVER A SLENDER BODY

by

James A. Pinaire, Jr.

December 1989

Thesis Advisor

Richard M. Howard

Approved for public release; distribution is unlimited.

90 07 20 008

REPORT DOCUMENTATION PAGE

1a REPORT SECURITY CLASSIFICATION <b>UNCLASSIFIED</b>		1b RESTRICTIVE MARKINGS	
2a SECURITY CLASSIFICATION AUTHORITY		3. DISTRIBUTION/AVAILABILITY OF REPORT Approved for public release; distribution is unlimited	
2b DECLASSIFICATION/DOWNGRADING SCHEDULE			
4 PERFORMING ORGANIZATION REPORT NUMBER(S)		5. MONITORING ORGANIZATION REPORT NUMBER(S)	
6a NAME OF PERFORMING ORGANIZATION Naval Postgraduate School	6b OFFICE SYMBOL (if applicable) Code 67	7a NAME OF MONITORING ORGANIZATION Naval Postgraduate School	
6c. ADDRESS (City, State, and ZIP Code) Monterey, California 93943-5000		7b. ADDRESS (City, State, and ZIP Code) Monterey, California 93943-5000	
8a. NAME OF FUNDING / SPONSORING ORGANIZATION	8b OFFICE SYMBOL (if applicable)	9. PROCUREMENT INSTRUMENT IDENTIFICATION NUMBER	
8c. ADDRESS (City, State, and ZIP Code)		10 SOURCE OF FUNDING NUMBERS	
		PROGRAM ELEMENT NO.	PROJECT NO.
		TASK NO.	WORK UNIT ACCESSION NO.
11. TITLE (Include Security Classification) EFFECTS OF FLOWFIELD TURBULENCE ON ASYMMETRIC VORTICES OVER A SLENDER BODY			
12. PERSONAL AUTHOR(S) Pinaire, James Alan			
13a. TYPE OF REPORT Master's Thesis	13b TIME COVERED FROM _____ TO _____	14. DATE OF REPORT (Year, Month, Day) 1989, December	15 PAGE COUNT 103
16. SUPPLEMENTARY NOTATION The views expressed in this thesis are those of the author and do not reflect the official policy or position of the Department of Defense or the U.S. Government.			
17 U.S. Government ACROSS		18 SUBJECT TERMS (Continue on reverse if necessary and identify by block number)	
FIELD	GROUP	Vertical Launch, Surface-to-Air-Missile, High Angle of Attack Aerodynamics, Turbulence, Body of Revolution, Vortex Asymmetry	
		110000	
19. ABSTRACT (Continue on reverse if necessary and identify by block number) The flowfield about a vertically-launched surface-to-air missile model at an angle of attack of 50 degrees and a Reynolds number of $1 \times 10^5$ was investigated in a low-speed wind tunnel at the Naval Postgraduate School. The location and intensity of the asymmetric vortices in the wake of the missile model were determined and the vortices were displayed using planar velocity vector, total pressure coefficient, and vorticity plots. The model configuration tested was a body-only configuration (wings, strakes, and tails removed). Two flowfield conditions were treated: the nominal ambient wind tunnel condition and a grid-generated turbulence condition. Flow visualization was conducted and video-taped for both the body-only and winged configurations. The following conclusions were reached: 1) the addition of turbulence decreased the vorticity but did not significantly change the patterns of the plots; 2) the addition of turbulence reduced the vorticity more at eleven body diameters than at six body diameters; 3) compared to the body-only case, the			
20 DISTRIBUTION/AVAILABILITY OF ABSTRACT <input checked="" type="checkbox"/> UNCLASSIFIED/UNLIMITED <input type="checkbox"/> SAME AS RPT <input type="checkbox"/> DTIC USERS		21. ABSTRACT SECURITY CLASSIFICATION Unclassified	
22a. NAME OF RESPONSIBLE INDIVIDUAL Richard M. Howard		22b. TELEPHONE (Include Area Code) (408) 646-2870	22c. OFFICE SYMBOL Code 67Ho

vorticity is reduced for the  $\downarrow x$  case but not for the "+" case for the turbulence condition; 4) flow visualization verified vortices movement away from the missile as the tested point was moved aft along the missile body. *Theses. ynd*

Accession For	
NTIS GRA&I	<input checked="" type="checkbox"/>
DTIC TAB	<input type="checkbox"/>
Unannounced	<input type="checkbox"/>
Justification	
By	
Distribution/	
Availability Codes	
Dist	Avail and/or Special
A-1	



Approved for public release; distribution is unlimited.

Effects of Flowfield Turbulence  
on Asymmetric Vortices  
Over a Slender Body

by

James A. Pinaire, Jr.  
Lieutenant, United States Navy  
B.S., Indiana Central University

Submitted in partial fulfillment  
of the requirements for the degree of

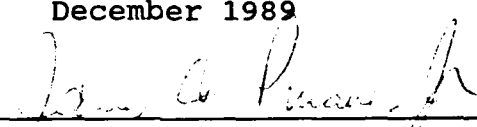
MASTER OF SCIENCE IN ENGINEERING SCIENCE

from the

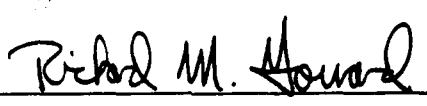
NAVAL POSTGRADUATE SCHOOL

December 1989

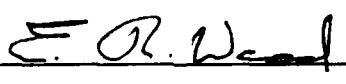
Author:

  
James A. Pinaire, Jr.

Approved by:

  
Richard M. Howard, Thesis Advisor

  
Eric P. Pagenkopf, Second Reader

  
E. R. Wood, Chairman  
Department of Aeronautics and Astronautics

## ABSTRACT

The flowfield about a vertically-launched surface-to-air missile model at an angle of attack of 50 degrees and a Reynolds number of  $1.1 \times 10^5$  was investigated in a low-speed wind tunnel at the Naval Postgraduate School. The location and intensity of the asymmetric vortices in the wake of the missile model were determined and the vortices were displayed using planar velocity vector, total pressure coefficient, and vorticity plots. The model configuration tested was a body-only configuration (wings, strakes, and tails removed). Two flowfield conditions were treated: the nominal ambient wind tunnel condition and a grid-generated turbulence condition. Flow visualization was conducted and video-taped for both the body-only configuration and the winged configurations. The following conclusions were reached: 1) the addition of turbulence decreased the vorticity but did not significantly change the patterns of the plots; 2) the addition of turbulence reduced the vorticity more at eleven body diameters than at six body diameters; 3) compared to the body-only case, the vorticity is reduced for the "x" case but not for the "+" case for the turbulence condition; 4) flow visualization verified vortices movement away from the missile as the tested point was moved aft along the missile body.

## TABLE OF CONTENTS

I.	INTRODUCTION . . . . .	1
A.	BACKGROUND . . . . .	1
B.	HIGH ANGLE OF ATTACK AERODYNAMICS . . . . .	4
C.	ASYMMETRIC VORTICES . . . . .	7
D.	TURBULENCE . . . . .	9
II.	EXPERIMENT AND PROCEDURES . . . . .	12
A.	OVERVIEW . . . . .	12
B.	APPARATUS . . . . .	14
1.	Wind Tunnel and Turbulence Grids . . . . .	14
2.	VLSAM Model and Mount . . . . .	18
3.	Traverser and Five-Hole Pressure Probe . . . . .	18
4.	Data Acquisition . . . . .	22
C.	EXPERIMENTAL CONDITIONS . . . . .	22
D.	SOFTWARE . . . . .	24
E.	EXPERIMENTAL PROCEDURE . . . . .	26
F.	FLOW VISUALIZATION EQUIPMENT . . . . .	28
III.	RESULTS AND DISCUSSION . . . . .	30
A.	CONFIGURATION 0B . . . . .	30
B.	CONFIGURATION 3B . . . . .	36

C. COMPARISON BETWEEN NO TURBULENCE AND TURBULENCE	39
D. COMPARISON BETWEEN BODY-ONLY CONFIGURATIONS . .	42
E. COMPARISON BETWEEN BODY-ONLY AND WINGED CONFIGURATIONS . . . . .	45
F. COMPARISON WITH FLOW VISUALIZATION . . . . .	54
IV. CONCLUSIONS AND RECOMMENDATIONS . . . . .	58
APPENDIX A. PPROBE PROGRAM . . . . .	61
APPENDIX B. CALP PROGRAM . . . . .	77
APPENDIX C. CONVERT PROGRAM . . . . .	84
APPENDIX D. VORTIC PROGRAM . . . . .	88
LIST OF REFERENCES . . . . .	90
INITIAL DISTRIBUTION LIST . . . . .	93

## LIST OF FIGURES

### Figure

1. Flow Regimes -----	5
2. Cross-flow Streamlines -----	7
3. The Planar Survey Grid -----	13
4. Naval Postgraduate School Wind Tunnel -----	14
5. Turbulence-Generating Grids -----	17
6. Planview of VLSAM Model with Pressure Probe and Grid in the Test Section of the Wind Tunnel -----	19
7. Specifications of VLSAM Model -----	20
8. 3-D Traversing Assembly -----	21
9. Five-Hole Pressure Probe -----	21
10. VLSAM Model Body Configurations -----	23
11. Flow Visualization System -----	29
12. Velocity Vectors-Configuration 0B -----	31
13. Total Pressure Coefficient-Configuration 0B -----	33
14. Vorticity-Configuration 0B -----	34
15. Vorticity-Configuration 0B -----	35
16. Velocity Vectors-Configuration 3B -----	37
17. Total Pressure Coefficient-Configuration 3B -----	38
18. Vorticity-Configuration 3B -----	40
19. Vorticity-Configuration 0B -----	41
20. Velocity Vectors-Configuration 0B -----	43
21. Total Pressure Coefficient-Configuration 0B -----	44
22. Velocity Vectors-Configuration 0C -----	46
23. Velocity Vectors-Configuration 3C -----	47

23. Velocity Vectors-Configuration 3C -----	47
24. Total Pressure Coefficient-Configuration 0C -----	48
25. Total Pressure Coefficient-Configuration 3C -----	49
26. Vorticity-Configuration 0C -----	50
27. Vorticity-Configuration 3C -----	51
28. Vorticity-Configuration 0A -----	52
29. Vorticity-Configuration 3A -----	53
30. Flow Visualization -----	55
31. Flow Visualization -----	56
32. Sketch of Vortex Core Positions -----	57

## I. INTRODUCTION

### A. BACKGROUND

Missile development in recent years has emphasized the capability for operation at high angle of attack due to demand for higher maneuverability and special mission requirements. This trend is amplified by the increasing demand to minimize the overall wingspan. Several examples of missile design which involve high angles of attack are vertical launching, missile storage separation from aircraft, launch from an aircraft container, the one-man anti-tank weapon, and the air-to-air and air-to-ground short range missile. These are examples where high angles of attack can be reached at subsonic Mach numbers. The flight Mach number in some cases can even range from low subsonic to high supersonic. In such flight conditions it is important to understand the flowfield around the missile and the effects on aerodynamic characteristics. [Ref. 1]

An example of such a missile is the U.S. Navy's vertically-launched surface-to-air missile (VLSAM). Upon launch it enters the ocean's surface environment at low velocity where it may encounter significant crosswinds resulting in a high angle of attack situation. In addition, the VLSAM launch conditions may include some degree of

turbulence caused by interaction of the air movement above the ocean surface, the ship's motion, and superstructure interference. [Ref. 2] High angle-of-attack conditions may result in the formation of asymmetric vortices along the missile body. These vortices induce side forces on the missile and can affect its flight aerodynamics. A vertically-launched anti-submarine rocket was lost due to asymmetric vortices caused by its high angle of attack and nose asymmetry [Ref. 3].

This thesis is a part of the research conducted at the Naval Postgraduate School (NPS) to understand the effects of turbulence on a VLSAM model at high angle of attack. Initially, Roane developed the missile model and procedure to measure various flowfield turbulence effects [Ref. 4]. Rabang studied the asymmetric-vortex-induced side force by varying turbulence, angle of attack, and roll angle. He concluded that turbulence with length scales comparable to the nose-generated vortices increased the side force and decreased flow unsteadiness. He also verified that nose roll angle can cause significant changes in the side forces and that the addition of low-aspect wings did not significantly change the magnitude of the side forces. [Ref. 2]

Lung mapped the location and shape of the asymmetric vortices, in a cross-plane six missile diameters from the nose, using a body-only configuration with and without

freestream turbulence, at 50 degree angle attack. He concluded that the strength of the vortices weakened and became more diffuse with turbulence. [Ref. 5]

Viniotis repeated the procedure at six diameters using two wing configurations: zero degree roll angle ("+" configuration) and 45 degree roll angle ("x" configuration).

He concluded that the addition of turbulence decreased vortex strength and the addition of wings causes the vortices to move closer to the missile body. [Ref. 6]

Johnson continued the study by mapping the flowfield in a cross-plane eleven diameters from the nose for the "+" and "x" configurations. He concluded that the addition of turbulence decreased the vortex strength with little change in the vortices' positions. He also noted that the vortex strength was greater for the "+" configuration than for the "x" configuration, but that the amount of change was much less with turbulence addition. [Ref. 7]

The purpose of this research was to study the vortices for the body-only configuration in turbulent and non-turbulent flow at eleven missile diameters from the missile nose. In addition, flow visualization was conducted for all missile configurations. Comparisons with the results of Lung and Johnson will be made to correlate the vortices' characteristics at six diameters and eleven diameters for all missile configurations.

## B. HIGH ANGLE OF ATTACK AERODYNAMICS

An important phenomenon of high angle-of-attack aerodynamics is the flow separation on body, wing, and tail surfaces and the shedding of free vortices. The flow separates along a line on the body surface via an interaction of the external flow with the laminar or turbulent boundary layer of the body. The separation causes the formation of feeding sheets which transfer the vorticity generated in the boundary layer into the external flow, which then roll up on the lee side of the body to form vortices. [Refs. 1,8]

A slender body of revolution experiences four distinct aerodynamic regimes as the angle of attack is increased from 0 to 90 degrees. The transition from one regime to the next as a function of angle of attack is also dependent on nose shape, overall fineness ratio, crossflow Mach number, Reynolds number, roll angle, free stream turbulence, and surface roughness. [Refs. 9,10]

Figure 1 shows schematics of the four flow patterns about an ogive-cylinder body and the corresponding characteristics of normal force and side force. At very low angles of attack (0 to 5 degrees) there is no noticeable boundary layer separation. In this regime the axial flow components dominate and the flow can be characterized as a classical potential flow field and an attached laminar or turbulent boundary layer. At intermediate angles of attack (5 to 20 degrees)

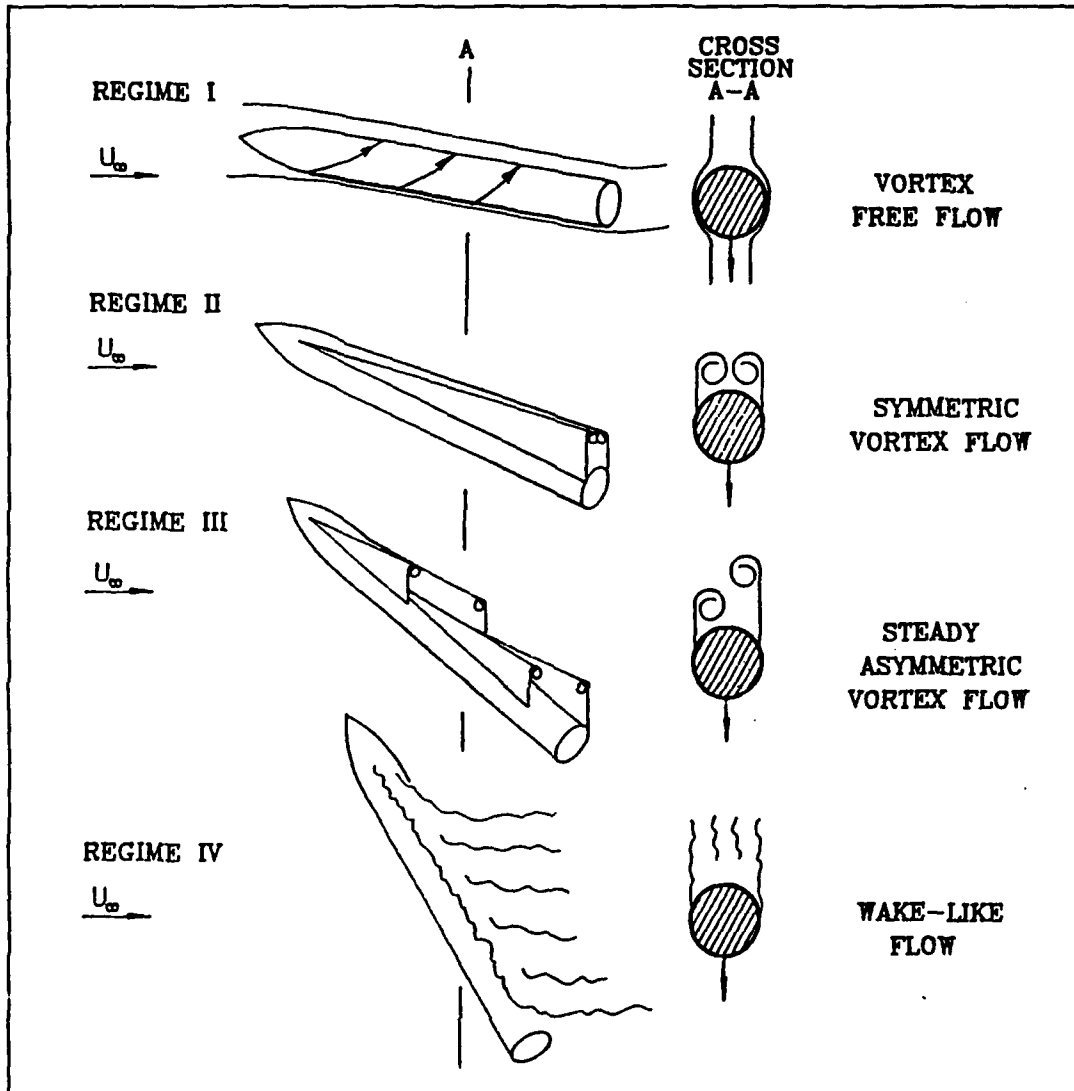
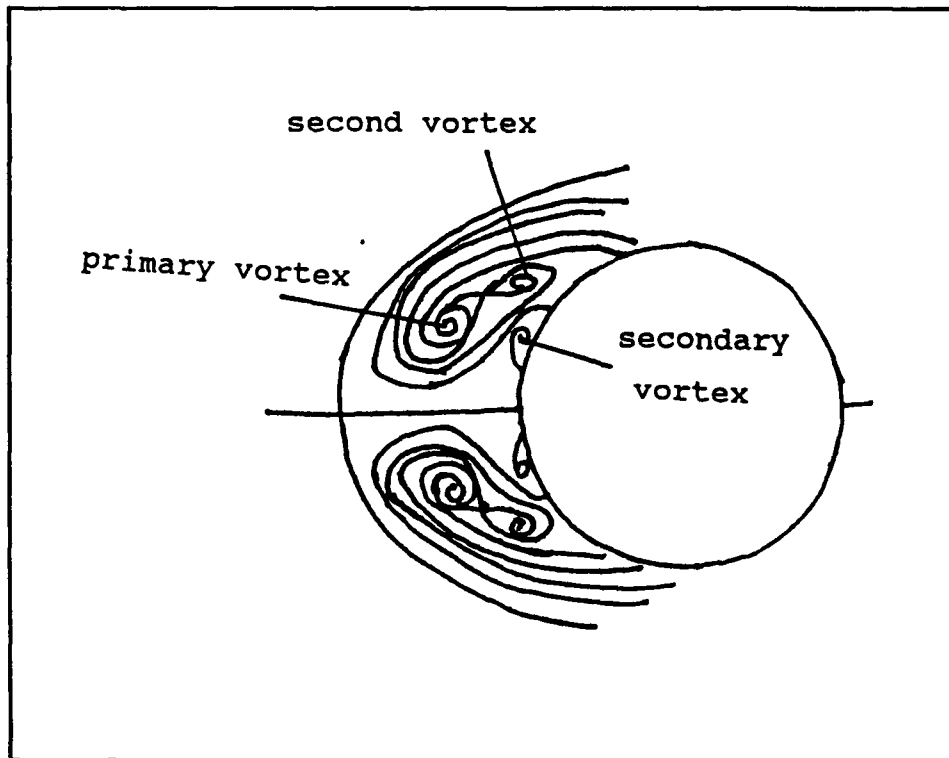


Figure 1. Flow Regimes [Ref. 2]

the boundary layer separates on the lee side of the body and rolls up into a symmetric vortex pair that originates from the apex of the body and extends to the base of the body. The vortices are steady with time and no side force or yawing moment is present. [Ref. 9]

In addition to the primary symmetric vortex pair, a second pair of vortices exists with the same rotational direction as the primary pair, positioned near the separation line as shown in Figure 2. The second interior vortices pair and the secondary vortices are induced by the primary vortices with rotation directions opposite to those of the primary vortices. The primary and the second vortices move away from the body and their cores become larger as the angle of attack increases. The second and secondary vortices are usually negligible in strength as compared to the primary vortices. [Ref.11]

In the next regime, 20 to 60 degrees, crossflow effects begin to dominate and the vortices may become asymmetric, producing a side force and yawing moment. The formation of asymmetric vortices is discussed in the next section. Lastly, at an angle of attack between 60 and 90 degrees, the crossflow completely dominates and the vortex shedding becomes unsteady, starting aft and moving forward as the angle of attack increases. The boundary layer is shed in the form of a Karman vortex street or random wake depending upon the



**Figure 2. Cross-flow Streamlines [Ref. 11]**

Reynolds number, Mach number, body geometry, etc. [Refs. 9,10,11]

### **C. ASYMMETRIC VORTICES**

As the angle of attack transitions through the 20 to 60 degree regime, the vortex flowfield on the lee side of slender bodies may become asymmetric, even without sideslip. These asymmetric vortices produce an undesirable side force and yawing moment which can make necessary a complex autopilot or degrade the mission effectiveness of the missile. The side forces may cause an unacceptable target miss distance, and the

yawing moments may reduce stability and controllability. [Refs.9,11] Reynolds number and Mach number affect the magnitude of the side force, but do not strongly influence the angle of attack for the onset of the side force. In general an increase in Mach number will decrease the magnitude of the side force. [Ref. 12,13]

The cause of asymmetric vortices formation is not completely understood, but there are two generally accepted theories. The first theory is that boundary-layer-induced asymmetry at the flow separation points causes the vortex flowfield to become asymmetric. The maximum vortex-induced normalized side force will occur in the critical Reynolds number regime where it is possible to have supercritical separation on one side of the body and subcritical separation on the other. [Refs. 14,6] The second theory suggests the principle cause of vortex flow asymmetry to be a hydrodynamic (inviscid) instability in the initially symmetric vortex formation. These vortices, which increase in strength with angle of attack, interact with the surrounding potential flowfield to form the asymmetric characteristic. [Refs. 12,15]

A vortex-switching phenomenon has been observed in which the vortex pattern rapidly switches from an almost symmetric to a highly asymmetric configuration [Ref. 13]. This switching phenomenon may result from a fluctuation in the separation characteristics on the missile, or may relate to

a second inviscid solution in the leeward flowfield [Ref. 16].

The large "steady" side forces observed by many investigators indicate that the detached vortices fluctuate about some mean asymmetric configuration [Ref. 13].

The missile fore-body has proven to be the dominating component concerning flow separation [Ref. 1]. The addition of wings does, however, cause the vortices to move closer to the body. This results in an increase of the effective angle of attack for the formation of the asymmetric vortices. [Ref. 18] The addition of strakes to a missile body greatly increases the lift and generates additional vortices which may alter the effect of the asymmetric vortices. The addition of tails has little effect on the flowfield and side forces of the forebody. Rabang has shown that the missile model retains the side force and length scale effects (described in the next section) of the induced vortices with the addition of strakes and wings. [Ref. 2]

#### D. TURBULENCE

Turbulence represents the presence of random, short duration variations in a flowfield with a given mean velocity. When considering the effects of turbulence on a body in a flowfield, it is important to compare the scale of the body to that of the turbulence. [Ref. 2]

Turbulence intensity measures the relative magnitude of high frequency velocity fluctuations in the flowfield. Greater intensities correspond to more kinetic energy in the turbulent flow. The turbulence intensity,  $T_u$ , is mathematically expressed by the ratio of the streamwise root-mean-square (rms) velocity fluctuation,  $u'$ , to the mean velocity component of the flowfield,  $U_\infty$ . [Ref. 2]

$$T_u = u' / U_\infty \quad (1)$$

Turbulence length scales are a measure of the time-averaged size of the fluid disturbance eddies. The turbulence length scale to body size ratio may determine the amount to which the turbulence affects the missile in the flowfield. Comparing the length scale to the missile length or missile diameter gives three possible results. For a length scale much greater than the body, the effect on the missile is similar to that of a steady-state flowfield. For a length scale on the same order as the body, the flowfield is non-steady and may cause rolling, pitching and yawing motion of the body. [Ref. 2] For a length scale much smaller than the body, most noticeably smaller than the missile diameter, the small-scale turbulence may affect the boundary layer development and flow separation over the missile body. [Ref. 19]

Since the length scale is an average of the disturbances, turbulence length scales of varying magnitude can be found in

a flowfield. These magnitude differences can be explained by the cascade effect. The turbulence eddies in the flowfield experience a strain in one direction which affects the scale of motion in the other directions as required by the conservation of angular momentum. The strain causes the eddies to break up into smaller scale and decreasing energy disturbances. The "cascade" of energy of turbulent motion continues to smaller and smaller scales until viscosity dissipates the smallest eddies. As the turbulence decreases in size and energy, the individual intensities decrease at a faster rate. These changes account for the dominance of the larger scale turbulence. [Ref. 20]

## II. EXPERIMENT AND PROCEDURES

### A. OVERVIEW

Pressure measurements were recorded in the VLSAM model wake to study the behavior of the asymmetric vortices. The body-only missile model was positioned at 50 degrees angle of attack for freestream conditions with and without generated turbulence in the Naval Postgraduate School low-speed wind tunnel. The pressure measurements were converted to total and planar velocity components, total pressure coefficients, and vorticity which were plotted to observe the vortices' characteristics.

Figure 3 shows the survey grid in an x-y plane which was perpendicular to the freestream flow 11 missile diameters aft from the missile nose, measured along the missile body. The survey grid measured 3.5 inches by 5.0 inches. Incremental step size was 0.25 inches, yielding 15 columns in the horizontal direction each having 21 points in the vertical direction. The grid was centered on the missile body and started 1.50 inches away from the missile body due to physical constraints of the sting mounting arm and probe.

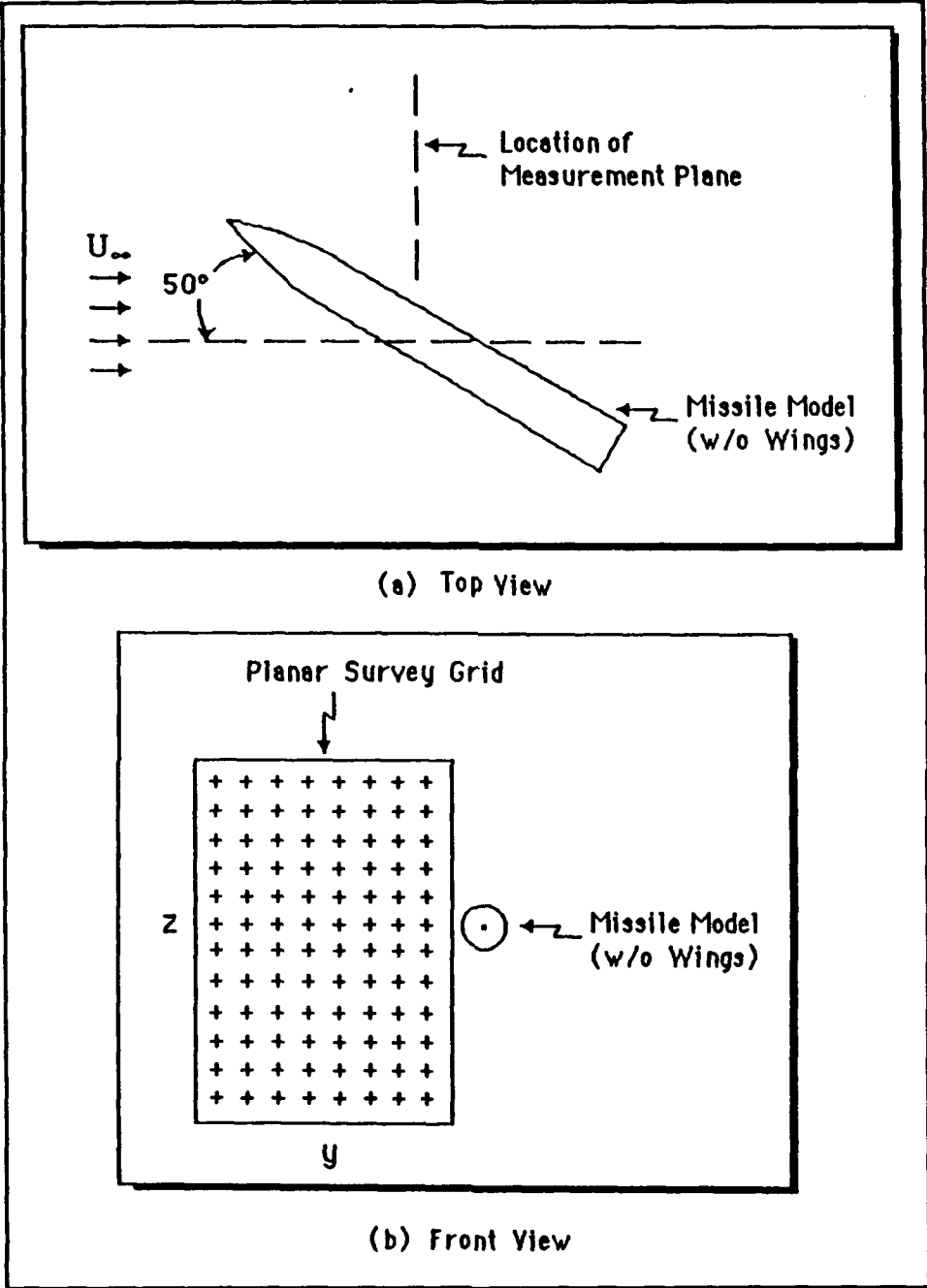


Figure 3. The Planar Survey Grid [Ref. 5]

## B. APPARATUS

Primary equipment used were the NPS wind tunnel, turbulence-generating grid, VLSAM model, three-axis traverser, five-hole pressure probe, data acquisition system, and data reduction/display software.

### 1. Wind Tunnel and Turbulence Grids

The low-speed, single-return, horizontal-flow wind tunnel is located in Halligan Hall at NPS (Figure 4).

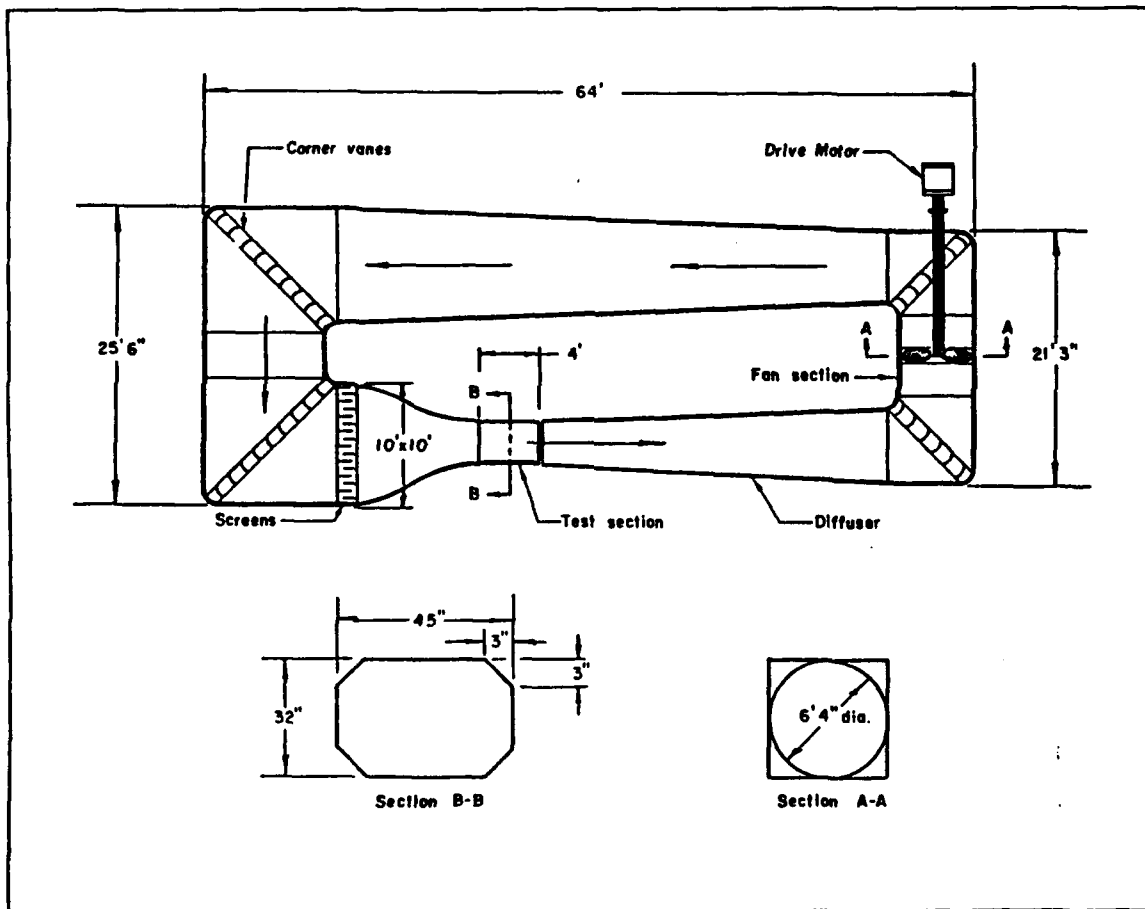


Figure 4. Naval Postgraduate School Wind Tunnel [Ref. 21]

The tunnel is powered by a 100-horsepower electric motor with a three-blade variable pitch fan and a four-speed Dodge truck transmission. Stator blades aft of the fan help to straighten the flow. Turbulence is reduced by two wire mesh screens upstream of the settling chamber and corner turning vanes. The test section is 45 inches by 32 inches with corner lighting enclosures that reduce the section area from 10 ft<sup>2</sup> to 9.88 ft<sup>2</sup>. A reflection plane in the test section decreases the useable height to 28 inches. The tunnel's contraction ratio is approximately 10:1. The tunnel was designed for test section velocities up to 290 ft/sec, operating at atmospheric pressure. A remote-controlled, flush-mounted turntable in the test section allows changing of model angle of attack in a horizontal plane. Wind tunnel temperature was measured in the settling chamber with a dial thermometer. Dynamic pressure was determined by the pressure difference between the static pressure in the settling chamber and in the test section by a water micro-manometer. The settling chamber and test section each have four static taps connecting to the manometer via a common manifold. [Ref.21] The measured pressure difference, measured in centimeters of water by the manometer, is converted to the test-section reference velocity by equation (2).

$$U_M = \{ (2 * 2.046 * \text{cm H}_2\text{O}) / (K * \rho) \}^{1/2} \quad (2)$$

Where:

$U_M$  = measured velocity (ft/sec)

2.046 = conversion factor

cm H<sub>2</sub>O = manometer reading in cm of H<sub>2</sub>O

K = wind tunnel calibration factor (for specific grid)

$\rho$  = air density (lb<sub>m</sub>/ft<sup>2</sup>)

The wind tunnel calibration factor, K, corrects for the fact that the actual dynamic pressure is slightly different than the measured static pressure difference between the static pressure in the settling chamber and in the test section. The value of the calibration factor was determined by plotting the actual dynamic pressure measured by a pitot-static tube in the test section versus the measured pressure difference. [Ref. 21] The relationship was found to be linear where the slope of the curve is the tunnel calibration factor. The value of K was determined to be 0.8891 for the no-grid configuration and 1.6545 for grid three. A large wall disturbance due to the grid frame accounts for the change in K. [Ref. 6]

Four square-mesh, square-bar, biplanar grids were designed and built by Roane to generate turbulence of varying intensities and length scales. Each grid, three constructed of wood and one of wire, was mounted in a wooden frame shown in Figure 5. [Ref. 4] The grid, placed 73 inches upstream of

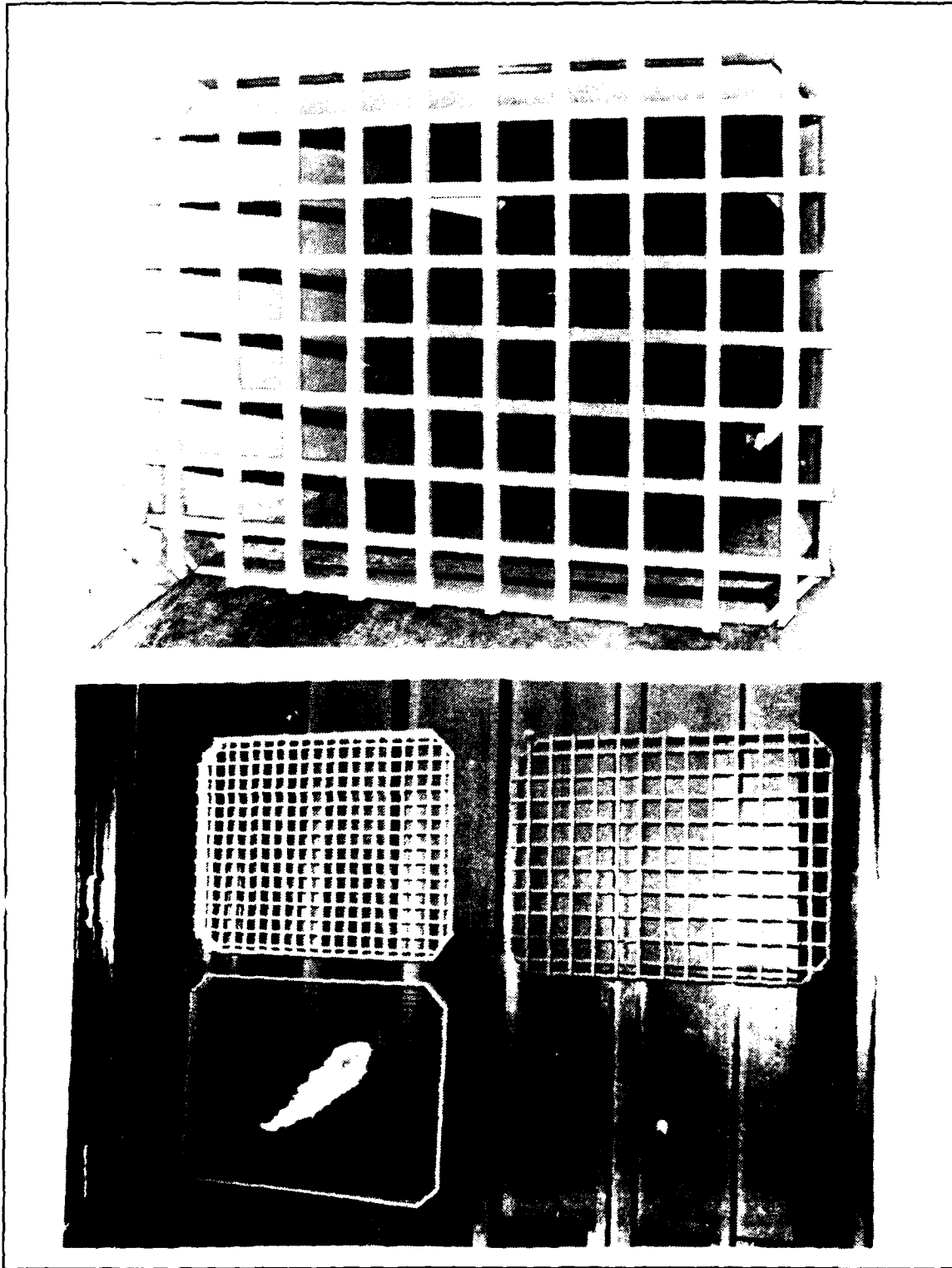


Figure 5. Turbulence-Generating Grids

the model pivot (Figure 6), creates nearly isotropic homogeneous turbulence. Table 1 summarizes measured turbulence intensities and estimated length scales determined by Roane.

## **2. VLSAM Model and Mount**

The VLSAM model is a cruciform tail-control missile with low aspect ratio wings. The nose, wings, strakes, and tails are detachable from a hollow cylindrical body which can be rotated in 45 degree increments. Figure 7 portrays the VLSAM specifications. [Ref. 2] The model was rigidly mounted in the test section using a sting mount attached to a rotating arm which allows the angle of attack to be changed (Figure 6).

## **3. Traverser and Five-Hole Pressure Probe**

The Velmex 8300 3-D traverser used three microcomputer-controlled stepping motors mounted on top the test section to allow for manual or computer operated movement of an attached five-hole pressure probe (Figure 8). Traverser movement was controlled using software (PPROBE) and a microcomputer.

Pressure measurements at each data point were acquired using a nulling five-hole pressure probe attached to the traverser (Figure 9). Pressure sample averages for each port were recorded at each data point and used to determine velocity, pitch angle, total pressure, total pressure coefficient, static pressure, and static pressure coefficient.

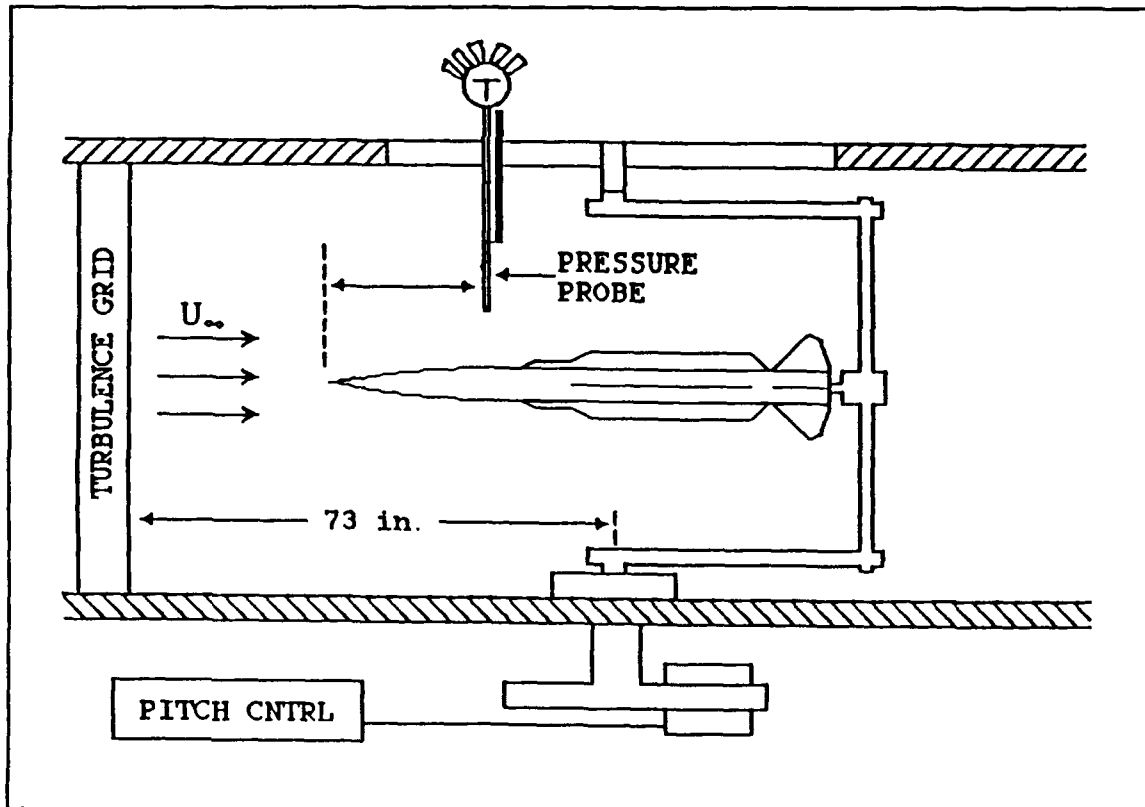
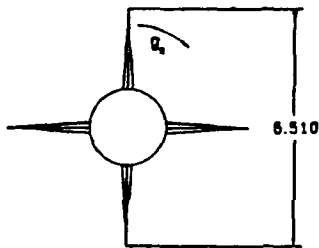


Figure 6. Planview of VLSAM Model with Pressure Probe and Grid in the Test Section of the Wind Tunnel (not drawn to scale) [Ref. 2]

Grid	Intensity (percent)	Length Scale (in.)	Turbulence/Model Dia.	Dynamic Pressure (lb/ft <sup>2</sup> )
One	3.31	1.84	1.05	15.35
Two	2.78	1.56	0.89	14.88
Three	1.88	1.08	0.62	16.38
Four	0.47	0.27	0.15	15.61
None	0.23	-	-	15.85

Table 1. Grid Turbulence Parameters [Ref. 5]

Total length = 22.85 in.  
 Base diameter = 1.75 in.  
 Length/diameter ratio = 13.06  
 Ogive nose length = 4.0 in.  
 Ogive/diameter ratio = 2.29  
 Wing span/root chord = 3.13 in./13.55 in.  
 Tail span/root chord = 5.50 in./1.70 in.  
 Center of pressure = 13.5 inches aft of nose tip (approx.)



NAVAL POSTGRADUATE SCHOOL  
 SURFACE-TO-AIR  
 MISSILE MODEL

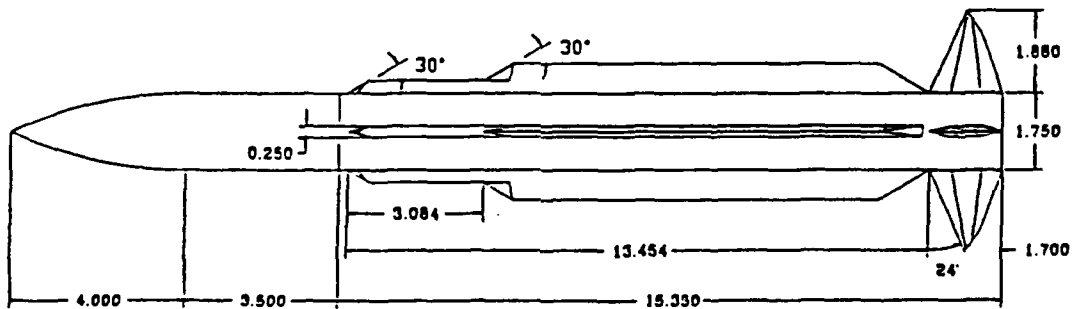


Figure 7. Specifications of VLSAM Model [Ref. 2]

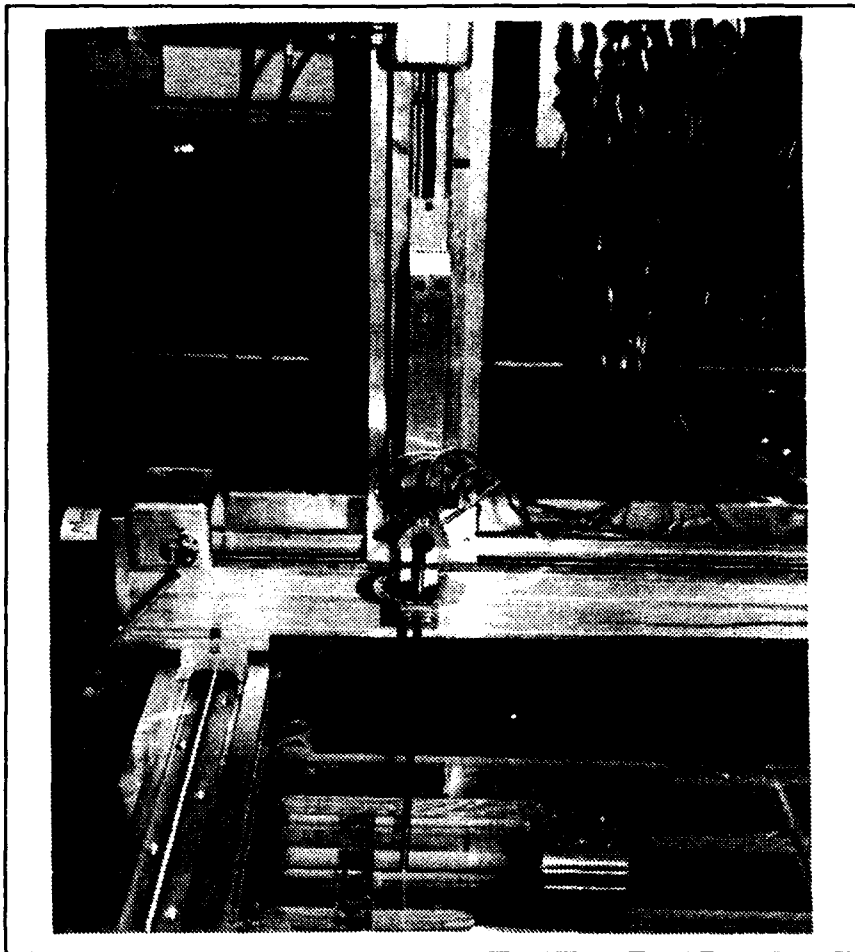


Figure 8. 3-D Traversing Assembly

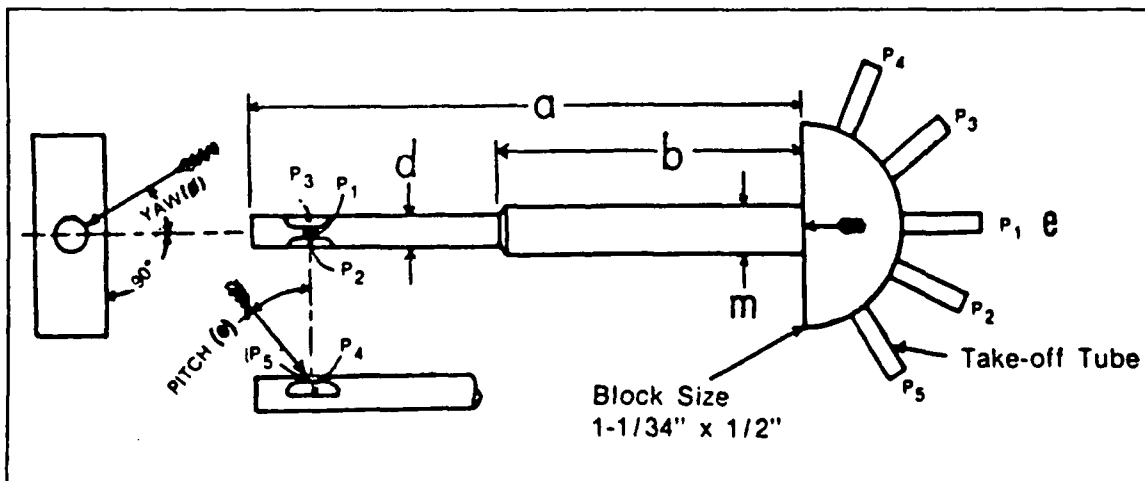


Figure 9. Five-Hole Pressure Probe [Ref. 22]

Probe port P1 measured stagnation pressure. Ports P2 and P3 were static ports connected to a portable manometer. Flow yaw angle was read directly by rotating the probe until P2 and P3 were equal. P4 and P5 were used with calibration curves to determine pitch angle. Velocities were found using the static and stagnation pressures as described previously. [Ref. 22]

#### 4. Data Acquisition

A 48-port scanivalve attached to the five-hole probe allowed the pressures to be measured and converted to voltages by one transducer. A Hewlett-Packard data acquisition system consisting of a relay multiplexer, digital multimeter, relay actuator, and software enabled system control from a microcomputer. [Refs. 6,7,24]

#### C. EXPERIMENTAL CONDITIONS

Test conditions used by Roane [Ref. 4], Lung [Ref. 5], Viniotis [Ref. 6], and Johnson [Ref. 7] were repeated to allow for data comparison.

(1) Turbulence grid three was used to generate freestream turbulence. Rabang found that grid three generated vortex-length-scale turbulence which had the largest side force effect on the missile. [Ref. 2]

(2) A Reynolds number of  $1.1 \cdot 10^5$  was obtained using reference pressure differences of 7.2 cm H<sub>2</sub>O for no grid and 10.0 cm H<sub>2</sub>O for grid three. These settings were determined

by Roane [Ref. 3] to insure comparable test section velocities for each tunnel configuration. These corrections are necessary because the pressure difference measured by the manometer includes an error resulting from disturbances caused by the screen. The calibration constants determined by Roane were used to calculate the actual dynamic pressure.

(3) Three body configurations were used. (Figure 10)

- Body A: wings and tails at 0 degree roll angle
- Body B: no wings or tails
- Body C: wings and tails at 45 degree roll angle

Body B was used for pressure measurements and all configurations were used for flow visualization.

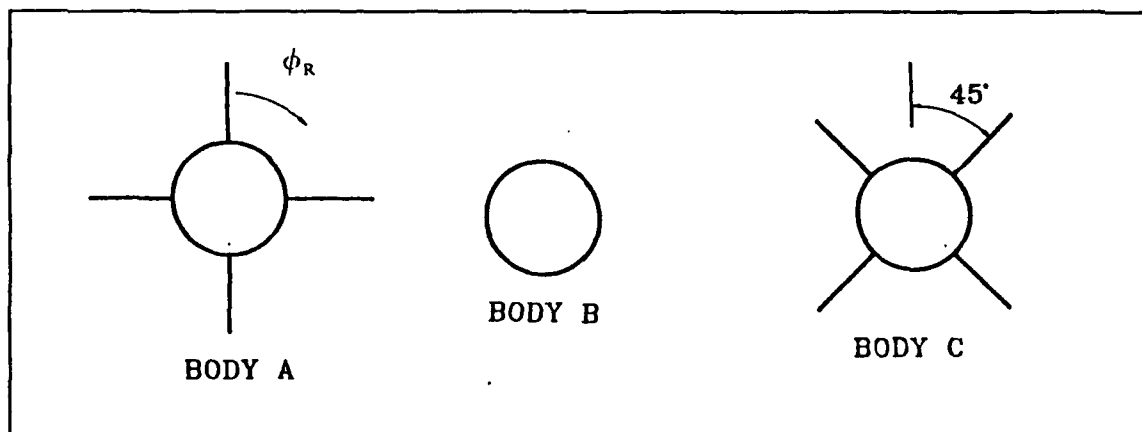


Figure 10. VLSAM Model Body Configurations [Ref. 2]

(4) The nose roll angle was set at position eight. Rabang [Ref. 2] found that the missile model's nose roll angle affected the side force coefficient, as suggested by previous

investigators. He determined that position eight produced the largest side force.

(5) Missile angle of attack was set at 50 degrees, determined by Rabang to be the angle of attack for the maximum side force. [Ref. 2]

(6) The data plane was at eleven body diameters from the nose corresponding to that used by Johnson. [Ref. 7]

(7) Wind tunnel temperature was not allowed to increase by more than 20 degrees during a data run. When the temperature reached the limit the run was stopped until the temperature cooled, at which point the testing resumed.

#### **D. SOFTWARE**

PPROBE (Appendix A) is a program written by Kindelspire [Ref. 25] and modified by Lung [Ref. 5] to control traverser movement. The operator may choose manual or computer control, the size of plane to be measured, and the step size for each movement.

CALP (Appendix B) is a program correlating transducer output voltage and pressure using a calibration manometer. The program was executed prior to and upon completion of the data collection run. CALP's output was converted to a slope-intercept equation using linear regression on a hand-held calculator. The two equations were averaged and the results used in CONVERT to calibrate the scanivalve transducer output.

CONVERT (Appendix C) is a program written by Lung [Ref. 5] which reads the PPROBE data file and computes total velocity, x and y components of velocity, pitch angle, total pressure, total pressure coefficient, static pressure, and static pressure coefficient for each data point. Velocities, pitch angle, and pressures were calculated using calibration curves provided by the probe manufacturer. Pressure coefficients were calculated using ambient room temperature and tunnel calibration factor (K), and were non-dimensionalized by the dynamic pressure. Equations (3) and (4) were used to calculate the static and total pressure coefficients, respectively.

$$C_{ps} = (P_{sl} - P_s) / Q \quad (3)$$

$$C_{pt} = (P_{tl} - P_t) / Q \quad (4)$$

Where:

- $C_{ps}$  = Static pressure coefficient
- $C_{pt}$  = Total pressure coefficient
- $Q$  = Freestream dynamic pressure
- $P_s$  = Freestream static pressure
- $P_t$  = Freestream total pressure
- $P_{sl}$  = Local static pressure
- $P_{tl}$  = Local total pressure

VORTIC is a program written by Johnson [Ref. 7] to compute the dimensionless vorticity using the velocity output from CONVERT using equation (5). (Appendix D)

$$V = \{ \partial (v/U_\infty) / \partial (x/d) \} - \{ \partial (u/U_\infty) / \partial (y/d) \} \quad (5)$$

Where:

V = vorticity

v = y component of the velocity

x = streamwise coordinate distance

u = x component of the velocity

y = transverse coordinate distance

TECPLOT is a commercial graphics program used to generate the velocity vector, pressure coefficient contour, and vorticity contour plots.

#### **E. EXPERIMENTAL PROCEDURE**

The following experimental procedure was used to collect data.

(1) The data acquisition equipment and wind tunnel were energized. Ambient tunnel temperature and pressure were recorded. The wind tunnel speed was monitored using the appropriate manual manometer value corresponding to the tunnel configuration previously discussed.

(2) Pressure calibration was performed and the results recorded.

(3) PPROBE was executed. The probe was positioned to the start point using manual control. Computer control was selected followed by grid size, increment distance and input file name. The probe was physically rotated until the

difference between  $P_2$  and  $P_3$  was approximately zero as indicated by the portable digital manometer. The yaw angle was read from the probe and entered on the computer. Each of the five pressure ports was automatically sampled ten times, averaged, and displayed on the computer screen. The values displayed were in units of volts and subsequently converted to pressure units. The  $P_1$  measurement had to be positive or a very small negative ( $> -0.5$  volts) value to ensure the probe was facing the correct direction. The difference between  $P_2$  and  $P_3$  values had to be less than 0.1 volts, which was approximately a 6.4% error of the dynamic pressure for the no-grid configuration and an 8.6% error of the dynamic pressure for the grid #3 configuration (the difference between  $P_2$  and  $P_3$  would ideally be zero). If either requirement was not satisfied, the probe was adjusted and the point resampled. At the completion of each column of data points PPROBE would automatically store the x-y position and corresponding average values and move the traverser to the next column. This procedure was repeated for the remaining data plane.

(4) CALP program was executed, the results were recorded, and the calibration curve was calculated as previously described.

(5) CONVERT and VORTIC programs were executed to obtain necessary data for plotting results.

(6) Output files from CONVERT and VCRTIC were converted to input file format for TECPLOT. Velocity vectors, pressure coefficient, and vorticity contours were then plotted.

#### F. FLOW VISUALIZATION EQUIPMENT

The flow visualization system was designed for the NPS low-speed wind tunnel by Chlebanowski [Ref. 26] and modified by Sommers [Ref. 27]. The system is depicted in Figure 11.

Smoke generated external to the tunnel by a portable fog/smoke machine was piped to a 10-gallon plenum chamber which served to dampen surges of smoke from the machine and allow the smoke to cool slightly. The smoke exited the plenum chamber and entered the contraction section of the tunnel via flexible hoses and copper tubing. The smoke then entered the freestream tunnel air three feet ahead of the missile model.

A laser sheet was used to illuminate a thin plane on the leeward side of the missile, allowing the flow phenomenon to be observed and recorded. The laser source was a class four Spectra-Physics, five watt, Argon-ion laser. The laser emitted a 1.25 mm blue-green beam through a Newport Corporation F-LFI laser fiber to a fiber optic handset, beam expander, and plano-cylindrical lens. The handset, expander, and lens were mounted to a manual traverse mechanism above the test section. The traverse allowed the laser sheet to be moved to any position along the missile.

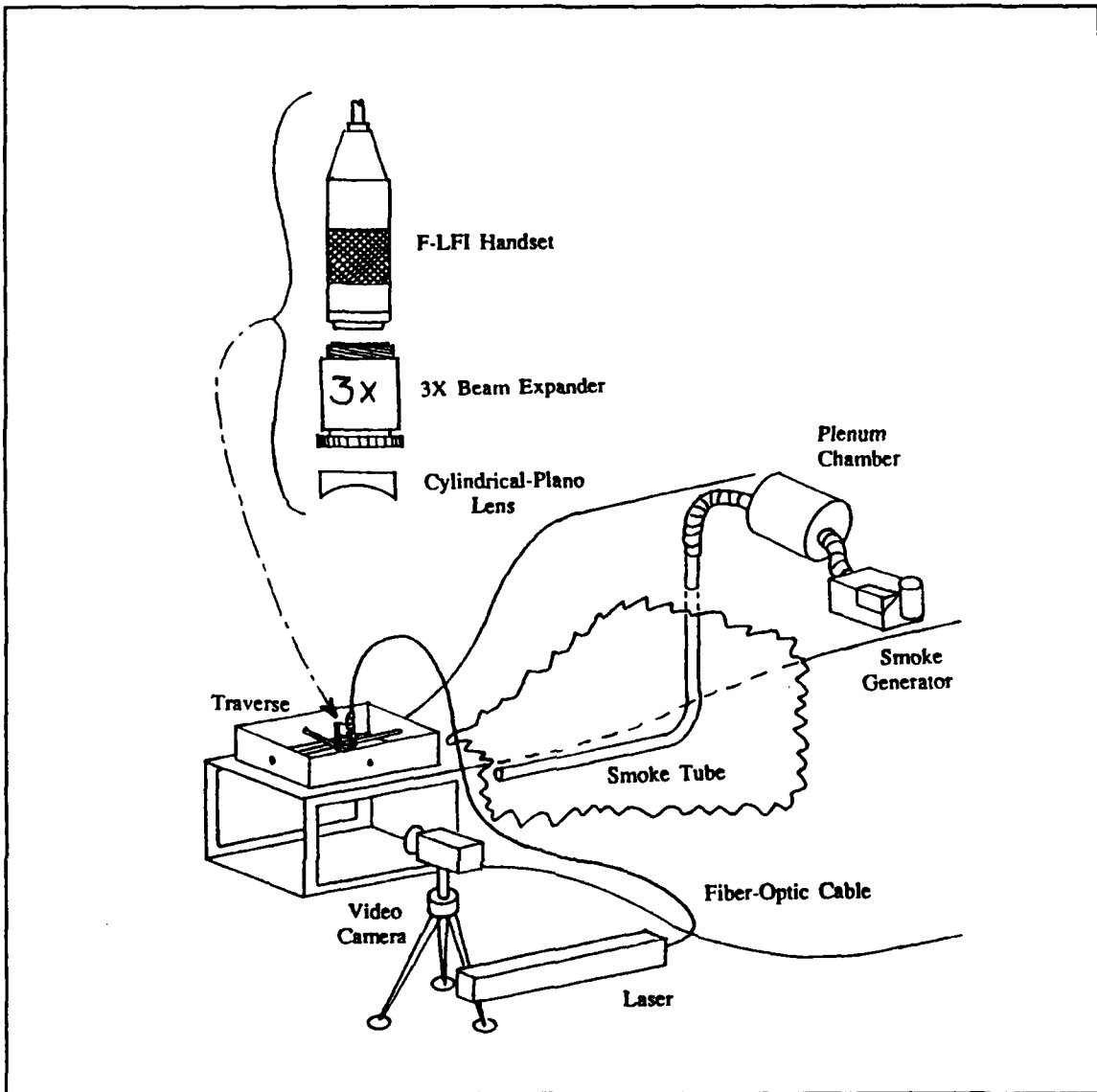


**Figure 11. Flow Visualization System [Ref. 27]**

The flow visualization runs were video-taped using a color video camera, 3/4-inch VCR, and color television monitor. Still photographs were taken of selected tape frames by the NPS Educational Media Department directly from the monitor screen.

### III. RESULTS AND DISCUSSION

The following sections discuss the velocity vector plots, total pressure coefficient contour plots, vorticity contour plots, and flow visualization photographs for the missile model configuration B (body-only) at eleven diameters. The results produced without using a turbulence grid are labeled "0B" and with turbulence grid three are labeled "3B".

The plots generated from Lung's data are at a survey grid plane six diameters (10.5 inches) aft from the missile nose. Lung also used the body-only configuration, but used grid one for turbulence generation.

The plots view the missile as it was mounted in the tunnel when observed in the direction of the tunnel freestream. All measurements are in inches (indicted by "), followed by the equivalent missile model base diameters (1.75 inches and indicated by d), and will be referenced from the leeward side of the missile body and the centerline. The terms "above" and "below" are relative to the missile centerline. "Away" indicates the distance from the center of the missile body.

#### A. CONFIGURATION 0B

The velocity vector plot (Figure 12) indicates the location of three vortices and shows the location of a saddle

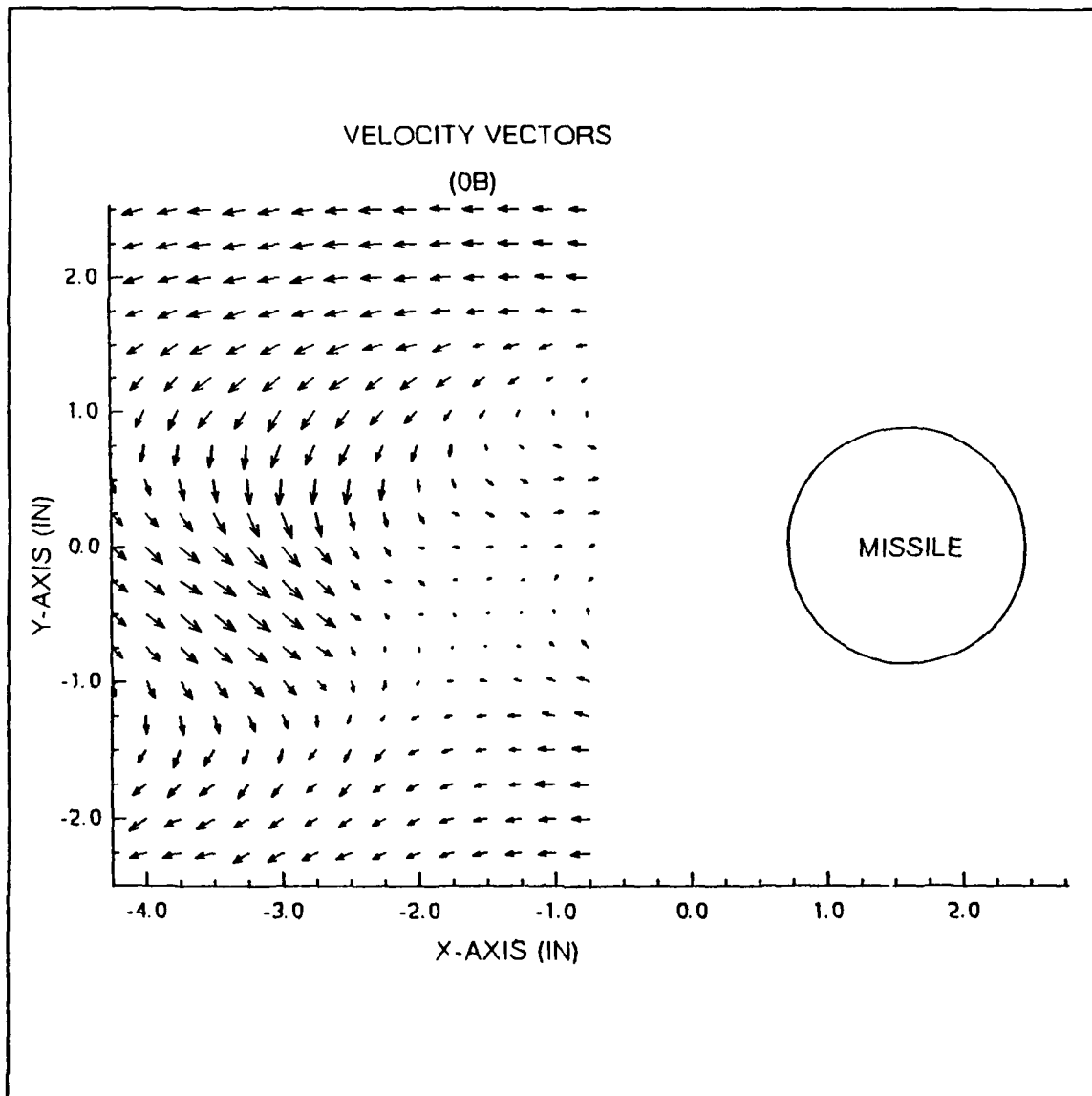


**Figure 12. Velocity Vectors-Configuration 0B**

point. The two larger vortices are asymmetric with the flow in opposite directions. The upper one is located about 1" (0.57d) above and 2 1/8" (1.21d) away. The lower outside one is located 1 1/2" (0.86d) below and 6 1/4" (3.57d) away. The lower inner one is located 7/16" (0.25d) below and 2 1/4" (1.29d) away. The saddle point is located 5/8" (0.36d) below and 3 1/8" (1.79d) away.

The total pressure coefficient plot (Figure 13) shows one large center of pressure loss located on the centerline and 4 1/4" (2.34d) away. The center does not coincide with any core from the velocity vector plot. The contours change from  $C_{pt}$  level five to level two (-0.29 to -0.82) in 3/4" in the upper half and in 1" in the lower half. This larger gradient in the upper half indicates a greater vortex strength.

The vorticity plot (Figure 14) shows three centers. The largest upper one is 5/16" (0.18d) above and 5 1/4" (3.00d) away. The smaller upper one, which is weaker, is 5/16" (0.18d) above and 4 1/2" (2.57d) away. The lower one is 1 3/16" (0.79d) below and 4 7/8" (2.79d) away. The zero value alternates above and below the missile centerline with no apparent pattern. The upper vorticity cores have positive vorticity. The lower one has negative vorticity and is smaller in magnitude than either of the upper two.

The vorticity plot from Lung (Figure 15) shows two centers. The upper one core is 3/4" (0.43d) above and 2 7/8"

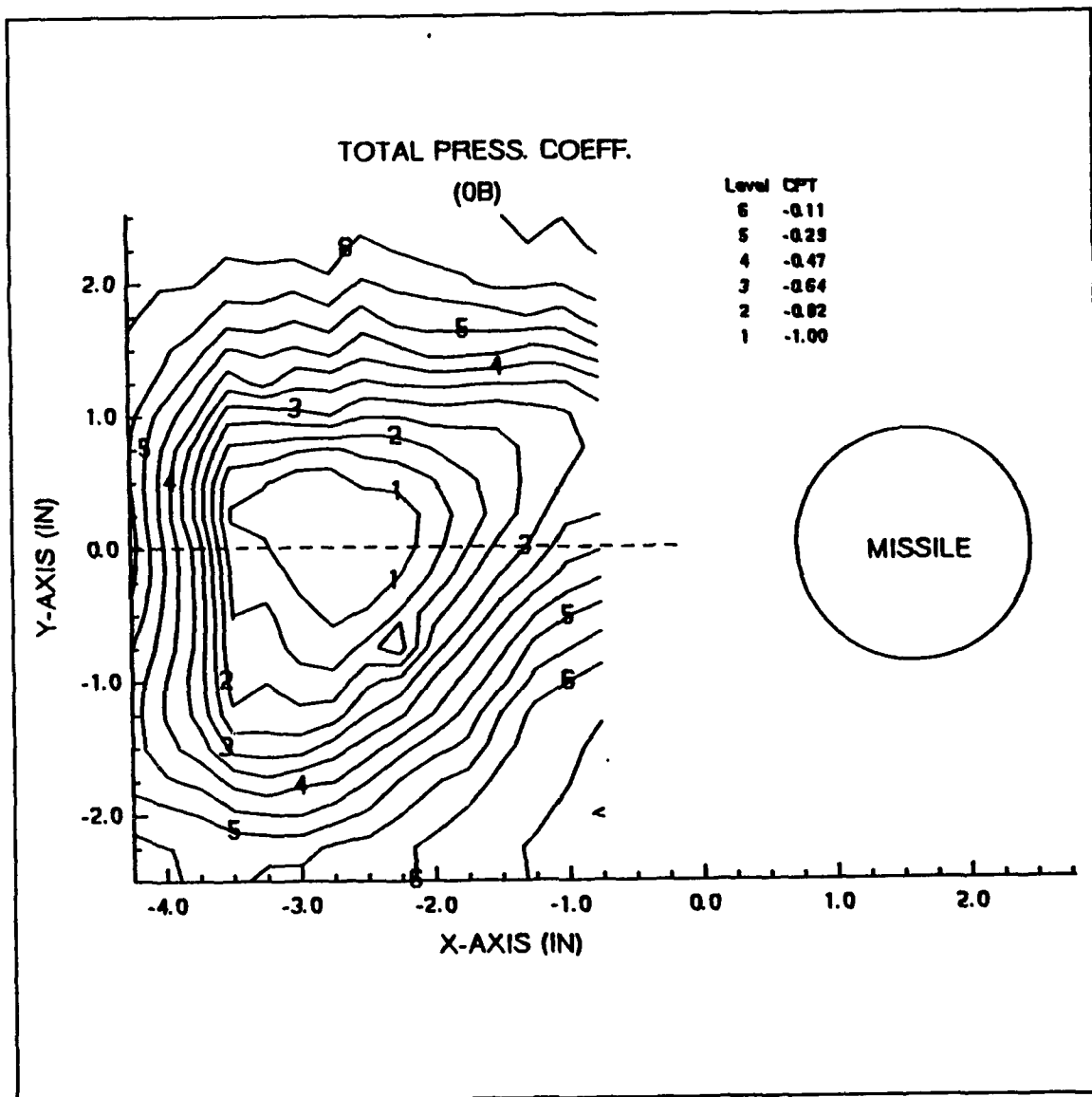


**Figure 13. Total Pressure Coefficient-Configuration 0B**

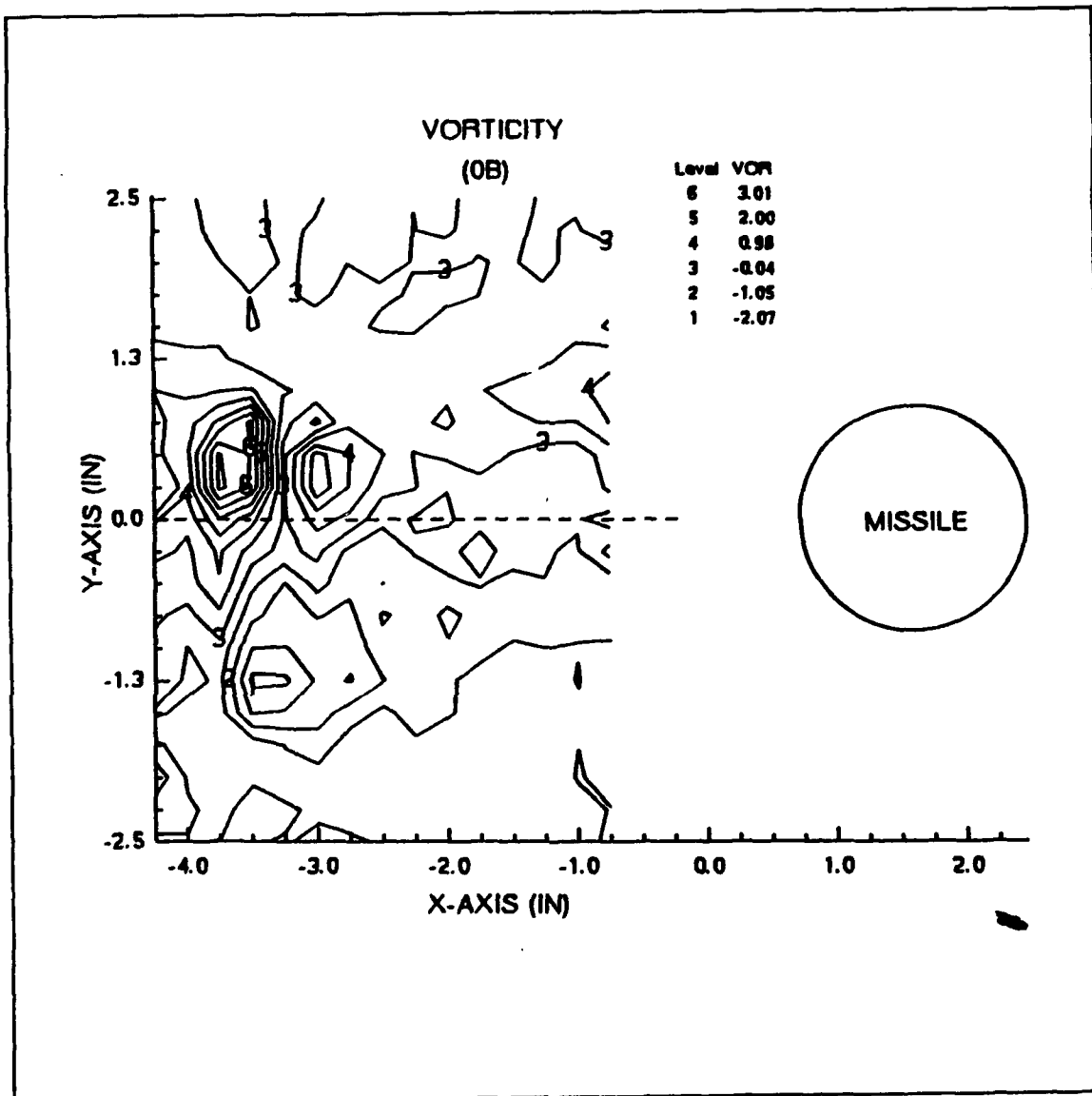


**Figure 14. Vorticity-Configuration 0B**

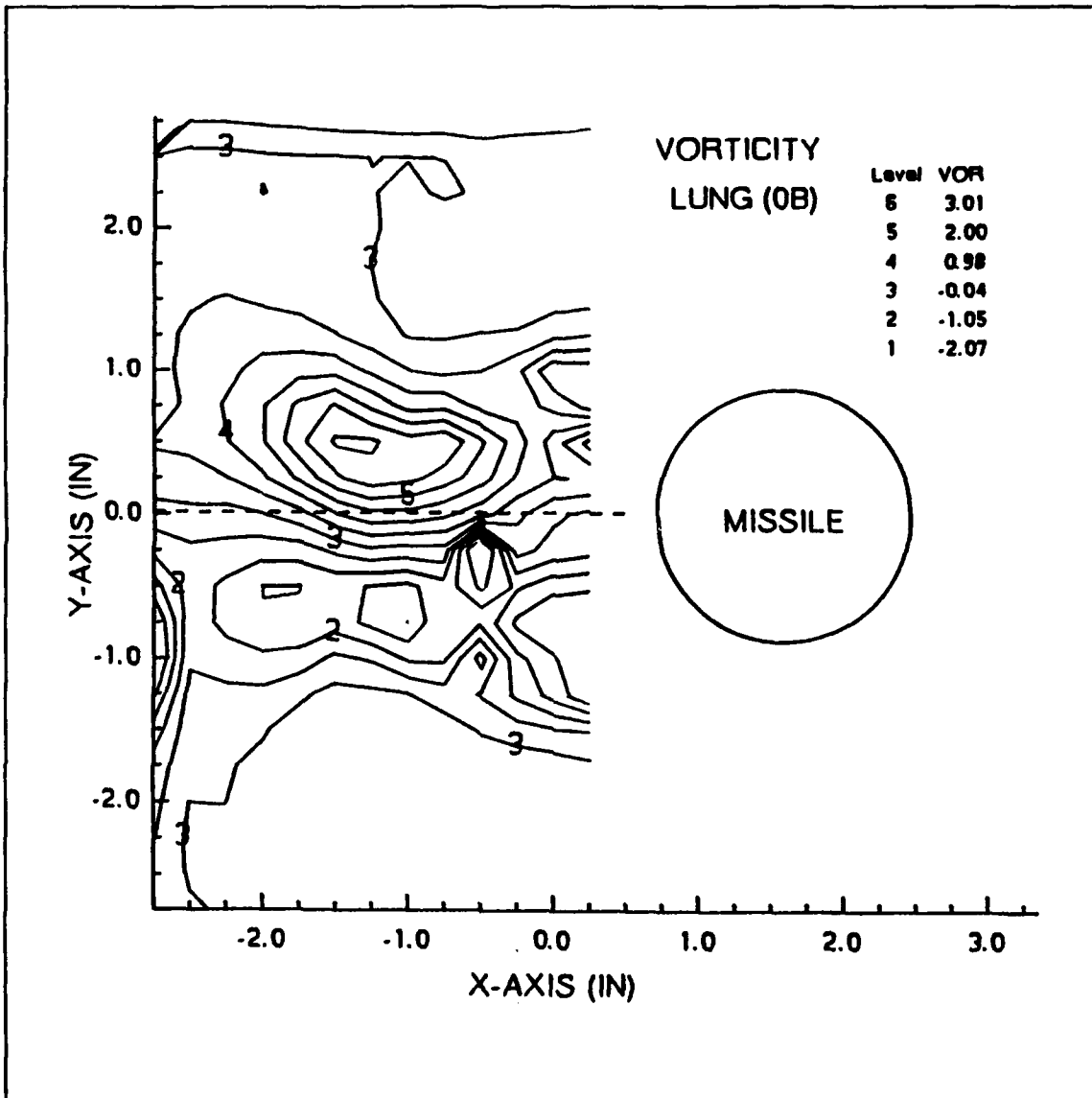


Figure 15. Vorticity-Configuration 0B (six diameters)

(1.64d) away. The lower one is  $5/8$ " below (0.36d), and  $3\ 1/4$ " (1.86d) away. The upper core has the largest magnitude and the greatest gradient. There also appear to be two centers at the inner edge of the survey grid, one above and one below the centerline.

#### B. CONFIGURATION 3B

The velocity vector plot (Figure 16) indicates the location of three vortices and a saddle point, similar to the 0B vector plot. The upper one is located  $7/8$ " (0.50d) above and  $2\ 1/8$ " (1.21d) away. The larger lower one is located  $1\ 1/2$ " (0.86d) below and  $6\ 3/8$ " (3.64d) away. The smaller lower one is located  $5/8$ " (0.39d) below and  $3\ 1/8$ " (1.79d) away. The saddle point is located  $5/8$ " (0.36d) below and  $3\ 1/8$ " (1.79d) away. The two larger vortices are asymmetric with opposite flow direction.

The total pressure coefficient plot (Figure 17) shows one large center of loss located  $5/16$ " (0.18d) above and  $4\ 5/8$ " (2.64d) away. The center does not coincide with any core from the velocity vector plot. The contours change from  $C_{pt}$  level six to level two (-0.28 to -0.86) in  $3/4$ " (0.43d) in the upper half and in  $1\ 1/4$ " (0.71d) in the lower half. This larger gradient change indicates a greater vortex strength in the upper half.

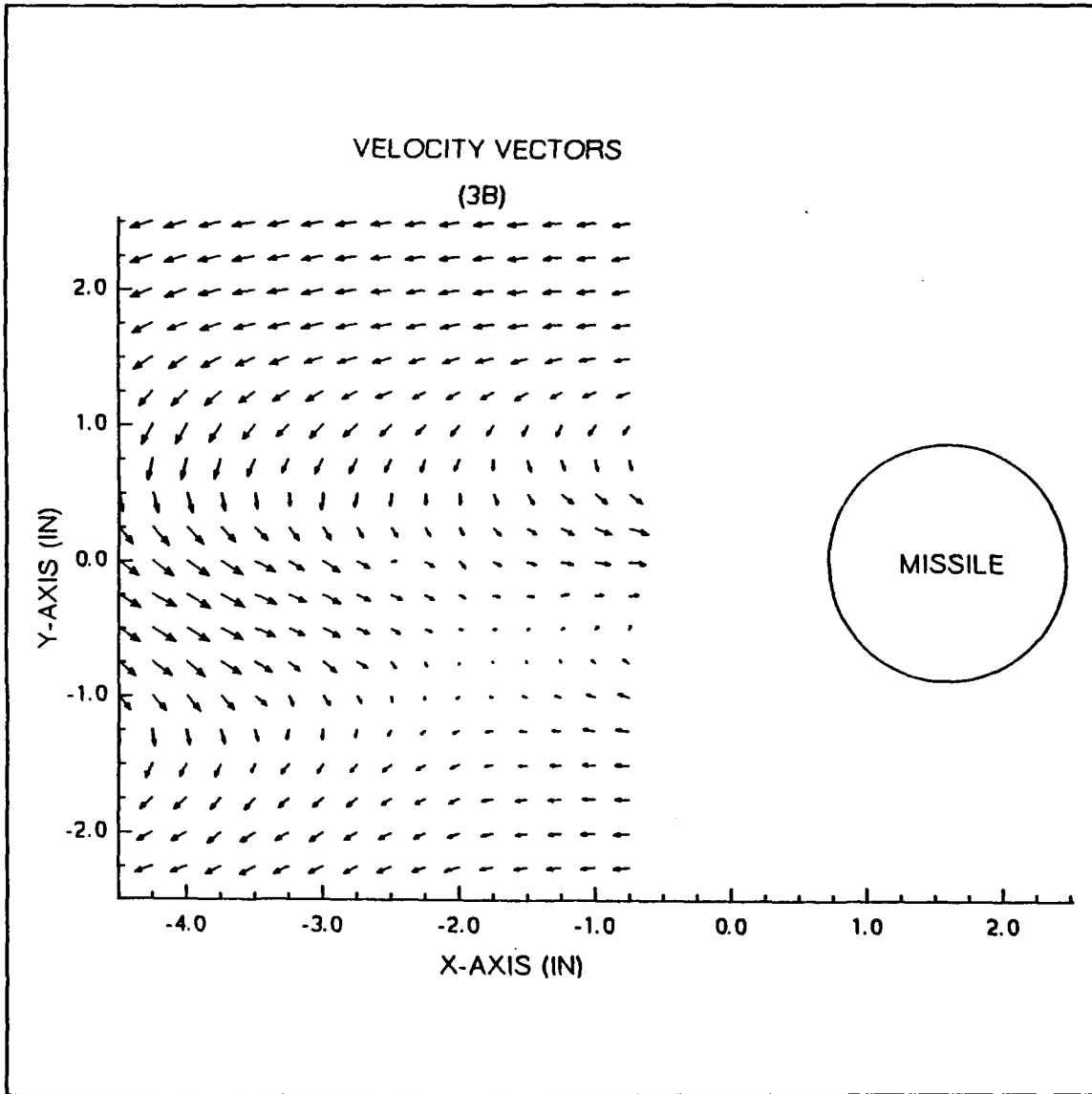


**Figure 16. Velocity Vectors-Configuration 3B**

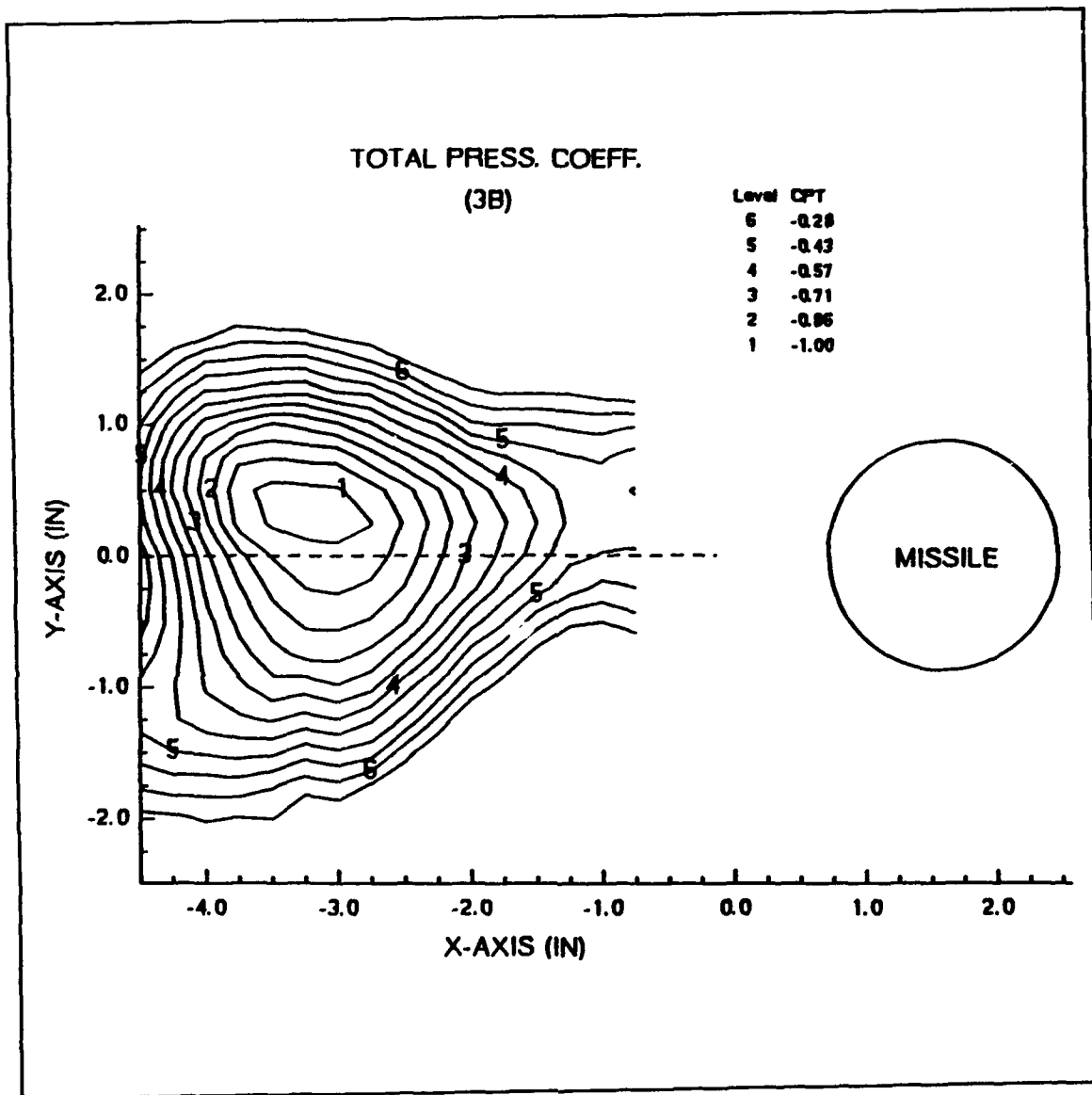


Figure 17. Total Pressure Coefficient-Configuration 3B

The vorticity plot (Figure 18) shows two centers. The upper one is  $1/2$ " (0.29d) above and  $5\ 1/2$ " (3.14d) away. The lower core is  $1\ 1/8$ " (0.64d) and  $5\ 1/4$ " (3.00d) away. The zero value is roughly along the missile centerline. The upper core has positive vorticity. The lower one has negative vorticity and is smaller in magnitude than the upper core.

The vorticity plot from Lung (Figure 19) represents turbulence added by use of grid #1. The plot shows one center  $1/2$ " (0.29d) above and 3" (1.71d) away. A second center is indicated in the lower half. The upper core has a much higher magnitude and gradient than the lower one.

#### **C. COMPARISON BETWEEN NO TURBULENCE AND TURBULENCE**

The addition of turbulence on the scale of the vortices did not affect the overall shapes of the plots. The effect on the velocity vector plot was to decrease the magnitudes, but the directions and core positions were approximately the same. The addition of turbulence did not change the magnitudes of the total pressure coefficient contours, but the gradient was much tighter and the center of the core moved up  $5/16$ " (0.18d). The vorticity strength was less and the gradients were greatly reduced with turbulence. The vorticity plots from Lung showed similar changes between the no turbulence and turbulence conditions at six diameters.

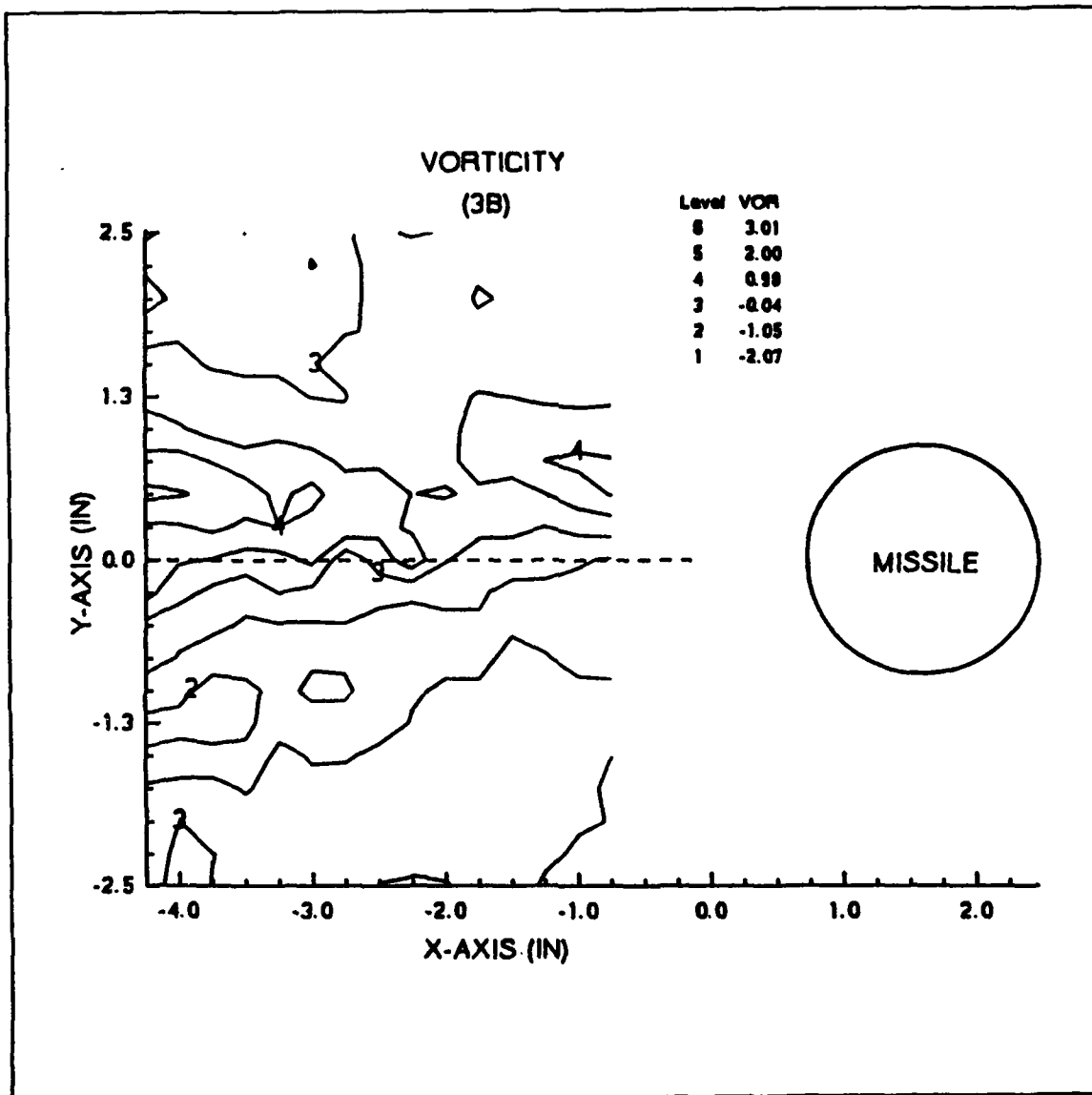


**Figure 18. Vorticity-Configuration 3B**

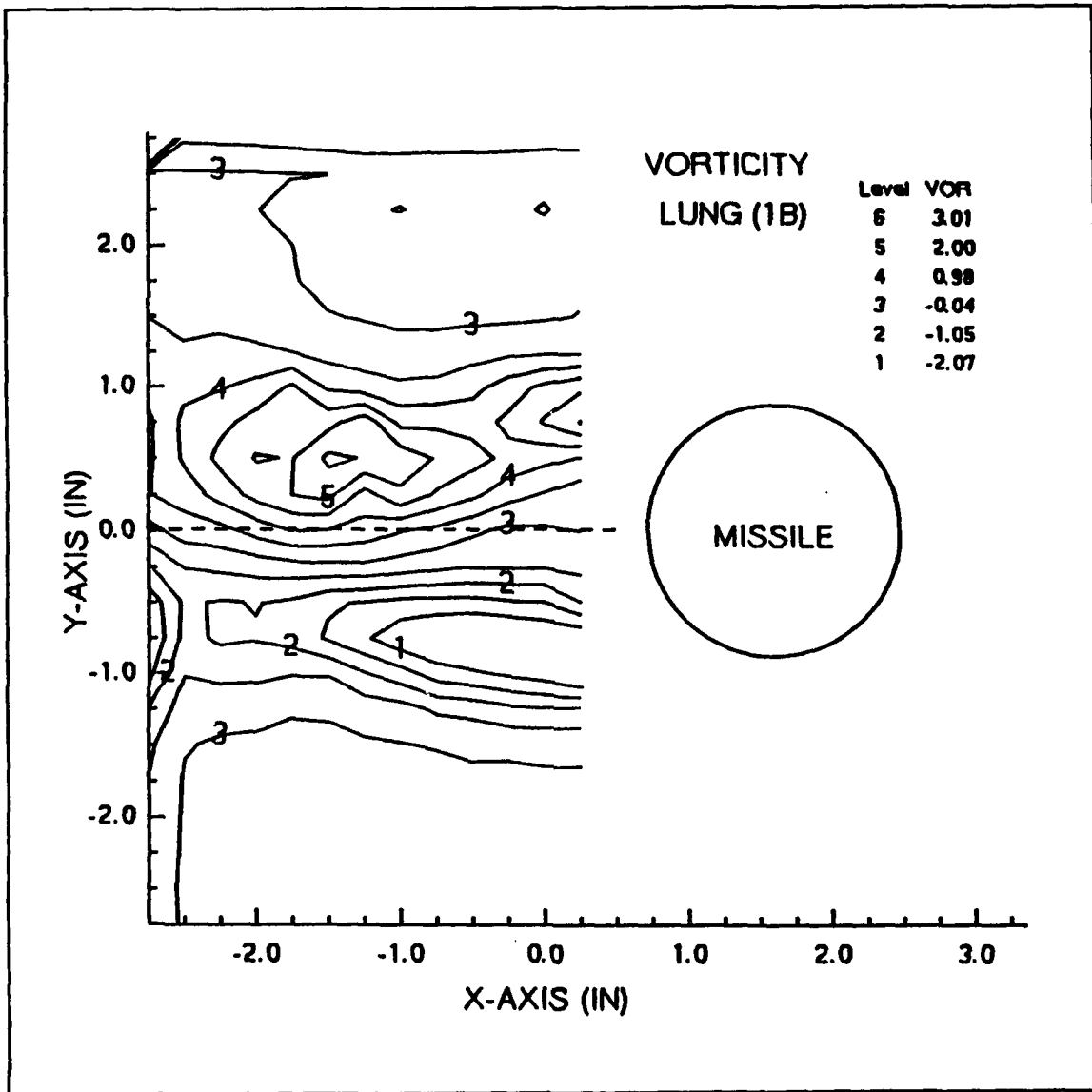


Figure 19. Vorticity-Configuration 0B (six diameters)

These results indicate that the added turbulence smoothes and steadies the flow, and results in a decrease in vorticity. This decrease in vorticity for added turbulence corresponds to Rabang's findings that the side force decreases with added turbulence for the body-only configuration [Ref. 2].

#### **D. COMPARISON BETWEEN BODY-ONLY CONFIGURATIONS**

Comparison of the vorticity plots for the body-only configuration at six diameters and eleven diameters for the no turbulence condition shows a higher vorticity strength at eleven diameters, but the gradients are approximately equal. The velocity vector plots (Figures 12,20) show that the positions of the vortex cores are farther away from the missile body at eleven diameters although the relative positioning is about the same. The total pressure coefficient plots (Figures 13,21) show two tight cores and a larger gradient at six diameters compared to one large core at eleven diameters. The second core is expected to be outside the survey grid.

For the turbulence condition, however, the vortex strength is much higher and the gradient is larger at six diameters. The velocity vector and total pressure coefficient plots show the same relative characteristics as the no turbulence condition.

These results indicate that the added turbulence reduces the vorticity at both six diameters and eleven diameters, but

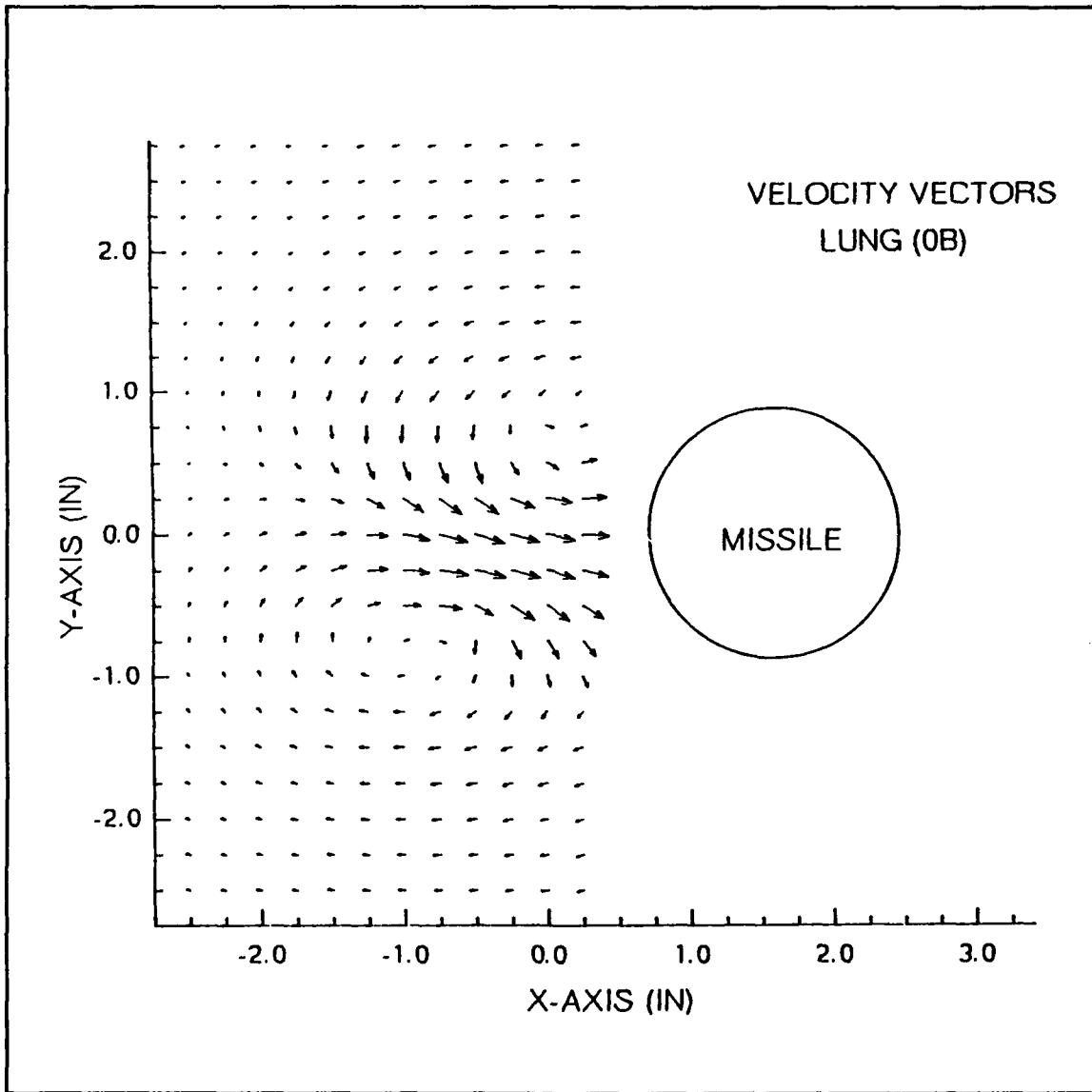
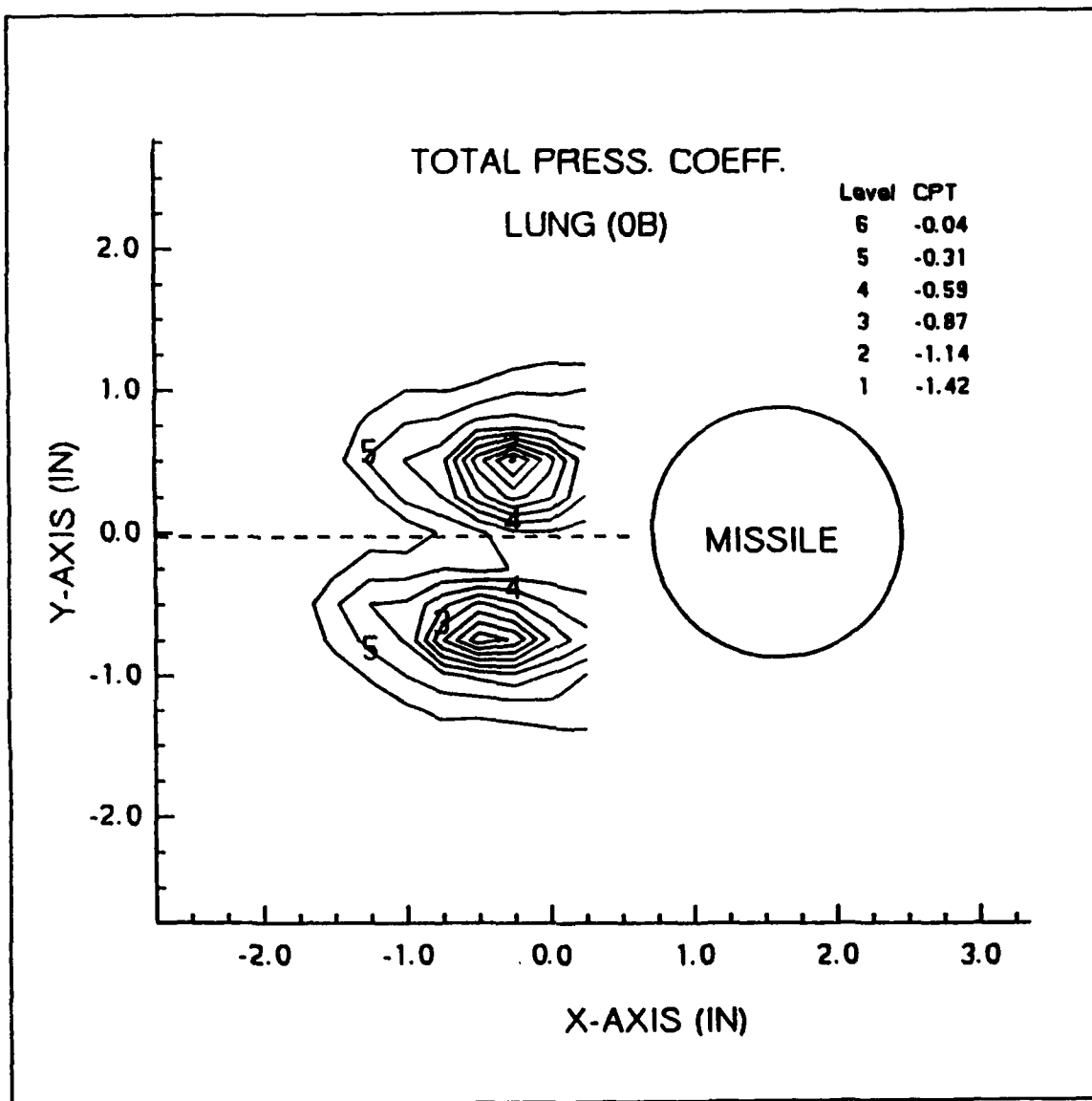


Figure 20. Velocity Vectors-Configuration 0B (six diameters)



**Figure 21. Total Pressure Coefficient-Configuration 0B (six diameters)**

the magnitude of the vorticity reduction is greater at eleven diameters.

#### **E. COMPARISON BETWEEN BODY-ONLY AND WINGED CONFIGURATIONS**

Comparison of the body-only ("0B" and "3B") configuration to the "x" ("0C" and "3C") and "+" ("0A" and "3A") configurations [Ref. 7] at eleven diameters shows the body-only configuration to have a strong resemblance to the "x" configuration and little resemblance to the "+" configuration for both the no turbulence and turbulence conditions. Comparisons of the velocity vector plots between "0C" and "3C" (Figures 22,23) and "0B" and "3B" (Figures 12,16) show the same positioning and flow directions of the vorticity cores and the saddle points. Comparison of the total pressure coefficient plots (Figures 13,17,24,25) show comparable coefficient magnitudes, but the body-only configurations have a much larger gradient. Comparison of the vorticity plots with the "x" configuration shows a higher vorticity for the body-only configuration with no turbulence (Figures 14,26) and comparable vorticity magnitudes for the turbulence condition (Figures 18,27). Comparisons with the "+" configurations (Figures 28,29) show that the body-only configuration magnitude is greater with no turbulence but is less for the turbulence condition.

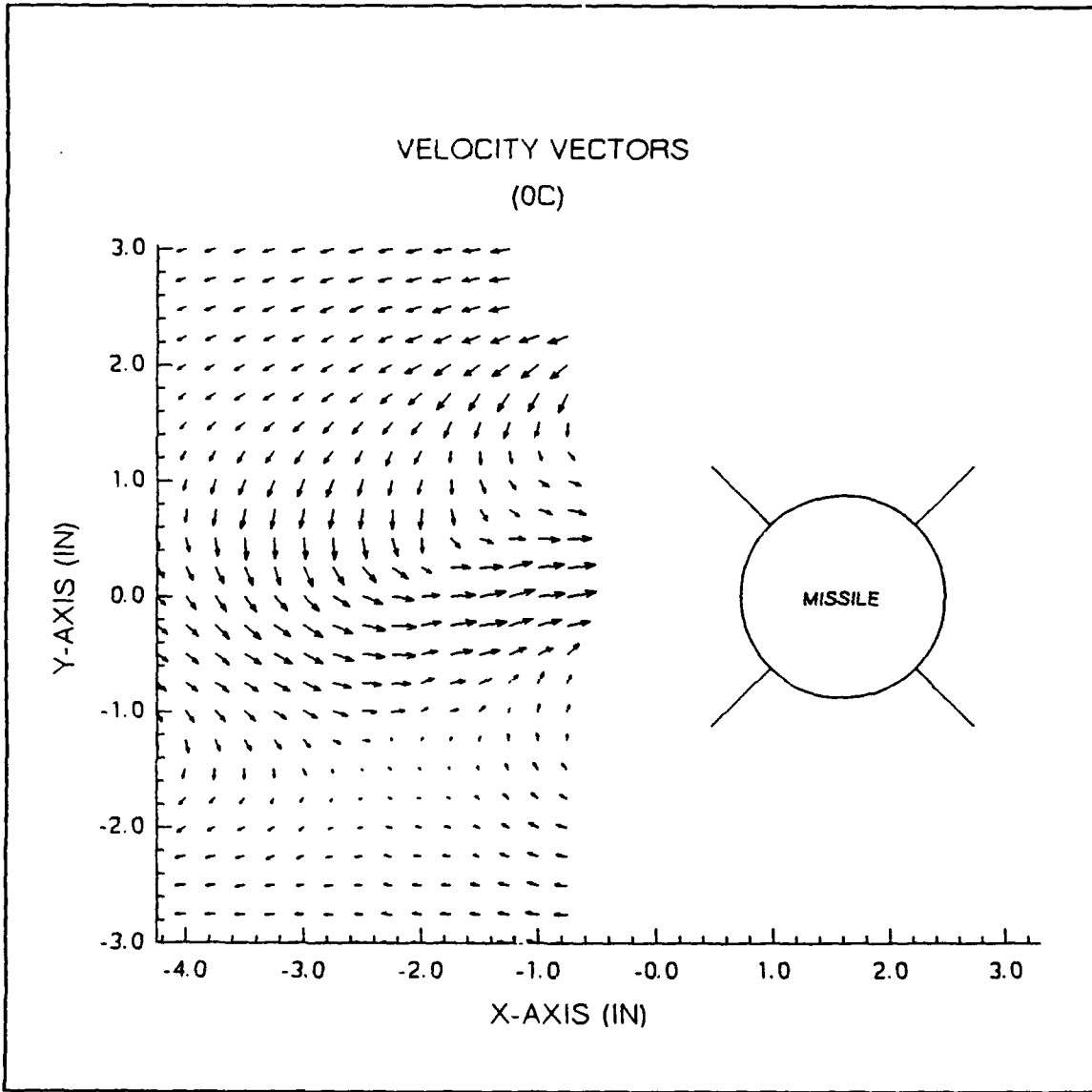


**Figure 22. Velocity Vectors-Configuration 0C**

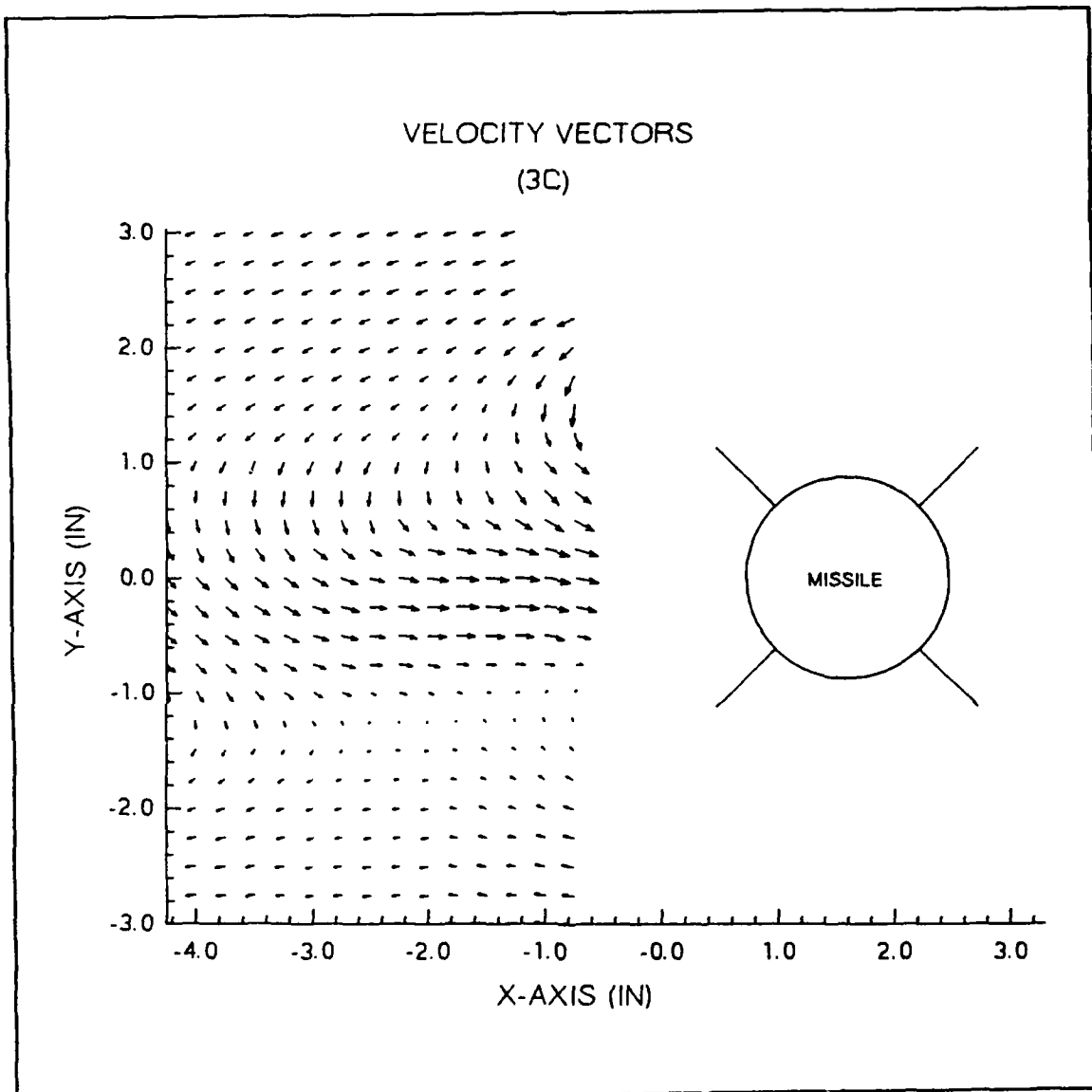


**Figure 23. Velocity Vectors-Configuration 3C**

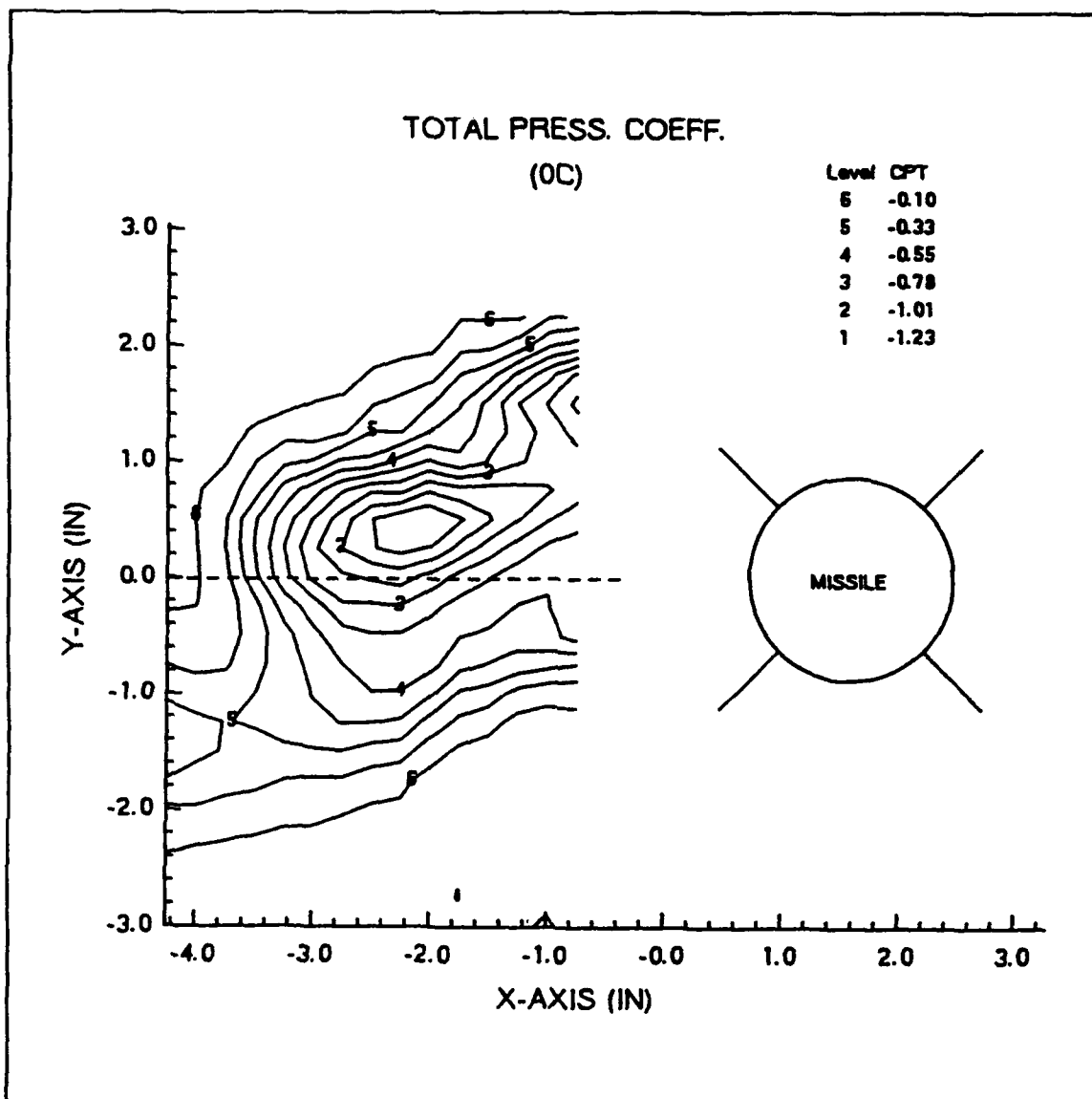


Figure 24. Total Pressure Coefficient-Configuration 0C

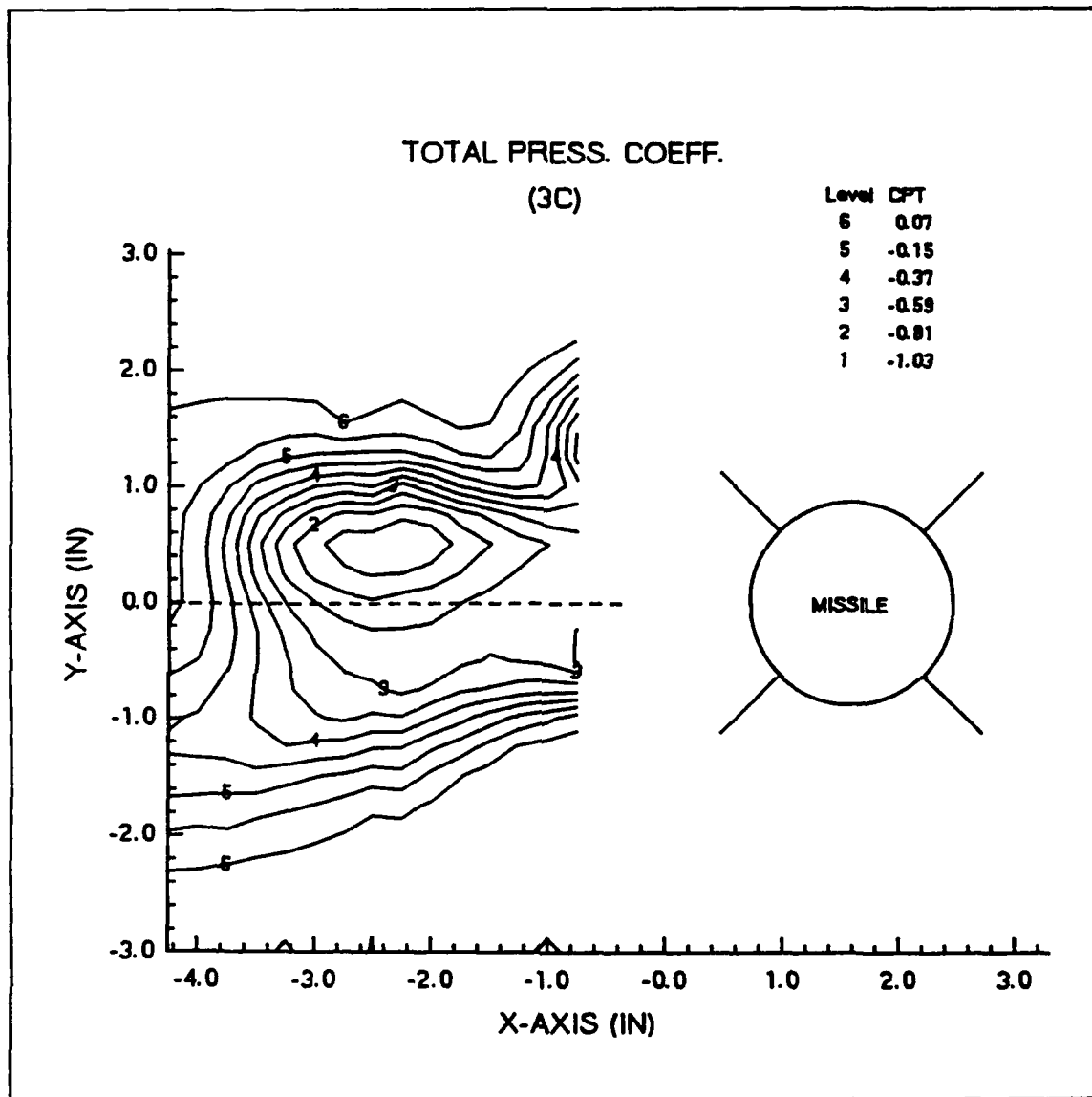
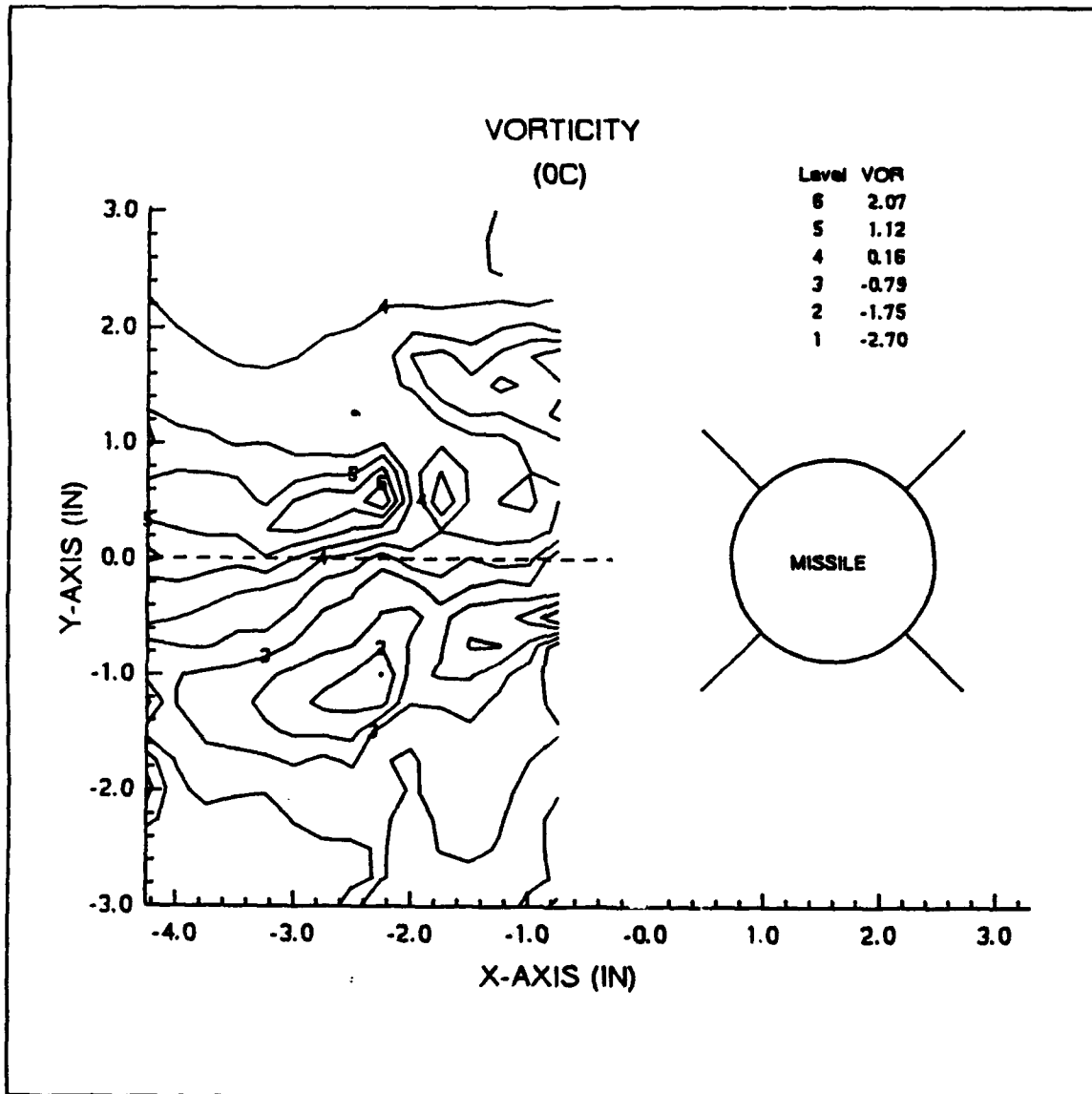
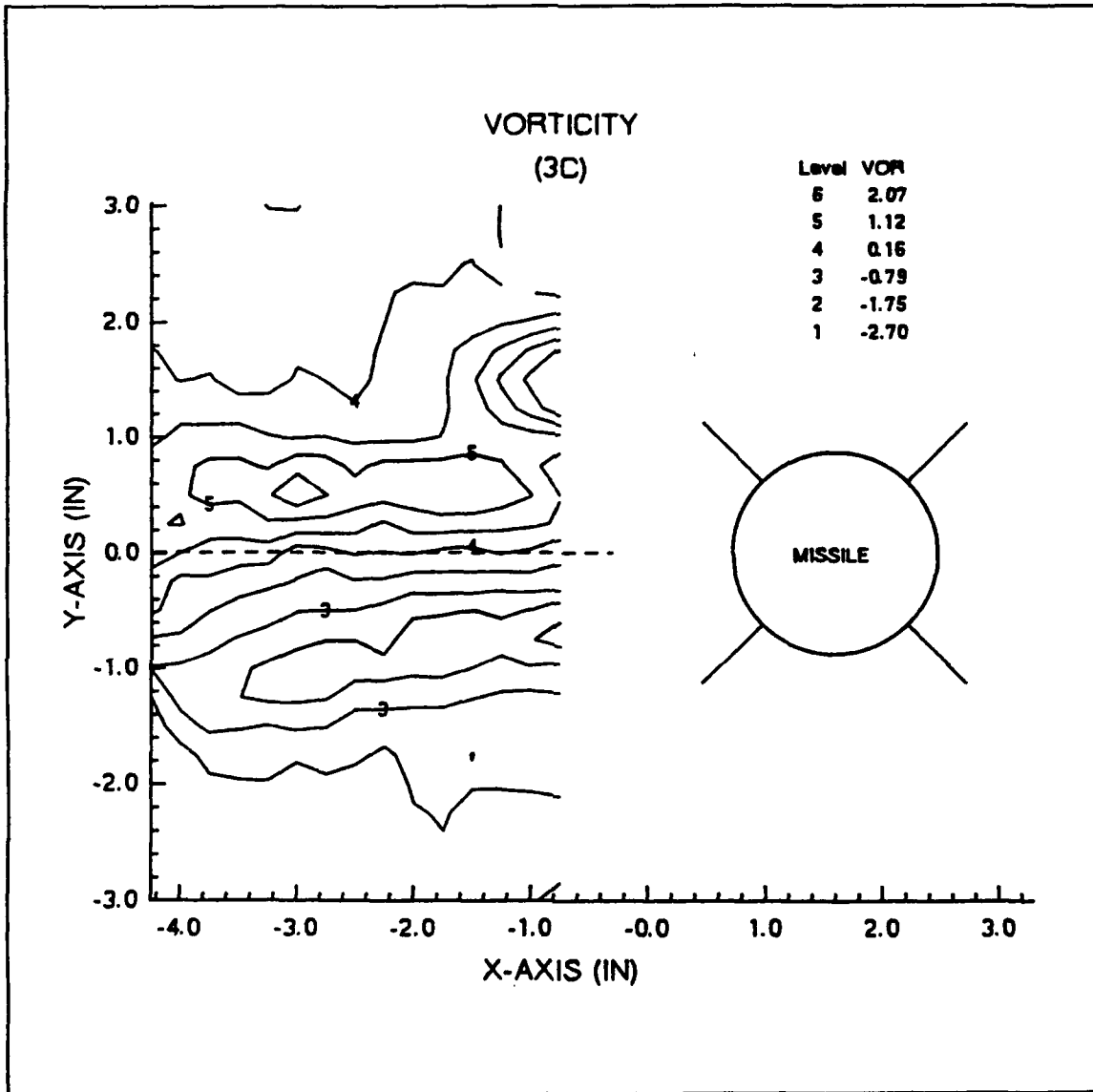


Figure 25. Total Pressure Coefficient-Configuration 3C



**Figure 26. Vorticity-Configuration OC**



**Figure 27. Vorticity-Configuration 3C**

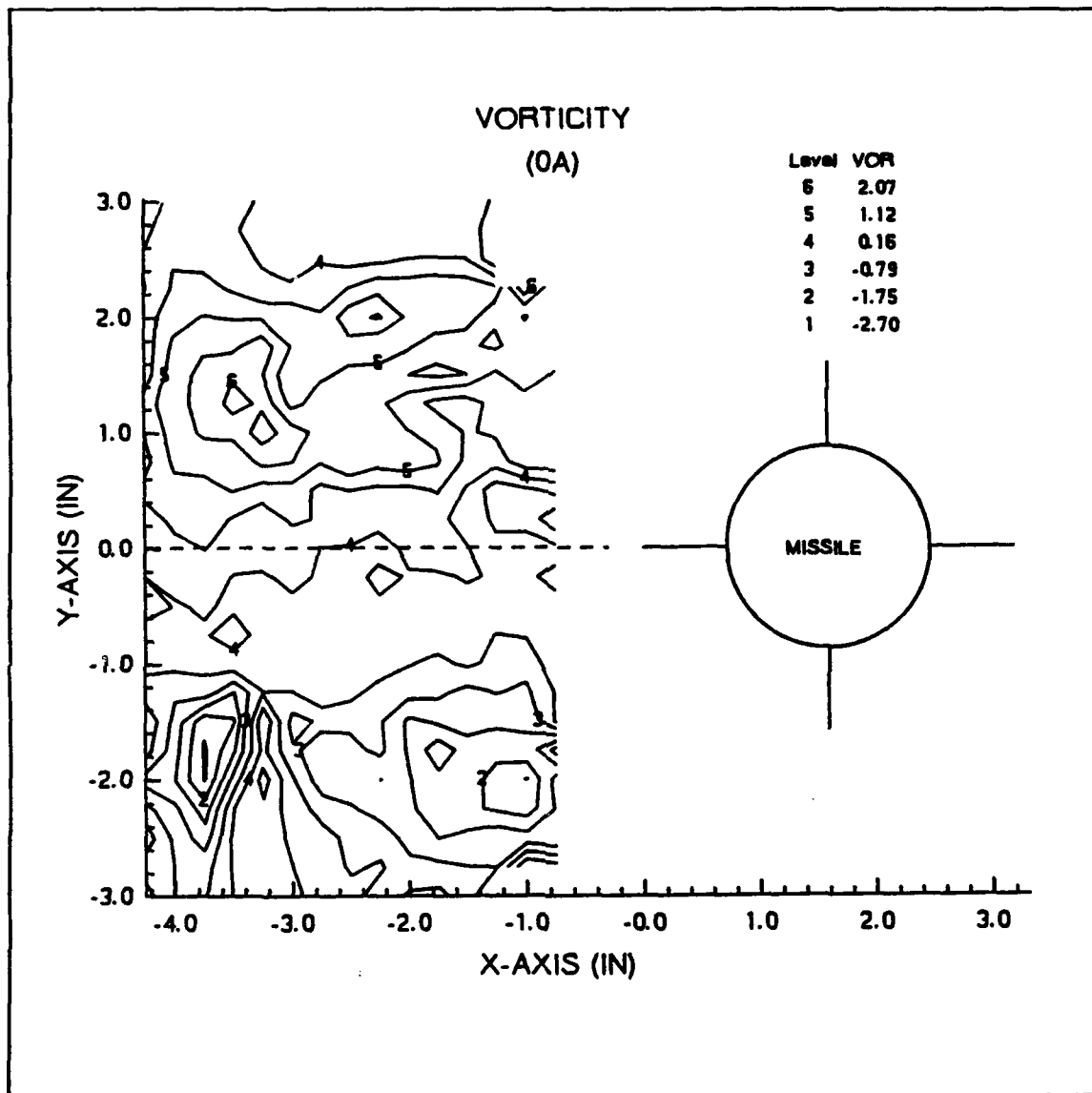


**Figure 28. Vorticity-Configuration 0A**

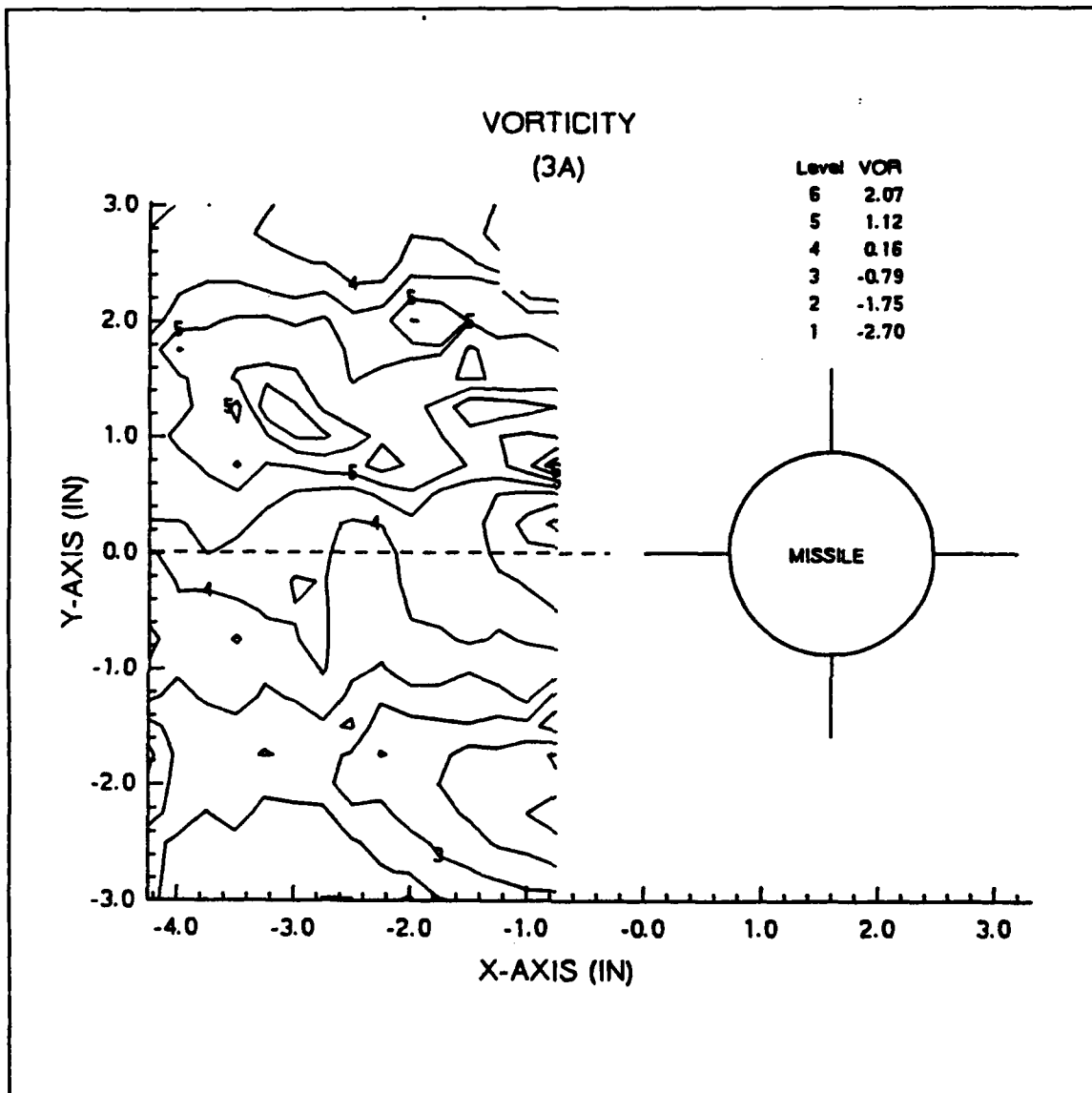


**Figure 29. Vorticity-Configuration 3A**

These results indicate that the addition of wings, strakes, and tails in the "x" configuration tends to reduce the magnitude of the vorticity with no turbulence. Again, as in the body-only configuration, the addition of turbulence of the nose-generated vortex scale appears to steady the flow and results in a decrease in vorticity for the "x" configuration. For the "+" configuration the turbulence has less of an effect on the vorticity magnitude, indicating a dependence on roll angle also. In addition, the amount of decrease in vorticity is larger for the body-only configuration.

#### **F. COMPARISON WITH FLOW VISUALIZATION**

Comparison of the body-only configuration velocity vector plots at six and eleven body diameters with flow visualization photographs (Figures 30,31) show that the velocity vector plot cores correspond to the asymmetric vortices formed on the lee side of the missile. Figure 32 is a sketch illustrating the vortex core movement away from the missile as the distance from the missile nose is increased from six to eleven body diameters.

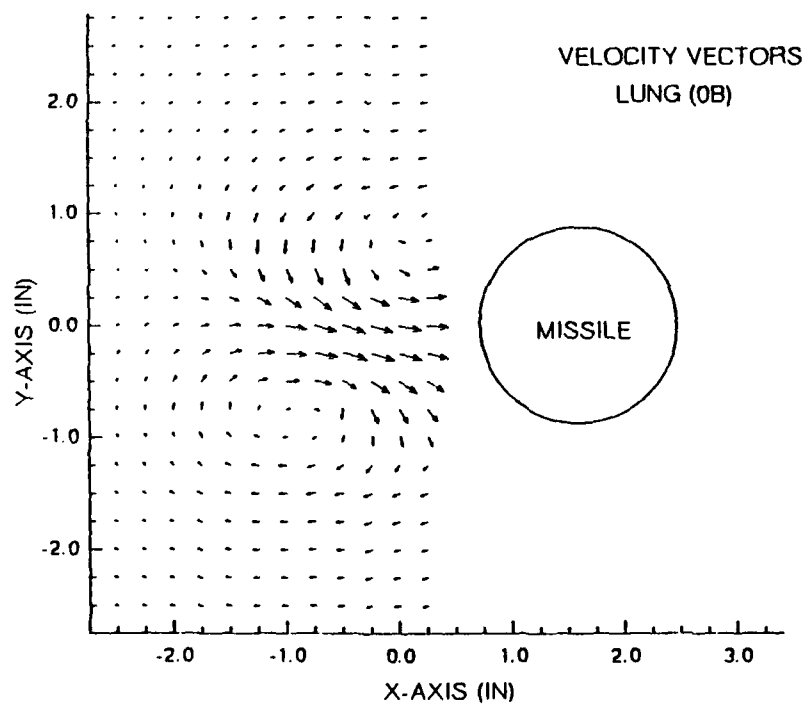


**Figure 30. Flow Visualization (six diameters)**

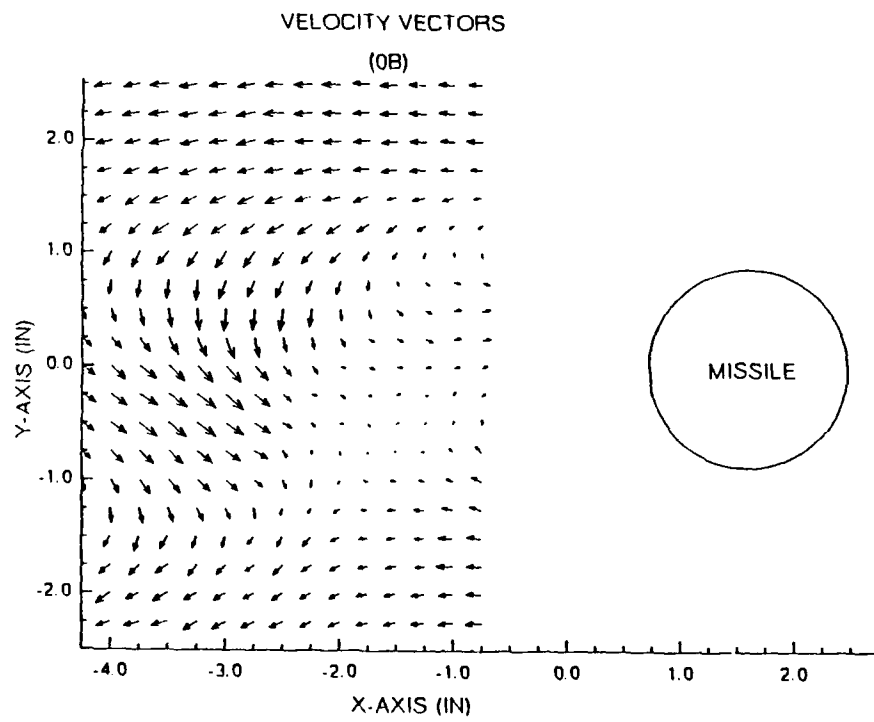
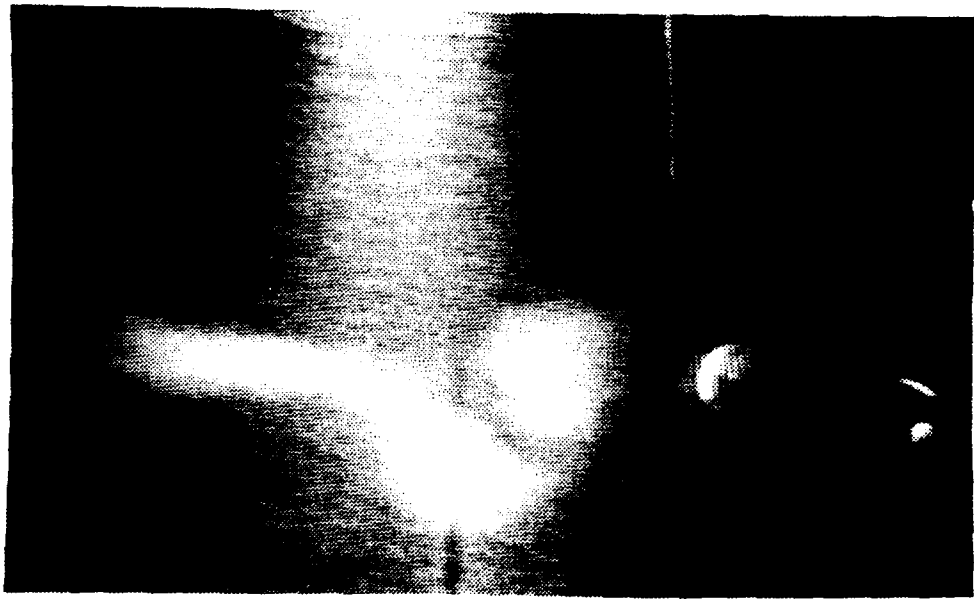


Figure 31. Flow Visualization (eleven diameters)

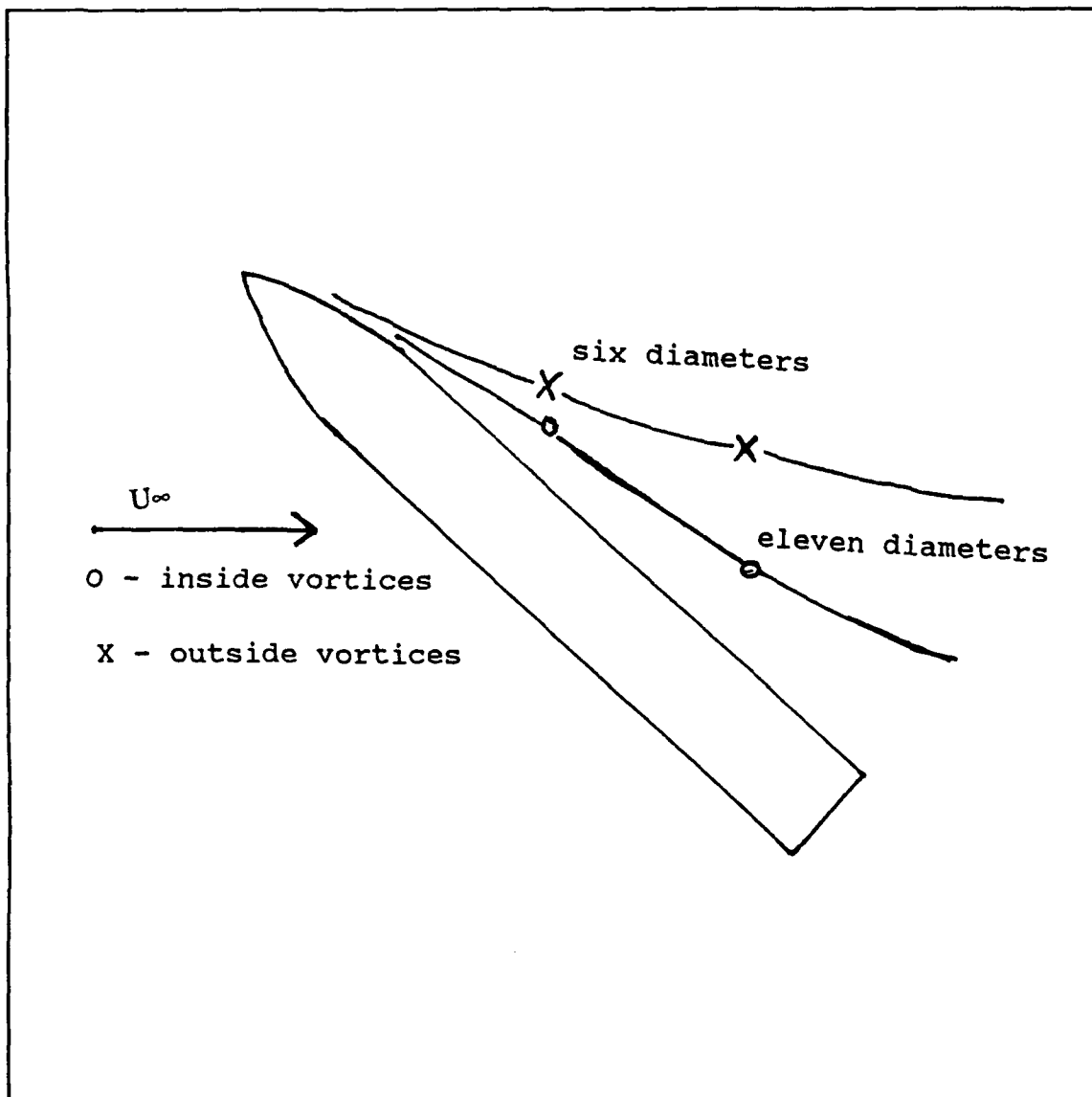


Figure 32. Sketch of Vortex Core Positions

#### IV. CONCLUSIONS AND RECOMMENDATIONS

The flowfield about a vertically-launched surface-to-air missile (VLSAM) model at high angle of attack was studied. The body-only configuration at eleven body diameters was tested and compared to the body-only configuration at six body diameters and with the winged configurations at eleven body diameters. The angle of attack was set at 50 degrees with a Reynolds number of  $1.1 \times 10^5$  for all data runs. All tests were conducted with both an ambient wind tunnel condition (no grid) and a condition with grid-generated turbulence on the scale of the nose-generated asymmetric vortices. The following conclusions were reached:

(1) Addition of turbulence for the body-only configuration tended to smooth and steady the flow. The turbulence reduced the vorticity level, but did not significantly change the positions of the vortices.

(2) The addition of turbulence had a greater effect on vorticity reduction at eleven body diameters than at six body diameters for the body-only configuration, based on the vorticity plots (Figures 14,15,18,19).

(3) The body-only plots at eleven body diameters are very similar to the "x" configuration at the same point, but different from the "+" configuration. Without turbulence, the vorticity levels for the body-only case are much larger than

for the "x" and the "+" configurations. With turbulence, however, the comparisons show that the vorticity levels were not only reduced but were approximately equal between the body-only and "x" configurations. However, compared to the "+" configuration, the vorticity levels were lower. Apparently the effect of added turbulence on vorticity is much greater for the body-only configuration than the winged configurations. The winged cases are also complicated by a dependence on roll angle. Rabang noted the same results on the side force magnitudes.

(4) The addition of wings had a significant effect on the reduction of the vorticity level without added turbulence. With turbulence, the addition of wings had a negligible effect on the vorticity level. Again, Rabang noted the same results on the side force magnitude. Apparently, the effects of added turbulence outweighs the effects of adding wings.

(5) The flow visualization experiment verified that the asymmetric vortices move away from the missile as distance is increased from the missile nose along the body axis, in a vary non-linear manner. The velocity vector plots tended to match the flow visualization results for the location of the vortex cores.

Recommendations for future research are:

(1) Conduct pressure measurements outside the present survey grid to determine characteristics of secondary vortices that may not have been located near the missile or farther away from the missile.

(2) Attempt to decrease the vortex asymmetry by modifying the present missile nose geometry.

## APPENDIX A. PPROBE PROGRAM

```

1 DEF SEG: CLEAR , &HFEE0: GOTO 4 'Begin PCIB Program Shell
2 GOTO 1000 ' User program
3 GOTO 900 ' Error handling
4 I=&HFEE0 ' Copyright Hewlett-Packard 1984,1985
5 PCIB.DIR$=ENVIRON$("PCIB")
6 I$=PCIB.DIR$+"\PCIBILC.BLD"
7 BLOAD I$,I
8 CALL I(PCIB.DIR$,I%,J%): PCIB.SEG=I%
9 IF J%=0 THEN GOTO 13
10 PRINT "Unable to load.";
11 PRINT " (Error #";J%;")"
12 END
13 '
14 DEF SEG=PCIB.SEG: O.S=5: C.S=10: I.V=15
15 I.C=20: L.P=25: LD.FILE=30
16 GET.MEM=35: L.S=40: PANELS=45: DEF.ERR=50
17 PCIB.ERR$=STRING$(64,32) : PCIB.NAME$=STRING$(16,32)
18 CALL DEF.ERR(PCIB.ERR,PCIB.ERR$,PCIB.NAME$,PCIB.GLBERR) :
PCIB.BASERR=255
19 ON ERROR GOTO 3
20 J=-1
21 I$=PCIB.DIR$+"\PCIB.SYN"
22 CALL O.S(I$)
23 IF PCIB.ERR<>0 THEN ERROR PCIB.BASERR
24 I=0
2         5             C             A             L             L
I.V(I, READ.REGISTER, READ.SELFID, DEFINE, INITIALIZE.SYSTEM)
26 IF PCIB.ERR<>0 THEN ERROR PCIB.BASERR
2         7             C             A             L             L
I.V(I, ENABLE.SYSTEM, DISABLE.SYSTEM, INITIALIZE, POWER.ON)
28 IF PCIB.ERR<>0 THEN ERROR PCIB.BASERR
29 CALL I.V(I, MEASURE, OUTPUT, START, HALT)
30 IF PCIB.ERR<>0 THEN ERROR PCIB.BASERR
3         1             C             A             L             L
I.V(I, ENABLE.INT.TRIGGER, DISABLE.INT.TRIGGER, ENABLE.OUTPUT, D
ISABLE.OUTPUT)
32 IF PCIB.ERR<>0 THEN ERROR PCIB.BASERR
33 CALL I.V(I, CHECK.DONE, GET.STATUS, SET.FUNCTION, SET.RANGE)
34 IF PCIB.ERR<>0 THEN ERROR PCIB.BASERR
35 CALL I.V(I, SET.MODE, WRITE.CAL, READ.CAL, STORE.CAL)
36 IF PCIB.ERR<>0 THEN ERROR PCIB.BASERR
37 CALL I.V(I, DELAY, SAVE.SYSTEM, J, J)
38 IF PCIB.ERR<>0 THEN ERROR PCIB.BASERR
39 I=1
40 CALL I.V(I, SET.GATETIME, SET.SAMPLES, SET.SLOPE, SET.SOURCE)

```

```

41 IF PCIB.ERR<>0 THEN ERROR PCIB.BASERR
42 CALL I.C(I,FREQUENCY,AUTO.FREQ,PERIOD,AUTO.PER)
43 IF PCIB.ERR<>0 THEN ERROR PCIB.BASERR
44 CALL I.C(I,INTERVAL,RATIO,TOTALIZE,R100MILLI)
45 IF PCIB.ERR<>0 THEN ERROR PCIB.BASERR
46 CALL I.C(I,R1,R10,R100,R1KILO)
47 IF PCIB.ERR<>0 THEN ERROR PCIB.BASERR
48 CALL I.C(I,R1OMEGA,R100OMEGA,CHAN.A,CHAN.B)
49 IF PCIB.ERR<>0 THEN ERROR PCIB.BASERR
50 CALL I.C(I,POSITIVE,NEGATIVE,COMN,SEPARATE)
51 IF PCIB.ERR<>0 THEN ERROR PCIB.BASERR
52 I=2
53 I=3
54 CALL I.V(I,ZERO.OHMS,SET.SPEED,J,J)
55 IF PCIB.ERR<>0 THEN ERROR PCIB.BASERR
56 CALL I.C(I,DCVOLTS,ACVOLTS,OHMS,R200MILLI)
57 IF PCIB.ERR<>0 THEN ERROR PCIB.BASERR
58 CALL I.C(I,R2,R20,R200,R2KILO)
59 IF PCIB.ERR<>0 THEN ERROR PCIB.BASERR
60 CALL I.C(I,R20KILO,R200KILO,R2MEGA,R2OMEGA)
61 IF PCIB.ERR<>0 THEN ERROR PCIB.BASERR
62 CALL I.C(I,AUTOM,R2.5,R12.5,J)
63 IF PCIB.ERR<>0 THEN ERROR PCIB.BASERR
64 I=4
6         5             C             A             L             L
I.V(I,SET.COMPLEMENT,SET.DRIVER,OUTPUT.NO.WAIT,ENABLE.HANDSH
AKE)
66 IF PCIB.ERR<>0 THEN ERROR PCIB.BASERR
6         7             C             A             L             L
I.V(I,DISABLE.HANDSHAKE,SET.THRESHOLD,SET.START.BIT,SET.NUM.
BITS)
68 IF PCIB.ERR<>0 THEN ERROR PCIB.BASERR
69 CALL I.V(I,SET.LOGIC.SENSE,J,J,J)
70 IF PCIB.ERR<>0 THEN ERROR PCIB.BASERR
71 CALL I.C(I,POSITIVE,NEGATIVE,TWOS,UNSIGNED)
72 IF PCIB.ERR<>0 THEN ERROR PCIB.BASERR
73 CALL I.C(I,OC,TTL,R0,R1)
74 IF PCIB.ERR<>0 THEN ERROR PCIB.BASERR
75 CALL I.C(I,R2,R3,R4,R5)
76 IF PCIB.ERR<>0 THEN ERROR PCIB.BASERR
77 CALL I.C(I,R6,R7,R8,R9)
78 IF PCIB.ERR<>0 THEN ERROR PCIB.BASERR
79 CALL I.C(I,R10,R11,R12,R13)
80 IF PCIB.ERR<>0 THEN ERROR PCIB.BASERR
81 CALL I.C(I,R14,R15,R16,J)
82 IF PCIB.ERR<>0 THEN ERROR PCIB.BASERR
83 I=6
8         4             C             A             L             L
I.V(I,SET.FREQUENCY,SET.AMPLITUDE,SET.OFFSET,SET.SYMMETRY)
85 IF PCIB.ERR<>0 THEN ERROR PCIB.BASERR
86 CALL I.V(I,SET.BURST.COUNT,J,J,J)

```

```

87 IF PCIB.ERR<>0 THEN ERROR PCIB.BASERR
88 CALL I.C(I,SINE,SQUARE,TRIANGLE,CONTINUOUS)
89 IF PCIB.ERR<>0 THEN ERROR PCIB.BASERR
90 CALL I.C(I,GATED,BURST,J,J)
91 IF PCIB.ERR<>0 THEN ERROR PCIB.BASERR
92 I=7
9       3           C           A           L           L
I.V(I,AUTOSCALE,CALIBRATE,SET.SENSITIVITY,SET.VERT.OFFSET)
94 IF PCIB.ERR<>0 THEN ERROR PCIB.BASERR
9       5           C           A           L           L
I.V(I,SET.COUPLING,SET.POLARITY,SET.SWEEPSPEED,SET.DELAY)
96 IF PCIB.ERR<>0 THEN ERROR PCIB.BASERR
9       7           C           A           L           L
I.V(I,SET.TRIG.SOURCE,SET.TRIG.SLOPE,SET.TRIG.LEVEL,SET.TRIG
.MODE)
98 IF PCIB.ERR<>0 THEN ERROR PCIB.BASERR
9       9           C           A           L           L
I.V(I,GET.SINGLE.WF,GET.TWO.WF,GET.VERT.INFO,GET.TIMEBASE.INFO)
100 IF PCIB.ERR<>0 THEN ERROR PCIB.BASERR
1       0           1           C           A           L           L
I.V(I,GET.TRIG.INFO,CALC.WFVOLT,CALC.WFTIME,CALC.WF.STATS)
102 IF PCIB.ERR<>0 THEN ERROR PCIB.BASERR
1       0           3           C           A           L           L
I.V(I,CALC.RISETIME,CALC.FALLTIME,CALC.PERIOD,CALC.FREQUENCY)
104 IF PCIB.ERR<>0 THEN ERROR PCIB.BASERR
1       0           5           C           A           L           L
I.V(I,CALC.PLUSWIDTH,CALC.MINUSWIDTH,CALC.OVERSHOOT,CALC.PRE
SHOOT)
106 IF PCIB.ERR<>0 THEN ERROR PCIB.BASERR
1       0           7           C           A           L           L
I.V(I,CALC.PK.TO.PK,SET.TIMEOUT,SCOPE.START,MEASURE.SINGLE.WF)
108 IF PCIB.ERR<>0 THEN ERROR PCIB.BASERR
109 CALL I.V(I,MEASURE.TWO.WF,J,J,J)
110 IF PCIB.ERR<>0 THEN ERROR PCIB.BASERR
111 CALL I.C(I,R10NANO,R100NANO,R1MICRO,R10MICRO)
112 IF PCIB.ERR<>0 THEN ERROR PCIB.BASERR
113 CALL I.C(I,R100MICRO,R1MILLI,R10MILLI,R100MILLI)
114 IF PCIB.ERR<>0 THEN ERROR PCIB.BASERR
115 CALL I.C(I,R1,R10,R20NANO,R200NANO)
116 IF PCIB.ERR<>0 THEN ERROR PCIB.BASERR
117 CALL I.C(I,R2MICRO,R20MICRO,R200MICRO,R2MILLI)
118 IF PCIB.ERR<>0 THEN ERROR PCIB.BASERR
119 CALL I.C(I,R20MILLI,R200MILLI,R2,R20)
120 IF PCIB.ERR<>0 THEN ERROR PCIB.BASERR
121 CALL I.C(I,R50NANO,R500NANO,R5MICRO,R50MICRO)
122 IF PCIB.ERR<>0 THEN ERROR PCIB.BASERR
123 CALL I.C(I,R500MICRO,R5MILLI,R50MILLI,R500MILLI)
124 IF PCIB.ERR<>0 THEN ERROR PCIB.BASERR
125 CALL I.C(I,R5,R50,CHAN.A,CHAN.B)
126 IF PCIB.ERR<>0 THEN ERROR PCIB.BASERR

```

```

127 CALL I.C(I,EXTERNAL,POSITIVE,NEGATIVE,AC)
128 IF PCIB.ERR<>0 THEN ERROR PCIB.BASERR
129 CALL I.C(I,DC,TRIGGERED,AUTO.TRIG,AUTO.LEVEL)
130 IF PCIB.ERR<>0 THEN ERROR PCIB.BASERR
131 CALL I.C(I,X1,X10,STANDARD,AVERAGE)
132 IF PCIB.ERR<>0 THEN ERROR PCIB.BASERR
133 I=8
134 CALL I.V(I,OPEN.CHANNEL,CLOSE.CHANNEL,J,J)
135 IF PCIB.ERR<>0 THEN ERROR PCIB.BASERR
136 CALL C.S
137 IF PCIB.ERR<>0 THEN ERROR PCIB.BASERR
138 I$=PCIB.DIR$+"\PCIB.PLD"
139 CALL L.P(I$)
140 IF PCIB.ERR<>0 THEN ERROR PCIB.BASERR
141 I$="DMM.01":I=3:J=0:K=0:L=1
142 CALL DEFINE(DMM.01,I$,I,J,K,L)
143 IF PCIB.ERR<>0 THEN ERROR PCIB.BASERR
144 I$="Func.Gen.01":I=6:J=0:K=1:L=1
145 CALL DEFINE(Func.Gen.01,I$,I,J,K,L)
146 IF PCIB.ERR<>0 THEN ERROR PCIB.BASERR
147 I$="Scope.01":I=7:J=0:K=2:L=1
148 CALL DEFINE(Scope.01,I$,I,J,K,L)
149 IF PCIB.ERR<>0 THEN ERROR PCIB.BASERR
150 I$="Counter.01":I=1:J=0:K=3:L=1
151 CALL DEFINE(Counter.01,I$,I,J,K,L)
152 IF PCIB.ERR<>0 THEN ERROR PCIB.BASERR
153 I$="Dig.In.01":I=4:J=0:K=4:L=1
154 CALL DEFINE(Dig.In.01,I$,I,J,K,L)
155 IF PCIB.ERR<>0 THEN ERROR PCIB.BASERR
156 I$="Dig.Out.01":I=4:J=1:K=4:L=1
157 CALL DEFINE(Dig.Out.01,I$,I,J,K,L)
158 IF PCIB.ERR<>0 THEN ERROR PCIB.BASERR
159 I$="Relay.Act.01":I=8:J=0:K=5:L=1
160 CALL DEFINE(Relay.Act.01,I$,I,J,K,L)
161 IF PCIB.ERR<>0 THEN ERROR PCIB.BASERR
162 I$="Relay.Mux.01":I=2:J=0:K=6:L=1
163 CALL DEFINE(Relay.Mux.01,I$,I,J,K,L)
164 IF PCIB.ERR<>0 THEN ERROR PCIB.BASERR
800 I$=ENVIRON$("PANELS")+"\PANELS.EXE"
801 CALL L.S(I$)
899 GOTO 2
900 IF ERR=PCIB.BASERR THEN GOTO 903
901 PRINT "BASIC error #";ERR;" occurred in line ";ERL
902 STOP
903 TMPERR=PCIB.ERR:IF TMPERR=0 THEN TMPERR=PCIB.GLBERR
904 PRINT "PC Instrument error #";TMPERR;" detected at line
";ERL
905 PRINT "Error: ";PCIB.ERR$
906 IF LEFT$(PCIB.NAME$,1)<>CHR$(32) THEN PRINT "Instrument:
";PCIB.NAME$
907 STOF

```

```

908 COMMON PCIB.DIR$,PCIB.SEG
909 COMMON LD.FILE,GET.MEM,PANELS,DEF.ERR
9      1      0      C      O      M      M      O      N
PCIB.BASERR,PCIB.ERR,PCIB.ERR$,PCIB.NAME$,PCIB.GLBERR
9      1      1      C      O      M      M      O      N
READ.REGISTER,READ.SELFID,DEFINE,INITIALIZE.SYSTEM,ENABLE.SY
STEM,DISABLE.SYSTEM,INITIALIZE,POWER.ON,MEASURE,OUTPUT,START
,HALT,ENABLE.INT.TRIGGER,DISABLE.INT.TRIGGER,ENABLE.OUTPUT,D
ISABLE.OUTPUT,CHECK.DONE,GET.STATUS      912      COMMON
SET.FUNCTION,SET.RANGE,SET.MODE,WRITE.CAL,READ.CAL,STORE.CAL
,DELAY,SAVE.SYSTEM,SET.GATETIME,SET.SAMPLES,SET.SLOPE,SET.SO
URCE,ZERO.OHMS,SET.SPEED,SET.COMPLEMENT,SET.DRIVER,OUTPUT.NO
.WAIT,ENABLE.HANDSHAKE,DISABLE.HANDSHAKE      913      COMMON
SET.THRESHOLD,SET.START.BIT,SET.NUM.BITS,SET.LOGIC.SENSE,SET
.FREQUENCY,SET.AMPLITUDE,SET.OFFSET,SET.SYMMETRY,SET.BURST.C
OUNT,AUTOSCALE,CALIBRATE,SET.SENSITIVITY,SET.VERT.OFFSET,SET
.COUPLING,SET.POLARITY,SET.SWEEPSPEED      914      COMMON
SET.DELAY,SET.TRIG.SOURCE,SET.TRIG.SLOPE,SET.TRIG.LEVEL,SET.
TRIG.MODE,GET.SINGLE.WF,GET.TWO.WF,GET.VERT.INFO,GET.TIMEBAS
E.INFO,GET.TRIG.INFO,CALC.WFVOLT,CALC.WFTIME,CALC.WF.STATS,C
ALC.RISETIME,CALC.FALLTIME,CALC.PERIOD      915      COMMON
CALC.FREQUENCY,CALC.PLUSWIDTH,CALC.MINUSWIDTH,CALC.OVERSHOOT
,CALC.PRESHOOT,CALC.PK.TO.PK,SET.TIMEOUT,SCOPE.START,MEASURE
.SINGLE.WF,MEASURE.TWO.WF,OPEN.CHANNEL,CLOSE.CHANNEL      916
C      O      M      M      O      N
FREQUENCY,AUTO.FREQ,PERIOD,AUTO.PER,INTERVAL,RATIO,TOTALIZE,
R100MILLI,R1,R10,R100,R1KILO,R1OMEGA,R100MEGA,CHAN.A,CHAN.B,
POSITIVE,NEGATIVE,COMN,SEPARATE,DCVOLTS,ACVOLTS,OHMS,R200MIL
LI,R2,R20,R200,R2KILO,R20KILO,R200KILO      917      COMMON
R2MEGA,R2OMEGA,AUTOM,R2.5,R12.5,POSITIVE,NEGATIVE,TWOS,UNSIG
NED,OC,TTL,R0,R1,R2,R3,R4,R5,R6,R7,R8,R9,R10,R11,R12,R13,R14
,R15,R16,SINE,SQUARE,TRIANGLE,CONTINUOUS,GATED,BURST,R10NANO
,R100NANO,R1MICRO,R10MICRO,R100MICRO      918      COMMON
R1MILLI,R10MILLI,R100MILLI,R1,R10,R20NANO,R200NANO,R2MICRO,R
20MICRO,R200MICRO,R2MILLI,R20MILLI,R200MILLI,R2,R20,R50NANO,
R500NANO,R5MICRO,R50MICRO,R500MICRO,R5MILLI,R50MILLI,R500MIL
LI,R5,R50,CHAN.A,CHAN.B,EXTERNAL,POSITIVE      919      COMMON
NEGATIVE,AC,DC,TRIGGERED,AUTO.TRIG,AUTO.LEVEL,X1,X10,STANDAR
D,AVERAGE
9      2      0      C      O      M      M      O      N
DMM.01,Func.Gen.01,Scope.01,Counter.01,Dig.In.01,Dig.Out.01,
Relay.Act.01,Relay.Mux.01 999 'End PCIB Program Shell
1000 REM This step initializes the HP system
1010 CLS
1020 OPTION BASE 1
1      0      3      0      D      I      M
P(5),PA(50,5),PP(50,5),XPT(50),YPT(50),X(50),Y(50),YAW(50)
1040 REM
1050 CALL INITIALIZE.SYSTEM(PGMSHEL.HPC)
1060 REM

```

```

1070 REM SET FUNCTIONON THE 'DMM' , 'RELAY MUX , 'RELAY
ACTUATOR'
1080 REM
1090 CALL SET.FUNCTION(DMM.01,DCVOLTS)
1100 CALL SET.RANGE(DMM.01,AUTOM)
1110 CALL DISABLE.INT.TRIGGER(DMM.01)
1120 CALL ENABLE.OUTPUT(RELAY.MUX.01)
1130 CALL ENABLE.OUTPUT(RELAY.ACT.01)
1140 REM ***** PROGRAM TRAVERSE *****
1150 REM
1160 REM          OPEN THE COM PORT AND INITIALIZE THE MOTOR
SETTINGS
1170 OPEN "com1:1200,n,8,1,rs,cs,ds,cd" AS #1
1180 REM SET MOTOR DEFAULT VALUES
1190 DATA 2000,2000,2000,2,2,2,0.000125,0.000125,0.000125
1200 READ V1,V2,V3,R1,R2,R3,C1,C2,C3
1210 REM DEFINE CHARACTERS FOR DATA REDUCTION ALGORITHM
1220 RN2$="RENAME A:RAW.DAT "
1230 HEAD1$ = " #      X      Y      P1      P2      P3
P4      P5      YAW  "
1240 FORMAT$= "##  ##.##  ##.##  ###.###  ###.###  ###.###
###.###  ###.###  ###.###"
1250 PRINT
1260 PRINT "*****"
1270 PRINT "** USER MUST SELECT 'CAPS LOCK' FUNCTION **"
1280 PRINT "*****"
1290 REM          DISPLAY MOTOR DEFAULT SETTINGS
1300 PRINT "          *****"
1310 PRINT "          INITIALIZED VALUES FOR ALL MOTOR
SETTINGS:"
1320 PRINT "          VELOCITY = 1000 STEPS/SEC"
1330 PRINT "          RAMP(MOTOR ACCELERATION) = 2 (6000
STEPS/SEC^2)"
1340 PRINT "          DEFAULT INCREMENTAL UNITS ARE
INCHES"
1350 PRINT "          *****"
1360 PRINT
1370 PRINT "NOTE!! USE MANUAL CONTROL TO INITIALIZE PROBE
POSITION BEFORE"
1380 PRINT "          SELECTING COMPUTER CONTROLLED MOVEMENT.
"
1390 PRINT
1400 INPUT "MANUAL CONTROL OR COMPUTER CONTROL (ENTER 'MAN'
or 'CP')";CON$
1410 IF CON$="CP" THEN 3490
1420 REM OPTION TO CHANGE DEFAULT SETTINGS OF VELOCITY OR
ACCELERATION RAMP
1430 PRINT
1440 PRINT
1450 PRINT " DO YOU WANT TO CHANGE THE VELOCITY OR
ACCELERATION RAMP"

```

```

1460 PRINT "          DEFAULT SETTINGS? (Y or N)"
1470 PRINT
1480 PRINT "IF 'NO', THIS PROGRAM WILL THEN LET YOU DEFINE
THE"
1490 PRINT "DISTANCE YOU WANT TO MOVE (IN INCHES). IF 'YES',"
1500 PRINT "YOU CAN CHANGE ANY OR ALL OF THE DEFAULT SETTINGS
FOR ANY MOTOR."
1510 PRINT
1520 PRINT
1530 PRINT
1540 INPUT "DO YOU WANT TO CHANGE ANY OF THE DEFAULT SETTINGS?
(Y or N)";D$
1550 IF D$="Y" THEN 1590
1560 IF D$="N" THEN 2220
1570 REM
1580 REM      **** OPERATOR SELECTED MOTOR VARIABLES ****
1590 PRINT
1600 PRINT
1610 INPUT "WHICH DEFAULT VALUE? (ENTER '1'FOR VELOC OR '2'
FOR ACCEL RAMP)";L
1620 ON L GOTO 1690,1930
1630 PRINT "DO YOU WANT TO CHANGE THE DEFAULT VELOCITY? (Y OR
N)"
1640 INPUT V$
1650 IF V$="Y" THEN 1690
1660 PRINT "DO YOU WANT TO CHANGE THE DEFAULT ACCELERATION
RAMP? (Y or N)"
1670 IF R$="Y" THEN 1990
1680 IF R$="N" THEN 1450
1690 PRINT
1700 PRINT
1710 INPUT "WHICH MOTOR VELOCITY DO YOU WISH TO CHANGE? (1,2,
or 3)";J
1720 ON J GOTO 1730,1830,1880
1730 PRINT
1740 PRINT
1750 INPUT "ENTER DESIRED VELOCITY OF MOTOR #1";V1
1760 PRINT
1770 PRINT
1780 PRINT
1790 PRINT "DO YOU WANT TO CHANGE VELOCITY OF ANOTHER MOTOR?
(Y OR N)"
1800 INPUT V$
1810 IF V$="Y" THEN 1690
1820 IF V$="N" THEN 1430
1830 PRINT
1840 PRINT
1850 INPUT "ENTER DESIRED VELOCITY OF MOTOR 2";V2
1860 PRINT
1870 GOTO 1780
1880 PRINT

```

```

1890 PRINT
1900 INPUT "ENTER DESIRED VELOCITY OF MOTOR #3";V3
1910 PRINT
1920 GOTO 1780
1930 PRINT
1940 PRINT
1950 INPUT "WHICH MOTOR ACCEL RAMP DO YOU WANT TO CHANGE? (1,
2, or 3)";K
1960 ON K GOTO 1970,2060,2120
1970 PRINT
1980 PRINT
1990 INPUT "ENTER DESIRED ACCELERATION RAMP OF MOTOR #1";R1
2000 PRINT
2010 PRINT
2020 PRINT "DO YOU WANT TO CHANGE THE ACCEL RAMP OF ANOTHER
MOTOR? (Y or N)?"
2030 INPUT RM$
2040 IF RM$="Y" THEN 1930
2050 IF RM$="N" THEN 1450
2060 PRINT
2070 PRINT
2080 INPUT "ENTER DESIRED ACCELERATION RAMP OF MOTOR #2";R2
2090 PRINT
2100 PRINT
2110 GOTO 2000
2120 PRINT
2130 PRINT
2140 INPUT "ENTER DESIRED ACCELERATION RAMP OF MOTOR #3";R3
2150 PRINT
2160 PRINT
2170 GOTO 2000
2180 REM
2190 REM DEFINE DISTANCE TO MOVE MOTOR
2200 PRINT
2210 PRINT
2220 PRINT
2230 REM INITIALIZE MOTOR INCREMENTS TO ZERO
2240 I1=0
2250 I2=0
2260 I3=0
2270 PRINT
2 2 8 0 P R I N T "
*****"
2290 PRINT " ** DEFINE WHICH MOTOR YOU WANT TO MOVE
**"
2300 PRINT " **
**"
2310 PRINT " ** NOTE!!! A POSITIVE ('+') INCREMENT TO
A MOTOR **"
2320 PRINT " ** MOVES TRAVERSER AWAY FROM THAT PARTICULAR
MOTOR **"

```

```

2330 PRINT " **
      ***"
2340 PRINT " ** -- MOTOR #1 MOVES THE PROBE UPSTREAM AGAINST
THE FLOW ***"
2350 PRINT " ** -- MOTOR #2 MOVES THE PROBE TOWARD THE ACCESS
WINDOW ***"
2360 PRINT " ** -- MOTOR #3 MOVES THE PROBE VERTICALLY
DOWNWARD ***"
2       3       7       0       P       R       I       N       T       "
*****"
2380 PRINT
2390 PRINT
2400 INPUT "WHICH MOTOR DO YOU WANT TO MOVE? (1,2, or 3)";L
2410 ON L GOTO 2420,2680,2970
2420 PRINT
2430 PRINT
2440 PRINT "HOW FAR DO YOU WANT TO MOVE MOTOR #1?"
2450 PRINT " ***** (ENTER DISTANCE IN INCHES) *****"
2460 INPUT I1
2470 PRINT
2480 PRINT" *****"
2490 PRINT
2500 PRINT "SUMMARY OF OPERATOR INPUTS:"
2510 PRINT "          MOTOR #1    VELOCITY = ";V1
2520 PRINT "          ACCELERATION RAMP = ";R1
2530 PRINT "          INCREMENTAL DISTANCE =
";I1;"INCHES"
2540 PRINT" *****"
2550 PRINT "DO YOU WANT TO CHANGE ANY OF THESE VALUES? (Y or
N)"
2560 PRINT
2570 PRINT "ENTER 'N' TO START MOTOR MOVEMENT.  ENTER 'Y' TO
RETURN"
2580 PRINT "TO VARIABLE SELECTION SUBROUTINE."
2590 INPUT V$
2600 IF V$="Y" THEN 1430
2610 GOSUB 3410
2620 PRINT
2630 PRINT "DO YOU WANT TO MOVE ANOTHER MOTOR ALSO? (Y or N)?"
2640 INPUT C$
2650 IF C$="Y" THEN 2220
2660 IF C$="N" THEN 3260
2670 PRINT
2680 PRINT
2690 PRINT "HOW FAR DO YOU WANT TO MOVE MOTOR #2?"
2700 PRINT " ***** (ENTER DISTANCE IN INCHES) *****"
2710 INPUT I2
2720 PRINT
2730 PRINT
2740 REM DISPLAY OPERATOR SELECTED MOTOR VARIABLES
2750 PRINT" *****"

```

```

2760 PRINT
2770 PRINT "SUMMARY OF OPERATOR INPUTS:"
2780 PRINT "          MOTOR #2    VELOCITY = ";V2
2790 PRINT "          ACCELERATION RAMP = ";R2
2800 PRINT "          INCREMENTAL DISTANCE =
";I2;"INCHES"
2810 PRINT" *****"
2820 PRINT
2830 PRINT
2840 PRINT "DO YOU WANT TO CHANGE ANY OF THESE VALUES? (Y or
N)"
2850 PRINT
2860 PRINT "ENTER 'N' TO START MOTOR MOVEMENT.  ENTER 'Y' TO
RETURN"
2870 PRINT "TO VARIABLE SELECTION SUBROUTINE."
2880 INPUT V$
2890 IF V$="Y" THEN 1430
2900 GOSUB 3410
2910 PRINT
2920 PRINT "DO YOU WANT TO MOVE ANOTHER MOTOR ALSO? (Y or N)?"
2930 INPUT C$
2940 IF C$="Y" THEN 2220
2950 IF C$="N" THEN 3260
2960 PRINT
2970 PRINT
2980 PRINT "HOW FAR DO YOU WANT TO MOVE MOTOR #3?"
2990 PRINT " ***** (ENTER DISTANCE IN INCHES) *****"
3000 INPUT I3
3010 PRINT
3020 PRINT
3030 REM DISPLAY OPERATOR SELECTED MOTOR VARIABLES
3040 PRINT" *****"
3050 PRINT
3060 PRINT "SUMMARY OF OPERATOR INPUTS:"
3070 PRINT "          MOTOR #3    VELOCITY = ";V3
3080 PRINT "          ACCELERATION RAMP = ";R3
3090 PRINT "          INCREMENTAL DISTANCE =
";I3;"INCHES"
3100 PRINT
3110 PRINT" *****"
3120 PRINT
3130 PRINT
3140 PRINT "DO YOU WANT TO CHANGE ANY OF THESE VALUES? (Y or
N)"
3150 PRINT
3160 PRINT "ENTER 'N' TO START MOTOR MOVEMENT.  ENTER 'Y' TO
RETURN"
3170 PRINT "TO VARIABLE SELECTION SUBROUTINE."
3180 INPUT V$
3190 IF V$="Y" THEN 1430
3200 GOSUB 3410

```

```

3210 PRINT
3220 PRINT
3230 INPUT "DO YOU WANT TO INPUT ANOTHER MANUAL MOTOR MOVEMENT
(Y or N)";M$
3240 IF M$="Y" THEN 2210
3250 PRINT
3260 PRINT "DO YOU WANT TO INPUT COMPUTER CONTROLLED MOTOR
MOVEMENT?"
3270 PRINT "          ***** NOTE!!! ***** "
3280 PRINT " ALL PREVIOUS MOTOR INCREMENT INPUTS HAVE BEEN
ZEROIZED."
3290 PRINT "PROGAM WILL LET YOU CHOOSE MANUAL OR CP-CONTROLLED
MOVEMENT."
3300 PRINT "***** (IF 'NO', THE PROGRAM WILL END). *****"
3310 PRINT
3320 INPUT "DO YOU WANT COMPUTER CONTROLLED MOTOR MOVEMENT (Y
or N)";N$
3330 IF N$="Y" THEN 3500
3340 PRINT
3350 PRINT
3360 PRINT
3370 PRINT "          *****"
3380 PRINT "          THE PROGRAM HAS ENDED."
3390 PRINT "          *****"
3400 END
3410 REM          ***** MOTOR MOVEMENT SUBROUTINE *****
3 4 2 0   P R I N T      # 1 ,      " & "          : P R I N T      # 1 ,
"E";"C1=";C1;" :C2=";C2;" :C3=";C3
3430 PRINT #1, "I1=";I1;" :V1=";V1;" :R1=";R1;
3440 PRINT #1, " :I2=";I2;" :V2=";V2;" :R2=";R2
3450 PRINT #1, "I3=";I3;" :V3=";V3;" :R3=";R3;" :@"
3460 RETURN
3470 REM          *****
3480 REM          *****
3490 PRINT
3500 REM ***** COMPUTER CONTROLLED MOVEMENT *****
3510 PRINT
3520 PRINT "THE PRESSURE DATA WILL BE WRITTEN TO FILES ON
DRIVE 'A' "
3530 PRINT
3540 PRINT "YOU WILL BE ASKED TO INPUT FILE NAMES FOR THESE."
3550 PRINT
3560 INPUT "IS A FORMATTED DISK IN DRIVE 'A'? PRESS 'ENTER'
TO CONTINUE";D$
3570 PRINT
3580 PRINT
3590 PRINT
3600 PRINT "          *****"
3610 PRINT "          **          NOTE !!!          **"
3620 PRINT "          ** COMPUTER CONTROLLED MOVEMENT          **"
3630 PRINT "          **          IS PROGRAMMED WITH A          **"

```

```

3640 PRINT "      ** DEFAULTED NEGATIVE MOTOR INCREMENT **"
3650 PRINT "      ** (i.e. MOTOR #3 WILL MOVE UPWARD **"
3660 PRINT "      ** BY ENTERING A (+) DISTANCE). **"
3670 PRINT "      ****"
3680 PRINT
3690 REM SET INITIAL MOVEMENT DISTANCE AND NUMBER OF DATA
POINTS TO ZERO
3700 HT=0
3710 WD=0
3720 DIST=0
3730 XPT=0
3740 YPT=0
3750 N=0
3760 PRINT
3770 PRINT
3780 INPUT "WHAT IS THE DIMENSION ( X , Y ) (IN INCHES) THAT
YOU WANT TO MEASURE." ;WD,HT
3790 PRINT
3800 INPUT "WHAT IS THE STEP (IN INCHES) THAT YOU WANT TO
MOVE." ;DIST
3810 YPT=INT(HT /DIST) + 1
3820 XPT=INT(WD /DIST)+ 1
3830 N=XPT*YPT
3840 PRINT
3850 PRINT "THERE ARE ";XPT;" * ";YPT;" = ";N;" POINTS TO BE
MEASURED "
3860 PRINT
3870 INPUT "ARE THE NUMBER OF POINTS IS OK.(Y OR N)";C$
3880 IF C$="N" THEN 3780
3890 CLS
3900 N=XPT
3910 IF (N < 1) OR (N > 99) GOTO 3780
3920 REM *** GENERATING STRING STRING SEGMENTS FOR DATA FILE
NAMES
3930 B$ = MID$(STR$(1), 2): REM ** STRING NUMBER "1"
3940 E$ = MID$(STR$(N), 2): REM ** ENDING STRING NUMBER "N"
3950 X$ = "XXXXXX"
3960 EX$ = ".DAT"
3970 CLS
3980 PRINT "DATA FILES WILL BE INCREMENTED FROM:"
3990 PRINT
4000 PRINT (X$ + B$ + EX$); " To "; (X$ + E$ + EX$)
4010 PRINT
4020 PRINT
4030 INPUT "ENTER DATA FILE NAME (6 CHARACTERS MAX -- NO
EXTENSION)";F2$
4040 PRINT
4050 PRINT
4060 IF LEN(F2$) > 6 OR LEN(F2$) < 1 GOTO 4030
4070 CLS

```

```

4080 PRINT N; "DATA FILES WILL BE GENERATED AND INCREMENTED
AS FOLLOWS:"
4090 PRINT
4100 PRINT
4110 PRINT (F2$ + B$ + EX$); " To "; (F2$ + E$ + EX$)
4120 PRINT
4130 PRINT
4140 INPUT "ARE THE NUMBER OF POINTS AND FILE NAMES OK.(Y OR
N)"; C$
4150 IF C$ = "N" GOTO 3780
4160 IF C$ = "Y" GOTO 4180
4170 GOTO 4140
4180 CLS
4190 PRINT
4200 PRINT
4210 REM SET INITIAL POSITION DATA
4220 X(1)=-DIST
4230 Y(1)=-DIST
4240 FOR IX=2 TO XPT+1
4250 X(IX)=0
4260 NEXT IX
4270 FOR JY=2 TO YPT+1
4280 Y(JY)=0
4290 NEXT JY
4300 FOR I=1 TO XPT
4302 I1=0
4304 I2=0
4306 I3=0
4310 FOR J=1 TO YPT
4320 REM MOTOR CP-CONTROLLED MOTOR MOVEMENT
4330 I1=0
4340 I2=0
4350 I3=0
4360 REM EACH POINT TAKE 10 TIMES READINGS
4370 X(I+1)=X(I)+DIST
4380 XPT(J)=X(I+1)
4390 Y(J+1)=Y(J)+DIST
4400 YPT(J)=Y(J+1)
4405 INPUT " ADJUST THE WHEEL TO MAKE THE P2 =P3, INPUT THE YAW
ANGLE";YAW(J)
4408 PRINT
4410 INPUT " PRESS 'ENTER' TO START THE MEASUREMENT";MOVE$
4420 REM
4430 REM READ FIVE CHANNELS AND DISPLAY THE DATA
4440 REM
4450 STEPPER=4
4460 SWITCH = 3
4470 HOMER=8
4480 DELAY1 = .1
4490 DELAY2 = 1
4500 REM SET THE S.V PORT TO #4

```

```

4510 FOR IL=1 TO 3
4520 THYME = TIMER
4530 CALL OUTPUT(RELAY.ACT.01,STEPPER)
4540 CHKTIME = TIMER
4550 IF CHKTIME < (THYME + DELAY1) GOTO 4540
4560 CALL OPEN.CHANNEL(RELAY.ACT.01,SWITCH)
4570 CLS
4580 NEXT IL
4590 PRINT
4600 PRINT " NOW IS POINT ";J
4610 REM START MEASURE FROM PORT 4 TO PORT 8
4620 FOR JJ=1 TO 5
4630 CALL OUTPUT(RELAY.ACT.01,STEPPER)
4640 CHKTIME = TIMER
4650 IF CHKTIME < (THYME + DELAY2) GOTO 4640
4660 REM EACH PORT SAMPLE 10 TIMES
4670 FOR II=1 TO 10
4680 ROUT=1
4690 CALL OUTPUT(RELAY.MUX.01,ROUT)
4700 CALL MEASURE(DMM.01,VOLTS)
4710 PA(II,JJ)=VOLTS
4720 NEXT II
4730 CALL OPEN.CHANNEL(RELAY.ACT.01,SWITCH)
4740 IF JJ=5 THEN 4760
4750 NEXT JJ
4760 REM HOME THE S.V PORT TO #48
4770 CALL OUTPUT(RELAY.ACT.01,HOMER)
4780 CALL OPEN.CHANNEL(RELAY.ACT.01,HOMER)
4790 REM
4800 REM DISPLAY THE SAMPLE DATA
4810 REM
4820 PRINT HEAD1$
4830 FOR IS= 1 TO 10
4 8 4 0 P R I N T U S I N G
FORMAT$;IS,XPT(J),YPT(J),PA(IS,1),PA(IS,2),PA(IS,3),PA(IS,4)
,PA(IS,5),YAW(J)
4850 NEXT IS
4860 REM
4870 REM AVERAGE THE DATA
4880 REM
4890 FOR JA = 1 TO 5
4900 TOTAL = 0
4910 FOR IA = 1 TO 10
4920 TOTAL = TOTAL + PA(IA,JA)
4930 NEXT IA
4940 AVERAGE = TOTAL /10
4950 P(JA)=AVERAGE
4960 NEXT JA
4970 PRINT
4980 PRINT "THE AVERAGES ARE: "
5000 PRINT HEAD1$

```

```

5010 FOR JD=1 TO 5
5020 PP(J,JD)=P(JD)
5030 NEXT JD
5 0 4 0 P R I N T U S I N G
FORMAT$,J,XPT(J),YPT(J),PP(J,1),PP(J,2),PP(J,3),PP(J,4),PP(J
,5),YAW(J)
5045 PRINT
5048 PRINT USING "THE NULLING ERROR IS +#.####";PP(J,3)-
PP(J,2)
5049 PRINT
5050 PRINT "DO YOU WANT RE-MEASURE AGAIN (Y / N)"
5060 PRINT
5062 PRINT "IF 'Y' WILL RE-SAMPLE AGAIN."
5064 PRINT
5070 INPUT "IF 'N' WILL MOVE THE TRAVERSER STEP UPWARD (WAIT
7 SEC)";C$
5075 PRINT
5080 IF C$="Y" THEN 4405
5082 IF C$="N" THEN 5090
5084 GO TO 5070
5090 IF J=YPT THEN 5160
5100 REM
5110 REM MOVE THE TRAVERSER STEP UPWARD.
5120 REM
5130 I3=-DIST
5140 GOSUB 3410
5150 NEXT J
5160 REM*** STORE DATA BEFORE NEXT SAMPLE***
5170 OPEN "A:\RAW.DAT" FOR OUTPUT AS #2
5180 PRINT #2 ,HEAD1$
5190 FOR ID=1 TO YPT
5 2 0 0 P R I N T # 2 , U S I N G
FORMAT$,ID,XPT(ID),YPT(ID),PP(ID,1),PP(ID,2),PP(ID,3),PP(ID,
4),PP(ID,5),YAW(ID) 5210 NEXT ID
5220 CLOSE #2
5230 REM *** GENERATING INCREMENTED DATA FILE NAME
5240 IF (I > 10) OR (I = 10) THEN I$ = MID$(STR$(I), 2)
5250 IF (I < 10) THEN I$ = (MID$(STR$(0), 2) + MID$(STR$(I),
2))
5260 FI2$ = (F2$ + I$ + EX$)
5270 PRINT
5280 PRINT " WRITING DATA FILE "; FI2$
5290 DF2$=RN2$+FI2$
5300 REM ** RENAME DATA FILE
5310 SHELL DF2$
5320 REM
5330 REM MOVE THE TRAVERSER TO THE NEXT SAMPLE POSITION
5340 REM
5350 PRINT
5360 IF I=XPT THEN 5430

```

```
5370 INPUT "THEN PRESS 'ENTER' FOR NEXT COLUMN SAMPLE( 90 SEC)
";MOVE$
5390 I2=-DIST
5400 I3=HT
5410 GOSUB 3410
5420 NEXT I
5430 CLS
5440 PRINT "ALL MOVEMENTS COMPLETE"
5450 PRINT
5460 PRINT
5470 PRINT "YOU WANT TO REPOSITION TRAVERSER FOR ANOTHER
MOVEMENT (Y OR N)?"
5480 PRINT
5490 PRINT "IF 'Y', THE PROGRAM WILL TAKE YOU TO MANUAL
CONTROL SUBROUTINE."
5500 PRINT "IF 'N', THE PROGRAM WILL END."
5510 PRINT
5520 INPUT "ANOTHER MOVEMENT";R$
5530 IF R$ = "Y" THEN 1370
5540 IF R$ = "N" THEN 3370
```

## APPENDIX B. CALP PROGRAM

```

1 DEF SEG: CLEAR , &HFEE0: GOTO 4 'Begin PCIB Program Shell
2 GOTO 1000 ' User program
3 GOTO 900 ' Error handling
4 I=&HFEE0 ' Copyright Hewlett-Packard 1984,1985
5 PCIB.DIR$=ENVIRON$("PCIB")
6 I$=PCIB.DIR$+"\PCIBILC.BLD"
7 BLOAD I$,I
8 CALL I(PCIB.DIR$,I%,J%): PCIB.SEG=I%
9 IF J%=0 THEN GOTO 13
10 PRINT "Unable to load.";
11 PRINT " (Error #";J%;" )"
12 END
13 '
14 DEF SEG=PCIB.SEG: O.S=5: C.S=10: I.V=15
15 I.C=20: L.P=25: LD.FILE=30
16 GET.MEM=35: L.S=40: PANELS=45: DEF.ERR=50
17 PCIB.ERR$=STRING$(64,32) : PCIB.NAME$=STRING$(16,32)
18 CALL DEF.ERR(PCIB.ERR, PCIB.ERR$, PCIB.NAME$, PCIB.GLBERR) :
PCIB.BASERR=255 19 ON ERROR GOTO 3
20 J=-1
21 I$=PCIB.DIR$+"\PCIB.SYN"
22 CALL O.S(I$)
23 IF PCIB.ERR<>0 THEN ERROR PCIB.BASERR
24 I=0
2         5             C           A           L           L
I.V(I, READ.REGISTER, READ.SELFID, DEFINE, INITIALIZE.SYSTEM)
26 IF PCIB.ERR<>0 THEN ERROR PCIB.BASERR
2         7             C           A           L           L
I.V(I, ENABLE.SYSTEM, DISABLE.SYSTEM, INITIALIZE, POWER.ON)
28 IF PCIB.ERR<>0 THEN ERROR PCIB.BASERR
29 CALL I.V(I, MEASURE, OUTPUT, START, HALT)
30 IF PCIB.ERR<>0 THEN ERROR PCIB.BASERR
3         1             C           A           L           L
I.V(I, ENABLE.INT.TRIGGER, DISABLE.INT.TRIGGER, ENABLE.OUTPUT, D
ISABLE.OUTPUT) 32 IF PCIB.ERR<>0 THEN ERROR PCIB.BASERR
33 CALL I.V(I, CHECK.DONE, GET.STATUS, SET.FUNCTION, SET.RANGE)
34 IF PCIB.ERR<>0 THEN ERROR PCIB.BASERR
35 CALL I.V(I, SET.MODE, WRITE.CAL, READ.CAL, STORE.CAL)
36 IF PCIB.ERR<>0 THEN ERROR PCIB.BASERR
37 CALL I.V(I, DELAY, SAVE.SYSTEM, J, J)
38 IF PCIB.ERR<>0 THEN ERROR PCIB.BASERR
39 I=1
40 CALL I.V(I, SET.GATETIME, SET.SAMPLES, SET.SLOPE, SET.SOURCE)
41 IF PCIB.ERR<>0 THEN ERROR PCIB.BASERR
42 CALL I.C(I, FREQUENCY, AUTO.FREQ, PERIOD, AUTO.PER)
43 IF PCIB.ERR<>0 THEN ERROR PCIB.BASERR

```

```

44 CALL I.C(I,INTERVAL,RATIO,TOTALIZE,R100MILLI)
45 IF PCIB.ERR<>0 THEN ERROR PCIB.BASERR
46 CALL I.C(I,R1,R10,R100,R1KILO)
47 IF PCIB.ERR<>0 THEN ERROR PCIB.BASERR
48 CALL I.C(I,R10MEGA,R100MEGA,CHAN.A,CHAN.B)
49 IF PCIB.ERR<>0 THEN ERROR PCIB.BASERR
50 CALL I.C(I,POSITIVE,NEGATIVE,COMN,SEPARATE)
51 IF PCIB.ERR<>0 THEN ERROR PCIB.BASERR
52 I=2
53 I=3
54 CALL I.V(I,ZERO.OHMS,SET.SPEED,J,J)
55 IF PCIB.ERR<>0 THEN ERROR PCIB.BASERR
56 CALL I.C(I,DCVOLTS,ACVOLTS,OHMS,R200MILLI)
57 IF PCIB.ERR<>0 THEN ERROR PCIB.BASERR
58 CALL I.C(I,R2,R20,R200,R2KILO)
59 IF PCIB.ERR<>0 THEN ERROR PCIB.BASERR
60 CALL I.C(I,R20KILO,R200KILO,R2MEGA,R20MEGA)
61 IF PCIB.ERR<>0 THEN ERROR PCIB.BASERR
62 CALL I.C(I,AUTOM,R2.5,R12.5,J)
63 IF PCIB.ERR<>0 THEN ERROR PCIB.BASERR
64 I=4
6         5             C         A         L         L
I.V(I,SET.COMPLEMENT,SET.DRIVER,OUTPUT.NO.WAIT,ENABLE.HANDSH
AKE) 66 IF PCIB.ERR<>0 THEN ERROR PCIB.BASERR
6         7             C         A         L         L
I.V(I,DISABLE.HANDSHAKE,SET.THRESHOLD,SET.START.BIT,SET.NUM.
BITS) 68 IF PCIB.ERR<>0 THEN ERROR PCIB.BASERR
69 CALL I.V(I,SET.LOGIC.SENSE,J,J,J)
70 IF PCIB.ERR<>0 THEN ERROR PCIB.BASERR
71 CALL I.C(I,POSITIVE,NEGATIVE,TWOS,UNSIGNED)
72 IF PCIB.ERR<>0 THEN ERROR PCIB.BASERR
73 CALL I.C(I,OC,TTL,R0,R1)
74 IF PCIB.ERR<>0 THEN ERROR PCIB.BASERR
75 CALL I.C(I,R2,R3,R4,R5)
76 IF PCIB.ERR<>0 THEN ERROR PCIB.BASERR
77 CALL I.C(I,R6,R7,R8,R9)
78 IF PCIB.ERR<>0 THEN ERROR PCIB.BASERR
79 CALL I.C(I,R10,R11,R12,R13)
80 IF PCIB.ERR<>0 THEN ERROR PCIB.BASERR
81 CALL I.C(I,R14,R15,R16,J)
82 IF PCIB.ERR<>0 THEN ERROR PCIB.BASERR
83 I=6
8         4             C         A         L         L
I.V(I,SET.FREQUENCY,SET.AMPLITUDE,SET.OFFSET,SET.SYMMETRY)
85 IF PCIB.ERR<>0 THEN ERROR PCIB.BASERR
86 CALL I.V(I,SET.BURST.COUNT,J,J,J)
87 IF PCIB.ERR<>0 THEN ERROR PCIB.BASERR
88 CALL I.C(I,SINE,SQUARE,TRIANGLE,CONTINUOUS)
89 IF PCIB.ERR<>0 THEN ERROR PCIB.BASERR
90 CALL I.C(I,GATED,BURST,J,J)
91 IF PCIB.ERR<>0 THEN ERROR PCIB.BASERR

```

```

92 I=7
9           3           C           A           L           L
I.V(I,AUTOSCALE,CALIBRATE,SET.SENSITIVITY,SET.VERT.OFFSET)
94 IF PCIB.ERR<>0 THEN ERROR PCIB.BASERR
9           5           C           A           L           L
I.V(I,SET.COUPLING,SET.POLARITY,SET.SWEEPSPEED,SET.DELAY)
96 IF PCIB.ERR<>0 THEN ERROR PCIB.BASERR
9           7           C           A           L           L
I.V(I,SET.TRIG.SOURCE,SET.TRIG.SLOPE,SET.TRIG.LEVEL,SET.TRIG
.MODE) 98 IF PCIB.ERR<>0 THEN ERROR PCIB.BASERR
9           9           C           A           L           L
I.V(I,GET.SINGLE.WF,GET.TWO.WF,GET.VERT.INFO,GET.TIMEBASE.IN
FO) 100 IF PCIB.ERR<>0 THEN ERROR PCIB.BASERR
1           0           1           C           A           L           L
I.V(I,GET.TRIG.INFO,CALC.WFVOLT,CALC.WFTIME,CALC.WF.STATS)
102 IF PCIB.ERR<>0 THEN ERROR PCIB.BASERR
1           0           3           C           A           L           L
I.V(I,CALC.RISETIME,CALC.FALLTIME,CALC.PERIOD,CALC.FREQUENCY)
104 IF PCIB.ERR<>0 THEN ERROR PCIB.BASERR
1           0           5           C           A           L           L
I.V(I,CALC.PLUSWIDTH,CALC.MINUSWIDTH,CALC.OVERSHOOT,CALC.PRE
SHOOT) 106 IF PCIB.ERR<>0 THEN ERROR PCIB.BASERR
1           0           7           C           A           L           L
I.V(I,CALC.PK.TO.PK,SET.TIMEOUT,SCOPE.START,MEASURE.SINGLE.WF)
108 IF PCIB.ERR<>0 THEN ERROR PCIB.BASERR
109 CALL I.V(I,MEASURE.TWO.WF,J,J,J)
110 IF PCIB.ERR<>0 THEN ERROR PCIB.BASERR
111 CALL I.C(I,R10NANO,R100NANO,R1MICRO,R10MICRO)
112 IF PCIB.ERR<>0 THEN ERROR PCIB.BASERR
113 CALL I.C(I,R100MICRO,R1MILLI,R10MILLI,R100MILLI)
114 IF PCIB.ERR<>0 THEN ERROR PCIB.BASERR
115 CALL I.C(I,R1,R10,R20NANO,R200NANO)
116 IF PCIB.ERR<>0 THEN ERROR PCIB.BASERR
117 CALL I.C(I,R2MICRO,R20MICRO,R200MICRO,R2MILLI)
118 IF PCIB.ERR<>0 THEN ERROR PCIB.BASERR
119 CALL I.C(I,R20MILLI,R200MILLI,R2,R20)
120 IF PCIB.ERR<>0 THEN ERROR PCIB.BASERR
121 CALL I.C(I,R50NANO,R500NANO,R5MICRO,R50MICRO)
122 IF PCIB.ERR<>0 THEN ERROR PCIB.BASERR
123 CALL I.C(I,R500MICRO,R5MILLI,R50MILLI,R500MILLI)
124 IF PCIB.ERR<>0 THEN ERROR PCIB.BASERR
125 CALL I.C(I,R5,R50,CHAN.A,CHAN.B)
126 IF PCIB.ERR<>0 THEN ERROR PCIB.BASERR
127 CALL I.C(I,EXTERNAL,POSITIVE,NEGATIVE,AC)
128 IF PCIB.ERR<>0 THEN ERROR PCIB.BASERR
129 CALL I.C(I,DC,TRIGGERED,AUTO.TRIG,AUTO.LEVEL)
130 IF PCIB.ERR<>0 THEN ERROR PCIB.BASERR
131 CALL I.C(I,X1,X10,STANDARD,AVERAGE)
132 IF PCIB.ERR<>0 THEN ERROR PCIB.BASERR
133 I=8
134 CALL I.V(I,OPEN.CHANNEL,CLOSE.CHANNEL,J,J)

```

```

135 IF PCIB.ERR<>0 THEN ERROR PCIB.BASERR
136 CALL C.S
137 IF PCIB.ERR<>0 THEN ERROR PCIB.BASERR
138 I$=PCIB.DIR$+"\PCIB.PLD"
139 CALL L.P(I$)
140 IF PCIB.ERR<>0 THEN ERROR PCIB.BASERR
141 I$="DMM.01":I=3:J=0:K=0:L=1
142 CALL DEFINE(DMM.01,I$,I,J,K,L)
143 IF PCIB.ERR<>0 THEN ERROR PCIB.BASERR
144 I$="Func.Gen.01":I=6:J=0:K=1:L=1
145 CALL DEFINE(FUNC.GEN.01,I$,I,J,K,L)
146 IF PCIB.ERR<>0 THEN ERROR PCIB.BASERR
147 I$="Scope.01":I=7:J=0:K=2:L=1
148 CALL DEFINE(SCOPE.01,I$,I,J,K,L)
149 IF PCIB.ERR<>0 THEN ERROR PCIB.BASERR
150 I$="Counter.01":I=1:J=0:K=3:L=1
151 CALL DEFINE(COUNTER.01,I$,I,J,K,L)
152 IF PCIB.ERR<>0 THEN ERROR PCIB.BASERR
153 I$="Dig.In.01":I=4:J=0:K=4:L=1
154 CALL DEFINE(DIG.IN.01,I$,I,J,K,L)
155 IF PCIB.ERR<>0 THEN ERROR PCIB.BASERR
156 I$="Dig.Out.01":I=4:J=1:K=4:L=1
157 CALL DEFINE(DIG.OUT.01,I$,I,J,K,L)
158 IF PCIB.ERR<>0 THEN ERROR PCIB.BASERR
159 I$="Relay.Act.01":I=8:J=0:K=5:L=1
160 CALL DEFINE(RELAY.ACT.01,I$,I,J,K,L)
161 IF PCIB.ERR<>0 THEN ERROR PCIB.BASERR
162 I$="Relay.Mux.01":I=2:J=0:K=6:L=1
163 CALL DEFINE(RELAY.MUX.01,I$,I,J,K,L)
164 IF PCIB.ERR<>0 THEN ERROR PCIB.BASERR
800 I$=ENVIRON$("PANELS")+"\PANELS.EXE"
801 CALL L.S(I$)
899 GOTO 2
900 IF ERR=PCIB.BASERR THEN GOTO 903
901 PRINT "BASIC error #";ERR;" occurred in line ";ERL
902 STOP
903 TMPERR=PCIB.ERR:IF TMPERR=0 THEN TMPERR=PCIB.GLBERR
904 PRINT "PC Instrument error #";TMPERR;" detected at line
";ERL
905 PRINT "Error: ";PCIB.ERR$
906 IF LEFT$(PCIB.NAME$,1)<>CHR$(32) THEN PRINT "Instrument:
";PCIB.NAME$ 907 STOP
908 COMMON PCIB.DIR$,PCIB.SEG
909 COMMON LD.FILE,GET.MEM,PANELS,DEF.ERR
9      1      0      C      O      M      M      O      N
PCIB.BASERR,PCIB.ERR,PCIB.ERR$,PCIB.NAME$,PCIB.GLBERR
9      1      1      C      O      M      M      O      N
READ.REGISTER,READ.SELFID,DEFINE,INITIALIZE.SYSTEM,ENABLE.SY
STEM,DISABLE.SYSTEM,INITIALIZE,POWER.ON,MEASURE,OUTPUT,START
,HALT,ENABLE.INT.TRIGGER,DISABLE.INT.TRIGGER,ENABLE.OUTPUT,D
ISABLE.OUTPUT,CHECK.DONE,GET.STATUS      912      COMMON

```

```

SET.FUNCTION, SET.RANGE, SET.MODE, WRITE.CAL, READ.CAL, STORE.CAL
, DELAY, SAVE.SYSTEM, SET.GATETIME, SET.SAMPLES, SET.SLOPE, SET.SO
URCE, ZERO.OHMS, SET.SPEED, SET.COMPLEMENT, SET.DRIVER, OUTPUT.NO
.WAIT, ENABLE.HANDSHAKE, DISABLE.HANDSHAKE      913      COMMON
SET.THRESHOLD, SET.START.BIT, SET.NUM.BITS, SET.LOGIC.SENSE, SET
.FREQUENCY, SET.AMPLITUDE, SET.OFFSET, SET.SYMMETRY, SET.BURST.C
OUNT, AUTOSCALE, CALIBRATE, SET.SENSITIVITY, SET.VERT.OFFSET, SET
.COUPLING, SET.POLARITY, SET.SWEEPSPEED      914      COMMON
SET.DELAY, SET.TRIG.SOURCE, SET.TRIG.SLOPE, SET.TRIG.LEVEL, SET.
TRIG.MODE, GET.SINGLE.WF, GET.TWO.WF, GET.VERT.INFO, GET.TIMEBAS
E.INFO, GET.TRIG.INFO, CALC.WFVOLT, CALC.WFTIME, CALC.WF.STATS, C
ALC.RISETIME, CALC.FALLTIME, CALC.PERIOD      915      COMMON
CALC.FREQUENCY, CALC.PLUSWIDTH, CALC.MINUSWIDTH, CALC.OVERSHOOT
, CALC.PRESHOOT, CALC.PK.TO.PK, SET.TIMEOUT, SCOPE.START, MEASURE
.SINGLE.WF, MEASURE.TWO.WF, OPEN.CHANNEL, CLOSE.CHANNEL      916
C          O          M          M          O          N
FREQUENCY, AUTO.FREQ, PERIOD, AUTO.PER, INTERVAL, RATIO, TOTALIZE,
R100MILLI, R1, R10, R100, R1KILO, R1OMEGA, R100OMEGA, CHAN.A, CHAN.B,
POSITIVE, NEGATIVE, COMN, SEPARATE, DCVOLTS, ACVOLTS, OHMS, R200MIL
LI, R2, R20, R200, R2KILO, R2OKILO, R200KILO      917      COMMON
R2MEGA, R2OMEGA, AUTOM, R2.5, R12.5, POSITIVE, NEGATIVE, TWOS, UNSIG
NED, OC, TTL, R0, R1, R2, R3, R4, R5, R6, R7, R8, R9, R10, R11, R12, R13, R14
, R15, R16, SINE, SQUARE, TRIANGLE, CONTINUOUS, GATED, BURST, R10NANO
, R100NANO, R1MICRO, R10MICRO, R100MICRO      918      COMMON
R1MILLI, R10MILLI, R100MILLI, R1, R10, R20NANO, R200NANO, R2MICRO, R
20MICRO, R200MICRO, R2MILLI, R20MILLI, R200MILLI, R2, R20, R50NANO,
R500NANO, R5MICRO, R50MICRO, R500MICRO, R5MILLI, R50MILLI, R500MIL
LI, R5, R50, CHAN.A, CHAN.B, EXTERNAL, POSITIVE      919      COMMON
NEGATIVE, AC, DC, TRIGGERED, AUTO.TRIG, AUTO.LEVEL, X1, X10, STANDAR
D , A V E R A G E 9 2 0 C O M M O N
DMM.01, FUNC.GEN.01, SCOPE.01, COUNTER.01, DIG.IN.01, DIG.OUT.01,
RELAY.ACT.01, RELAY.MUX.01 999 'End PCIB Program Shell
1000 REM
1010 REM This step initializes the HP system
1020 CLS
1030 OPTION BASE 1
1040 DIM P(10), PA(50,6), PP(50,6), XPT(40), CAL(40)
1050 CALL INITIALIZE.SYSTEM(PGMSHEL.HPC)
1060 REM
1070 REM All PC devices now have an initial state
1080 REM Set function on the DMM and Relay MUX
1090 REM
1100 CALL SET.FUNCTION(DMM.01, DCVOLTS)
1110 CALL SET.RANGE(DMM.01, AUTOM)
1120 CALL DISABLE.INT.TRIGGER(DMM.01)
1130 CALL ENABLE.OUTPUT(RELAY.MUX.01)
1140 FORMAT$="## ##.#### ##.#### ##.#### ##.#### ##.#### ##.####
##.####" 1200 FOR I=1 TO 10
1210 CAL(I)=0.0
1220 NEXT I
1510 REM

```

```

1520 REM READ THE VOLTAGE OF 48TH CHANNEL AND DISPLAY THE
DATA
1530 REM
1540 PRINT " CHOOSE 6 POINTS"
1550 PRINT
1550 PRINT "THE CALIBRATION WILL BE STORES IN 'CAL.DAT'"
1560 REM
1570 REM Begin sampling loop
1580 REM
1600 FOR J=1 TO 1
1610 PRINT
1630 FOR JJ=1 TO 6
1631 INPUT "INPUT THE CALIBRATION PRESSURE";CAL(JJ)
1632 INPUT "PRESS 'ENTER' TO START MEASUREMENT";MOVE$
1640 FOR II=1 TO 10
1650 ROUT=1
1660 CALL OUTPUT(RELAY.MUX.01,ROUT)
1670 CALL MEASURE(DMM.01,VOLTS)
1680 PA(II,JJ)=VOLTS
1690 NEXT II
1700 IF JJ=6 THEN 1740
1730 NEXT JJ
1740 REM
1750 REM DISPLAY THE SAMPLE DATA
1760 REM
1780 FOR IS= 1 TO 10
1 7 9 0 P R I N T U S I N G
FORMAT$;IS,PA(IS,1),PA(IS,2),PA(IS,3),PA(IS,4),PA(IS,5),PA(I
S,6) 1800 NEXT IS
1810 REM
1820 REM AVERAGE THE DATA
1830 REM
1840 FOR JA = 1 TO 6
1850 TOTAL = 0
1860 FOR IA = 1 TO 10
1870 TOTAL = TOTAL + PA(IA,JA)
1880 NEXT IA
1890 AVERAGE = TOTAL /10
1900 P(JA)=AVERAGE
1920 NEXT JA
1930 PRINT
1940 PRINT "THE AVERAGE ARE: "
2000 FOR JD=1 TO 6
2010 PP(J,JD)=P(JD)
2020 NEXT JD
2 0 5 5 P R I N T U S I N G
FORMAT$;J,PP(J,1),PP(J,2),PP(J,3),PP(J,4),PP(J,5),PP(J,6) 2070
PRINT
2080 INPUT "DO YOU WANT RE-MEASURE AGAIN ? (Y / N)";C$
2090 IF C$="Y" THEN 1580
2101 REM*** STORE DATA BEFORE NEXT SAMPLE***

```

```
2102 OPEN "A:\CAL.DAT" FOR OUTPUT AS #2
2106 FOR ID=1 TO 6
2107 PRINT #2,USING FORMAT$;ID,PP(J, ID),CAL(ID)
2108 NEXT ID
2109 CLOSE #2
2210 NEXT J
```

## APPENDIX C. CONVERT PROGRAM

```

*****
*****
* THIS PROGRAM CONVERTS THE VOLTAGE OF TRANSDUCER INTO
* PHYSICAL *
* PRESSURE, VELOCITY, YAW ANGLE AND PITCH ANGLE. THOSE DATA ARE
*
* USED FOR PLOT PROGRAM LATER.
*
*****
*****
CHARACTER*12 FNAME
CHARACTER*12 NAME
CHARACTER*12 FONAME
CHARACTER*2 A(50)
CHARACTER*80 ST
REAL K,INTR
INTEGER COLS,RWS,DTPTS
DATA A/'01','02','03','04','05','06','07','08','09',
*      '10','11','12','13','14','15','16','17','18',
*      '19','20','21','22','23','24','25','26','27',
*      '28','29','30','31','32','33','34','35','36',
*      '37','38','39','40','41','42','43','44','45',
*      '46','47','48','49','50'/
WRITE (*,'(A\)' ) ' # OF COLS (AWAY FROM MSL) = '
READ (*,'(I5)' ) COLS
WRITE (*,'(A\)' ) ' # OF DATA PTS IN A COL (UP/DOWN) =
,
READ (*,'(I5)' ) RWS
WRITE (*,'(A\)' ) ' DATA FILE NAME? (IE R001A2XX.DAT)
,
READ (*,'(A12)' ) NAME
WRITE (*,'(A\)' ) ' PI (F4.2) = '
READ (*,'(F4.2)' ) PI
WRITE (*,'(A\)' ) ' PF (F4.2) = '
READ (*,'(F4.2)' ) PF
WRITE (*,'(A\)' ) ' TI (F3.1) = '
READ (*,'(F3.1)' ) TI
WRITE (*,'(A\)' ) ' TF (F3.1) = '
READ (*,'(F3.1)' ) TF
WRITE (*,'(A\)' ) ' K (F6.4) = '
READ (*,'(F6.4)' ) K
WRITE (*,'(A\)' ) ' SLOPE FOR DELTAP (F9.6) = '
READ (*,'(F9.6)' ) SLOPE
WRITE (*,'(A\)' ) ' INTERCEPT FOR DELTAP (F9.6) = '
READ (*,'(F9.6)' ) INTR

```

```

WRITE (*,'(A\)' ) ' QM1 FACTOR (F4.2) = '
READ (*,'(F4.2)') QM1FAC
WRITE (*,'(A\)' ) ' X OFFSET = '
READ (*,'(F5.2)') XOFF
WRITE (*,'(A\)' ) ' Y OFFSET = '
READ (*,'(F5.2)') YOFF
WRITE (*,'(A\)' ) ' OUTPUT FILE NAME = '
READ (*,'(A12)') FONAME
* CONVERT THE PRESSURE UNIT FROM inHg TO psf
PATM=(PI+PF)*35.3631
R=1716.5
E=0.0123
T=(TI+TF)/2.+460
RO=PATM/(R*T)
DTPTS=RWS*COLS
* OPEN A NEW FILE TO STORE THE REDUCED DATA
OPEN(2,FILE=FONAME,STATUS='NEW')
WRITE(2,222) DTPTS
222 FORMAT (I5)
* OPEN A SEQUENTIAL OF DATA FILE
DO 20 I=1, COLS
NAME(7:8)=A(I)
FNAME=NAME
OPEN(1,FILE=FNAME)
READ(1,100,END=20) ST
100 FORMAT(A65)
15 READ(1,1000,END=30) NO,X,Y,V1,V2,V3,V4,V5,BETA
1000 FORMAT(I2,F7.2,F6.2,5F9.3,F8.2)
* CONVERT THE VOLTAGE TO PRESSURE IN LBF/FT**2
P1=DELTAP(V1,SLOPE,INTR)*2.0475+PATM
P2=DELTAP(V2,SLOPE,INTR)*2.0475+PATM
P3=DELTAP(V3,SLOPE,INTR)*2.0475+PATM
P4=DELTAP(V4,SLOPE,INTR)*2.0475+PATM
P5=DELTAP(V5,SLOPE,INTR)*2.0475+PATM
* CALCULATE THE PITCH ANGLE IN DEGREES
P=(P4-P5)/(P1-P2)
IF (P.GT.0.80) P=0.80
IF (P.LT.-0.80) P=-0.80
ALPHA=FPITCH(P)
* CALCULATE THE VELOCITY IN FT/SEC
YSLOP=FYSLOP(ALPHA)
VELM=SQRT((2*YSLOP*(P1-P2))/(RO*K))
VEL=VELM*(1+E)
* CALCULATE THE LOCAL DYNAMIC PRESSURE
QM1=QM1FAC*2.0475/K
QM=RO*VEL**2/2.
Q1=QM1*(1+2*E)
Q=QM*(1+2*E)
* CALCULATE THE YAW ANGLE IN DEGREES
YAW=FYAW(BETA+5.0)
* CALCULATE THE VELOCITY COMPONENTS

```

```

      BETAR=YAW*.017453
      ALPHAR=(ALPHA-17.942)*.017453
      VELY=VEL*SIN(ALPHAR)
      VELX=VEL*COS(ALPHAR)*SIN(BETAR)
*   CALCULATE THE TOTAL PRESSURE IN LBF/IN**2
      PTC=FPT(ALPHA)
      PT1=P1-Q*PTC
      PT=PT1/144.
      CPT=(PT1-PATM-Q1)/Q1
*   CALCULATE THE STATIC PRESSURE IN LBF/IN**2
      PS1=PT1-Q
      PS=PS1/144
      CPS=(PS1-PATM)/Q1
*   WRITE VALUES TO OUTPUT FILE
      WRITE(2,2000)-X+XOFF,Y+YOFF,VEL,VELX,VELY,YAW,
C      ALPHA-17.942,PT,CPT,PS,CPS
2000  FORMAT(11F10.3)
      GO TO 15
30    CLOSE(1)
20    CONTINUE
      CLOSE(2)
      STOP
      END
*****
* THIS FUNCTION CONVERTS THE VOLTAGE TO PHYSICAL PRESSURE
FUNCTION DELTAP(X,SLOPE,INTR)
REAL INTR
DELTAP=X*SLOPE+INTR
END
*****
* THIS FUNCTION CALCULATES THE PITCH ANGLE
FUNCTION FPITCH(X)
FPITCH=3.759+53.7568*X-1.3085*X**2-1.6583*X**3
*      -0.8061*X**4+16.5115*X**5
      END
*****
* THIS FUNCTION CALCULATES THE VELOCITY PRESSURE COEFFICIENT
FUNCTION FYSLOP(X)
IF(X.LT.-10)THEN
  FYSLOP=0.981-0.0102*X-3.000E-4*X**2-2.500E-6*X**3
ELSE IF((X.GE.-10).AND.(X.LE.10))THEN
  FYSLOP=0.98-0.006*X+2.000E-4*X**2
ELSE
  FYSLOP=0.9801-0.0035*X-1.143E-4*X**2+5.833E-6*X**3
END IF
END
*****
* THIS FUNCTION CALCULATES THE YAW ANGLE
FUNCTION FYAW(X)
IF((X.GE.0).AND.(X.LE.180)) THEN
  FYAW=-X

```

```

ELSE
  FYAW=360-X
END IF
END
*****
* THIS FUNCTION CALCULATES THE TOTAL PRESSURE COEFFICIENT
  FUNCTION FPT(X) .
  IF(X.LE.-30) THEN
    FPT=-0.01
  ELSE IF((X.GT.-30).AND.(X.LT.-20)) THEN
    FPT=0.02+1.00E-3*X
  ELSE IF((X.GE.-20).AND.(X.LE.30)) THEN
    FPT=0
  ELSE
    FPT=0.03-1.00E-3*X
  END IF
END

```

## APPENDIX D. VORTIC PROGRAM

```

CHARACTER*12 FNAME,OFNAME
REAL VEL,VX(13,23),VY(13,23),VOR(13,23),VORX(13,23)
REAL VELX,VELY,X,Y,DH,VORY(13,23),XC(13,23),YC(13,23)
WRITE(*,'(A\)' ) ' DATA FILE NAME ? '
READ (*,'(A12)') FNAME
WRITE (*,'(A\)' ) ' OUTPUT FILE NAME ? '
READ (*,'(A12)') OFNAME
OPEN (3,FILE=OFNAME,STATUS='NEW')
OPEN (2,FILE=FNAME)
10  READ (2,100,END=20) X,Y,VEL,VELX,VELY
100  FORMAT (5F10.3)
C  COMPUTE INDICES FOR ARRAYS
    J=INT((Y/.25)+12.0)
    I=INT((-X/.25)-1.0)
C  COMPUTE NON-DIMEN. VELOCITIES
    VX(I,J)=VELX/VEL
    VY(I,J)=VELY/VEL
    XC(I,J)=X
    YC(I,J)=Y
    GO TO 10
C  COMPUTE NON-DIMEN. STEP SIZE
C  DELTA H=2*GRID STEP DISTANCE/MISSILE DIAMETER
20  DH=(2.0*.25)/1.75
C  COMPUTE VALUES FOR THE Y VORTICITY IN X DIR. ARRAY
    DO 30 J=1,23
      DO 40 I=1,13
C  IF STATEMENTS DEFINE BOUNDARIES
        IF(I.EQ.1) THEN
          VORY(I,J)=(-3.*VY(I,J)+4.*VY(I+1,J)-VY(I+2,J))/DH
        ELSE IF(I.EQ.15) THEN
          VORY(I,J)=(3.*VY(I,J)-4.*VY(I-1,J)+VY(I-2,J))/DH
        ELSE
          VORY(I,J)=(VY(I+1,J)-VY(I-1,J))/DH
        ENDIF
      40  CONTINUE
    30  CONTINUE
C  COMPUTE VALUES FOR THE X VORTICITY IN Y DIR. ARRAY
    DO 35 J=1,23
      DO 45 I=1,13
C  IF STATEMENTS DEFINE BOUNDARIES
        IF(J.EQ.1) THEN
          VORX(I,J)=(-3.*VX(I,J)+4.*VX(I,J+1)-VX(I,J+2))/DH
        ELSE IF (J.EQ.21) THEN
          VORX(I,J)=(3.*VX(I,J)-4.*VX(I,J-1)+VX(I,J-2))/DH
        ELSE
          VORX(I,J)=(VX(I,J+1)-VX(I,J-1))/DH

```

```
                ENDIF
45  CONTINUE
35  CONTINUE
C  COMPUTE THE VORTICITY FOR EACH POINT
    DO 50 I=1,13
      DO 55 J=1,23
        VOR(I,J)=VORY(I,J)-VORX(I,J)
        WRITE (3,200)XC(I,J), YC(I,J), VOR(I,J)
200  FORMAT (3F10.3)
55  CONTINUE
50  CONTINUE
    CLOSE (2)
    CLOSE (3)
    STOP
    END
```

## LIST OF REFERENCES

1. Gregoriou, Gregor, *Modern Missile Design For High Angle-of Attack*, AGARD/VKI Lecture Series No. 121, High Angle of Attack Aerodynamics, March 1982.
2. Rabang, M.P., *Turbulence Effects on the High Angle of Attack Aerodynamics of a Vertically-launched Missile*, Master's Thesis, Naval Postgraduate School, Monterey, CA, June 1988.
3. Dunne, Anthony L., and others, *VLA Missile Development and High Angle of Attack Behavior*, NEAR Conference on Missile Aerodynamics Proceedings, Monterey, CA, November, 1988.
4. Roane, D.P., *The Effect of a Turbulent Airstream on a Vertically-launched Missile at High Angles of Attack*, Master's Thesis, Naval Postgraduate School, Monterey, CA, December 1987.
5. Lung, M.H., *Flowfield Measurements in the Vortex Wake of a Missile at High Angle of Attack in Turbulence*, Master's Thesis, Naval Postgraduate School, Monterey, CA, December 1988.
6. Viniotis, J.J., *Flowfield Effects of Launch on a Vertically-Launched Missile*, Master's Thesis, Naval Postgraduate School, Monterey, CA, June 1989.
7. Johnson, Dan A., *Flowfield Measurements in the Wake of a Missile at High Angle Attack*, Master's Thesis, Naval Postgraduate School, Monterey, CA, September 1989.
8. Gregoriou, Gregor, and Knoche, H.G., *High Incidence Aerodynamics of Missiles During Launch Phase*, MBB GMBH Report UA-523/80, January 1980.
9. Ericsson, Lars E., and Redding, J. Peter, *Asymmetric Vortex Shedding from Bodies of Revolution*, Tactical Missile Aerodynamics, American Institute of Aerodynamics and Astronautics, Inc., 1986.
10. Dahlem, Valentine, and others, *High Angle of Attack Missile Aerodynamics at Mach Numbers 0.3 to 1.5*, AFWAL-TR-80-3070, November 1980.
11. Genxing, Wu, Tzehsing, Wang, and Shixhong, Tian, *Investigation of Vortex Patterns on Slender Bodies at High Angles Of Attack*, Journal of Aircraft, Volume 23, Number 4, pp. 321-325, April 1986.

12. Keener, Earl R., and Chapman, Gary T., *Onset of Aerodynamic Side Forces at Zero Sideslip on Symmetric Forebodies at High Angles of Attack*, AIAA Paper 74-770, August 1974.
13. Deffenbaugh, F.D., and Koerner, *Asymmetric Vortex Wake Development on Missiles at High Angles of Attack*, *Journal of Spacecraft*, Volume 14, Number 3, pp. 155-162, March 1977.
14. Ericsson, L.E., and Reding, J.P., *Steady and Unsteady Vortex-Induced Asymmetric Load on Slender Vehicles*, *Journal of Spacecraft*, Volume 10, Number 2, March-April 1981.
15. Keener, E.R., and Chapman, G.T., *Similarity in Vortex Asymmetries over Slender Bodies and Wings*, *AIAA Journal*, Volume 15, Number 9, pp. 1370-1372, September 1977.
16. Howard, Richard M., Rabang, M. Peter, and Roane, Donald P., *Aerodynamic Effects of a Turbulent Flowfield on a Vertically-Launched Missile*, AIAA Paper 89-0329, 1989.
17. Jorgensen, Leland H., and Nelson, Edgar R., *Experimental Aerodynamic Characteristics for a Cylindrical Body of Revolution with Side Strakes and Various Noses at Angles of Attack From 0° to 58° and Mach Numbers from 0.6 to 2.0*, NASA TM X-3130, March 1975.
18. Deane, J.R., *Missile Body Vortices and Their Interaction with Lifting Surfaces*, AGARD/VKI Lecture Series No. 121, High Angle of Attack Aerodynamics, March 1982.
19. Castro, I.P., *Effects of Free Stream Turbulence on Low Reynolds Number Boundary Layers*, *Journal of Fluids Engineering*, Volume 106, pp. 298-306, September 1984.
20. Bradshaw, P., *An Introduction to Turbulence and its Measurement*, Pergamon Press, 1971.
21. *Laboratory Manual for Slow-Speed Wind Tunnel Testing*, Department of Aeronautics, Naval Postgraduate School, Monterey, CA, 1983.
22. Velmex, Inc., *User's Guide to 3800 Series Stepping Motor Controller/Drivers*, East Bloomfield, NY, January 1988.
23. United Sensors, Inc., *5-Hole Probes Calibration Manual*, Watertown, MA, June 1988.
24. Hewlett-Packard, Inc., *PC Instruments System Owner's Guide Using HP 610618 System Interface*, February 1986.

25. Kindelspire, D.W., *The Effects of Freestream Turbulence on Airfoil Boundary Layer Behavior at Low Reynolds Number*, Master's Thesis, Naval Postgraduate School, Monterey, CA, September 1988.
26. Chlebanowski, J.S. Jr., *Flow Visualization by Laser Sheet*, Master's Thesis, Naval Postgraduate School, Monterey, CA, March 1988.
27. Sommers, J.D., *An Experimental Investigation of Support Strut Interference on a Three-Percent Fighter Model at High Angles of Attack*, Master's Thesis, Naval Postgraduate School, Monterey, CA, September 1989.

**INITIAL DISTRIBUTION LIST**

	<b>No. Copies</b>
1. Defense Technical Information Center Cameron Station Alexandria, VA 22304-6145	2
2. Library, Code 0142 Naval Postgraduate School Monterey, CA 93943-5002	2
3. Chairman Department of Aeronautics, Code 67 Naval Postgraduate School Monterey, CA 93943-5000	1
4. Commander Naval Surface Warfare Center, Code G205 Dahlgren, VA 22448-5000	1
5. Standard Missile Program Office PMS 422, G205 ATTN: Thomas McCants Dr. Jesse East Naval Surface Warfare Center Dahlgren, VA 22448-5000	2
6. Commander Naval Weapons Center, Code 406 China Lake, CA 93555	1
7. Commander Naval Surface Weapons Center Silver Spring, MD 20903-5000	1
8. Commander Pacific Missile Test Center Point Mugu, CA 93041	1
9. NASA Ames Research Center Technical Library Moffett Field, CA 94035	1
10. Prof. R. M. Howard Department of Aeronautics, Code 67Ho Naval Postgraduate School Monterey, CA 93943-5000	7

- |  |   |
|--|---|
| 11. LT. Lung, Ming-Hung<br>No. 114-5 Chung-Ching Rd.<br>Taichung Taiwan 400<br>Republic of China | 1 |
| 12. LT. J. J. Viniotis, USN<br>379 Ocean Avenue<br>Massapequa Pk, NY 11762                       | 1 |
| 13. LT. J. A. Pinaire, USN<br>RR1 Box 406-B<br>Corydon, IN 47112                                 | 2 |